

Rydberg atoms and their applications

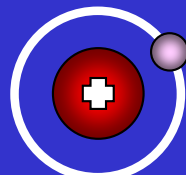
**I.I.Rybtsev^{1,2}, I.I.Beterov^{1,2,3}, E.A.Yakshina^{1,2,3},
D.B.Tretyakov^{1,2}, V.M.Entin¹, I.N.Ashkarin^{1,2}, A.M.Faruk²,
N.V.Alyanova^{1,3}, P.I.Betleni^{1,2}, N.O.Zhuravlev²**

¹ *Rzhanov Institute of Semiconductor Physics SB RAS, Novosibirsk, Russia*

² *Novosibirsk State University, 630090 Novosibirsk, Russia*

³ *Institute of Laser Physics SB RAS, Novosibirsk, Russia*

Atom in a ground state with $n \sim 1$

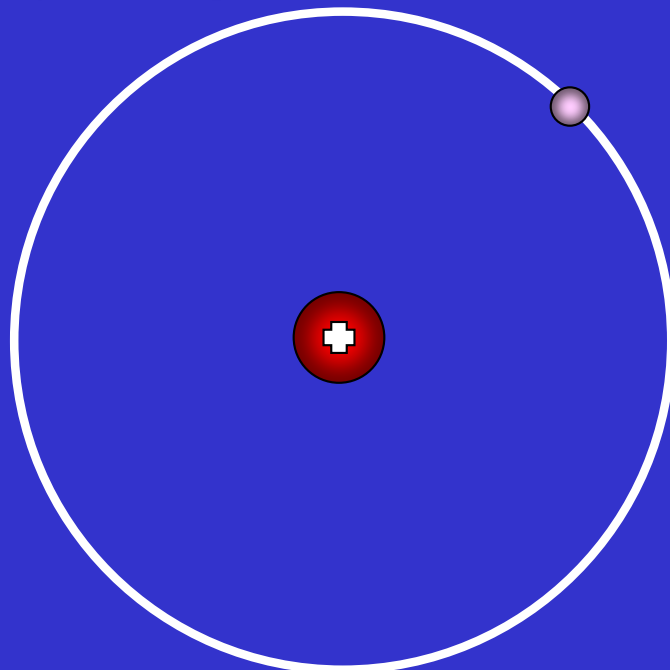


Quantum numbers: n, L

n - principal quantum number

L - orbital moment

Rydberg atom with $n \gg 1$



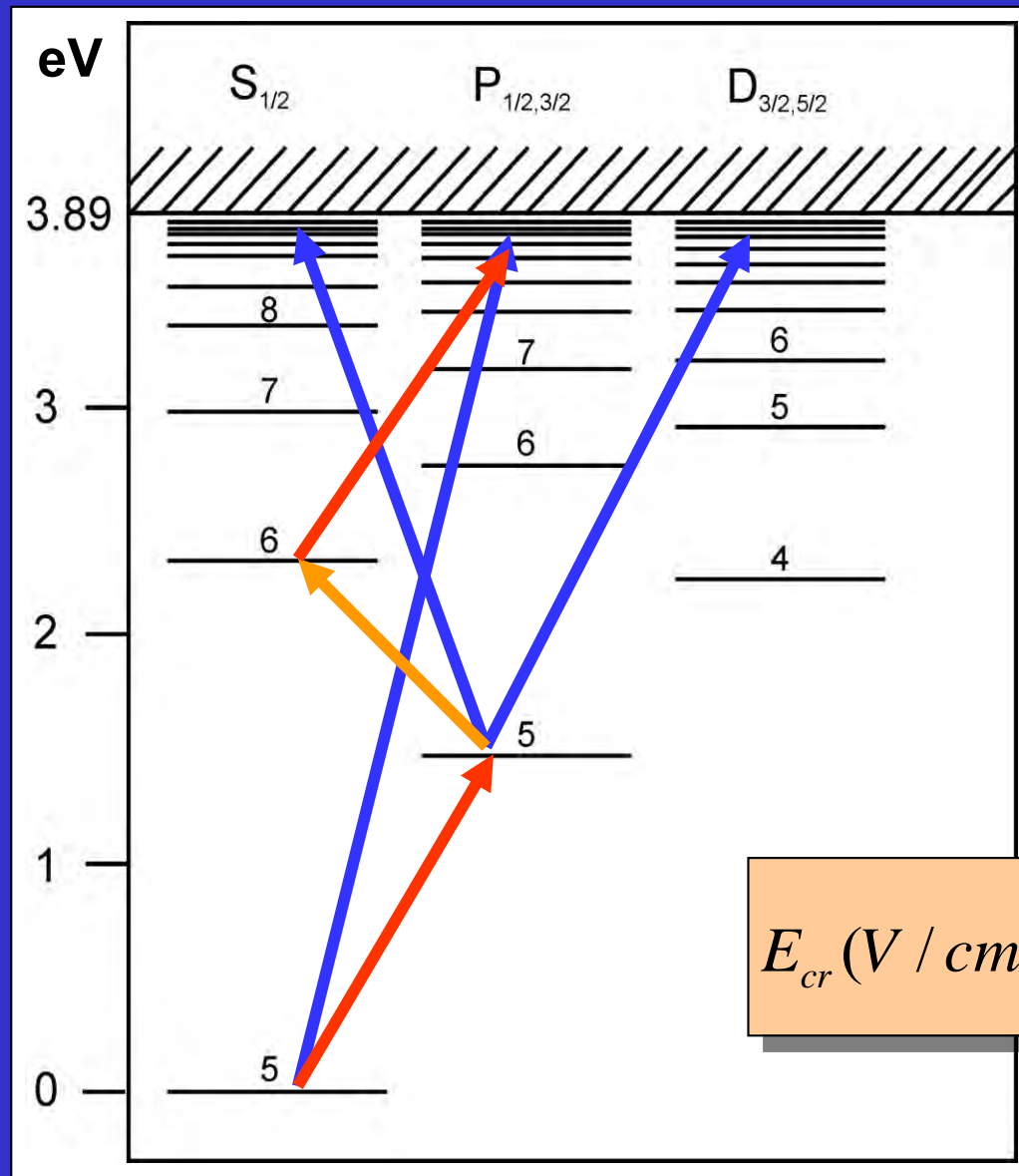
$$E_n = -\frac{Ry}{n^2}$$

$$E_n = -\frac{Ry}{(n - \delta_L)^2}$$

$$r_n \sim n^2$$

Rydberg atoms

Energy levels in Rb atoms



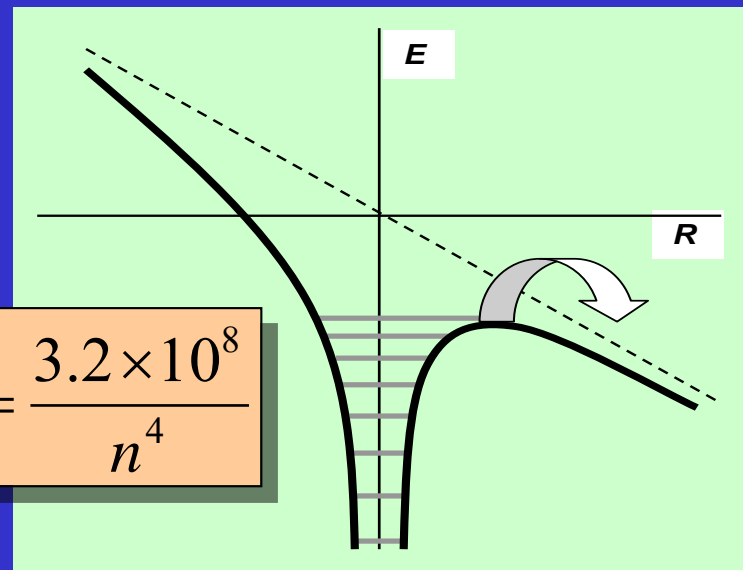
$$E_n = -\frac{Ry}{(n-\delta_L)^2}$$

$$r_n \sim n^2$$

$$\tau_n \sim n^3 - n^5$$

$$\alpha_n \sim n^7$$

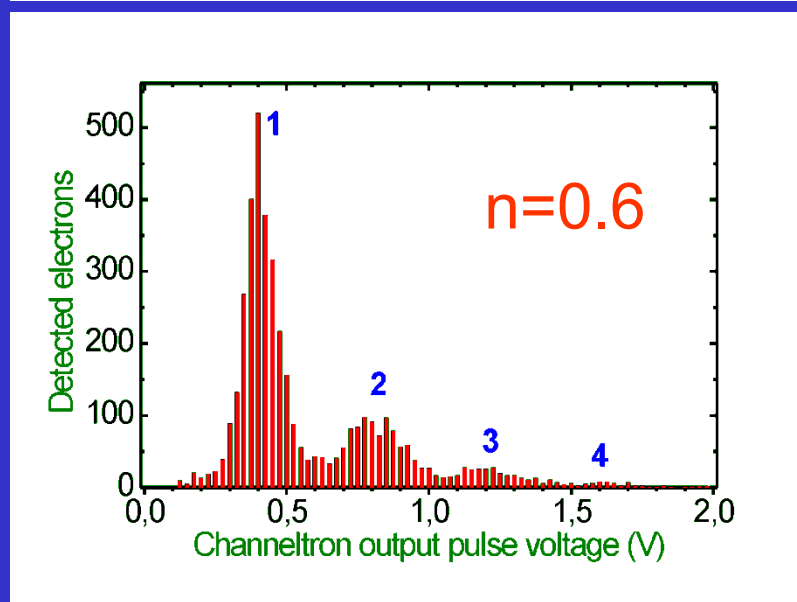
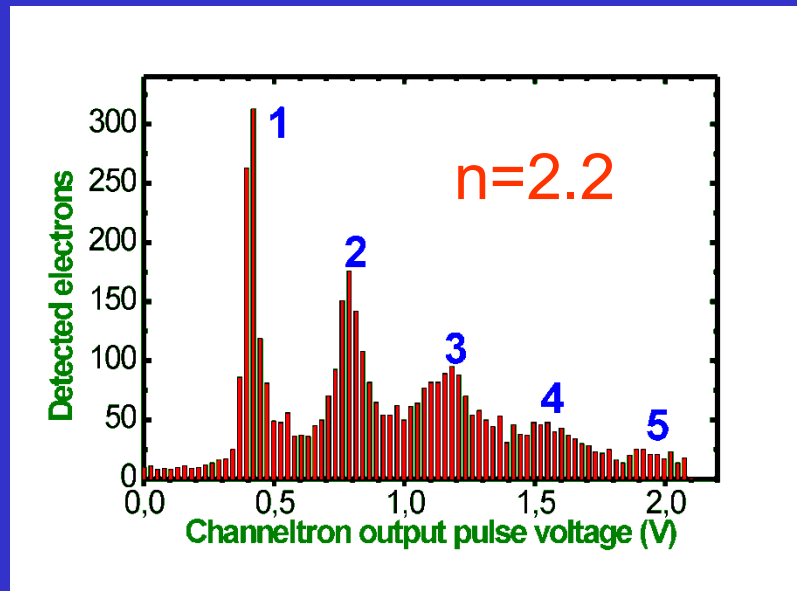
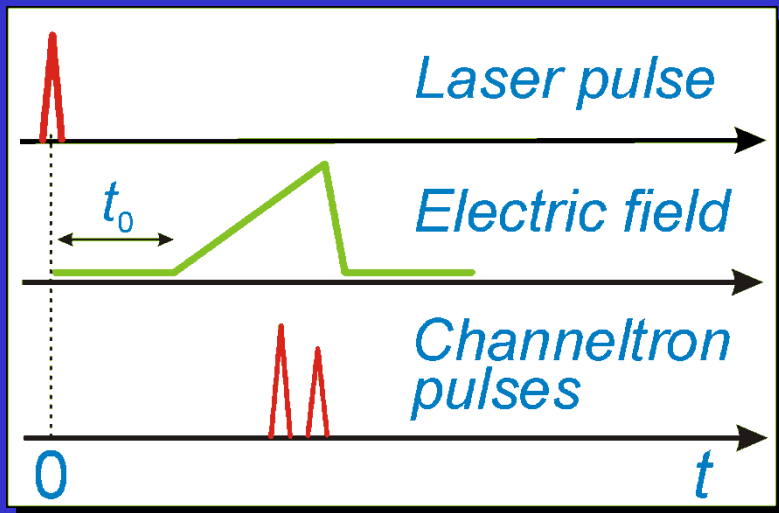
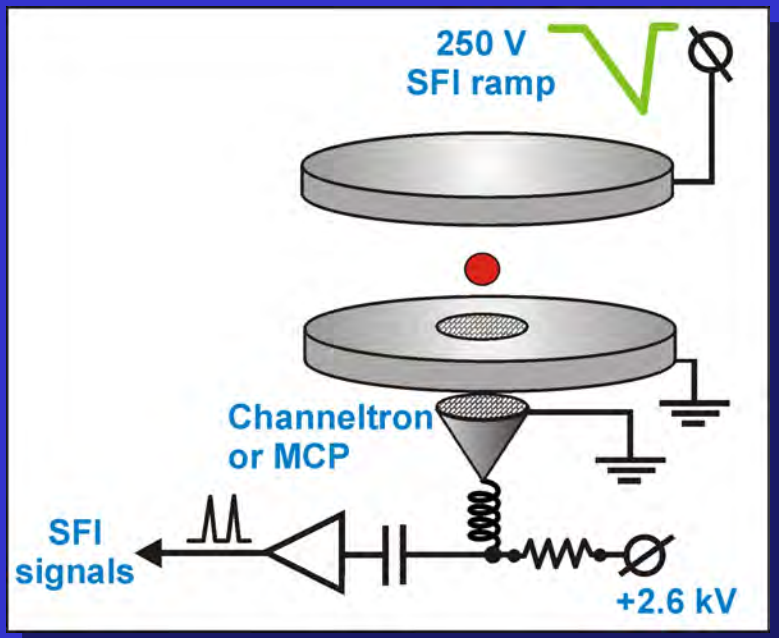
$$E_{cr} (V/cm) = \frac{3.2 \times 10^8}{n^4}$$



Selective Field Ionization detector

Atom counting with CEM

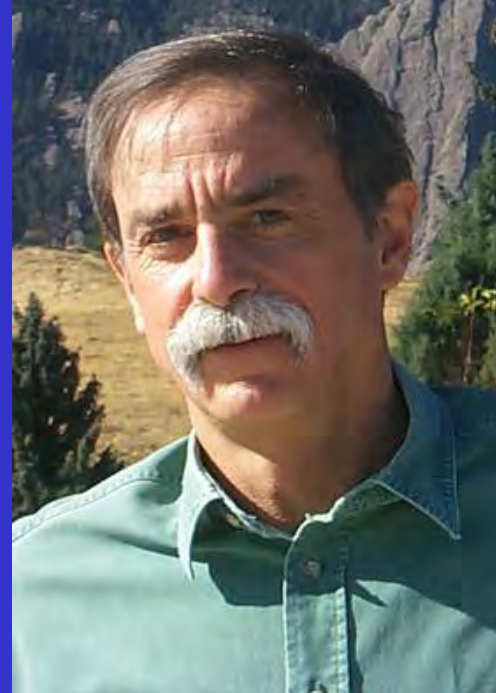
Ryabtsev et al., PRA 76 (2007) 012722



MOTIVATION

- Laser and microwave spectroscopy
- Collisions and chemionization
- Photoionization
- Ultracold plasmas
- Many-body phenomena
- Neutral atom quantum computing
- Single-photon sources
- Electric-field sensors

Nobel Prize laureates for physics in 2012



Serge Haroche

Born: 1944, Casablanca, Morocco

Affiliation at the time of the award: Collège de France, Paris, France, École Normale Supérieure, Paris, France

Prize motivation: "for ground-breaking experimental methods that enable measuring and manipulation of individual quantum systems"

David J. Wineland

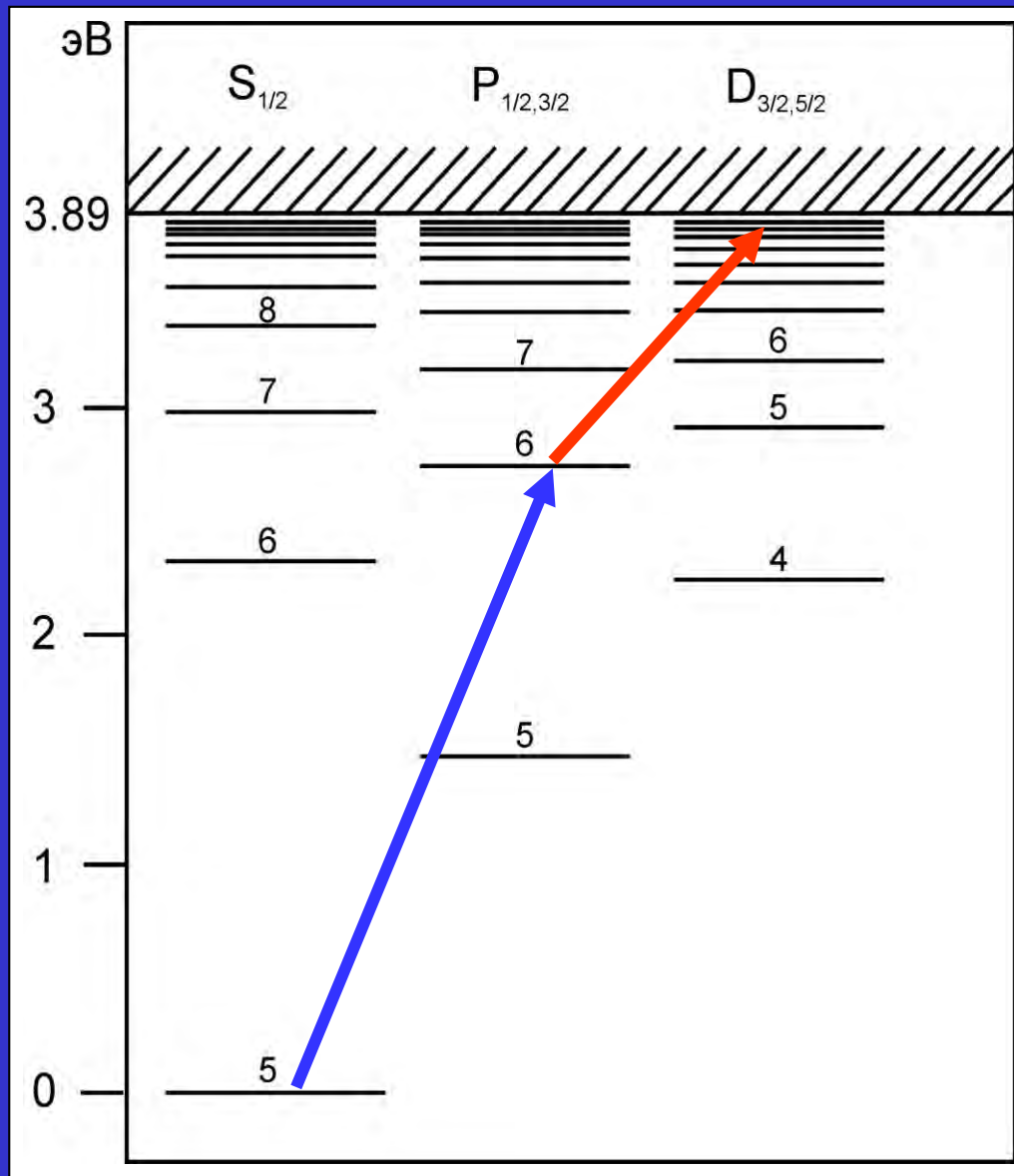
Born: 1944, Milwaukee, WI, USA

Affiliation at the time of the award: National Institute of Standards and Technology, Boulder, CO, USA, University of Colorado, Boulder, CO, USA

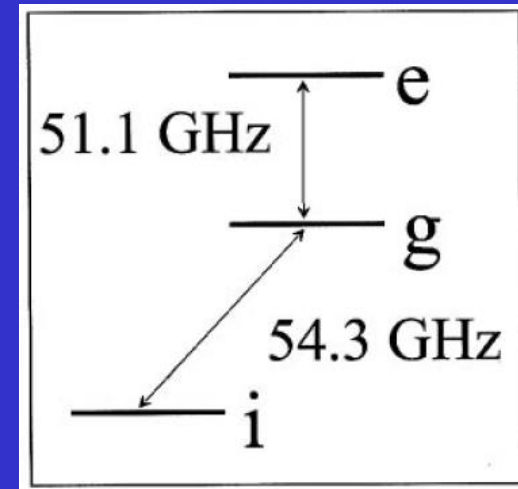
Prize motivation: "for ground-breaking experimental methods that enable measuring and manipulation of individual quantum systems"

Experiments of S.Haroche

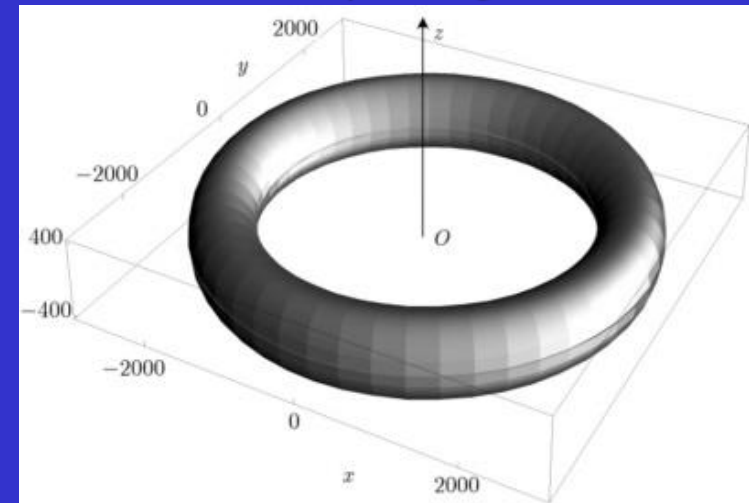
Energy levels in Rb atoms



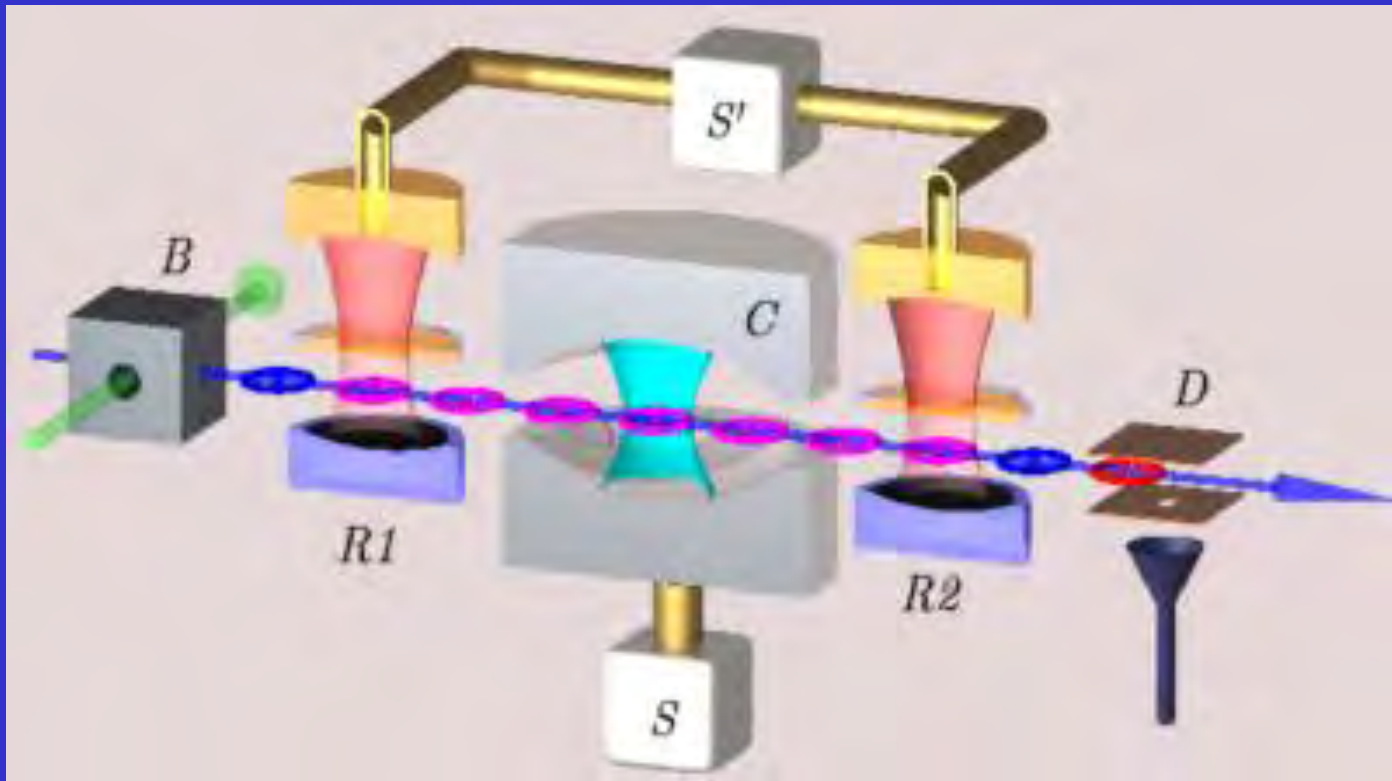
Microwave transition



Circular Rydberg state

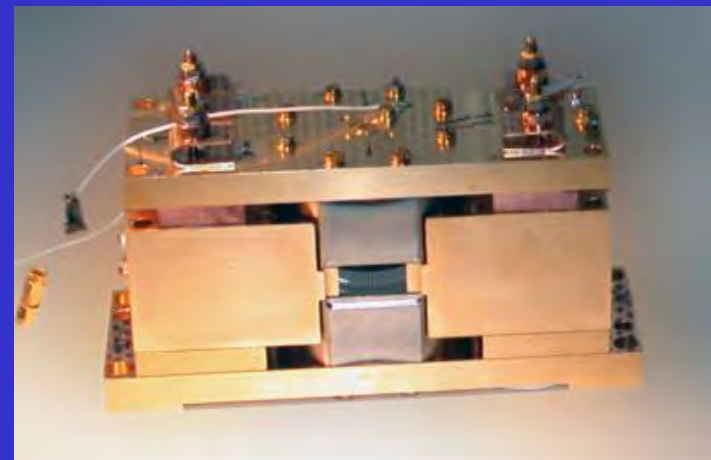


Experiments of S.Haroche



$$E_n = (n + 1/2) \hbar \omega$$

$$P_n = e^{-\mu} \mu^n / n!$$



Experiments of S.Haroche

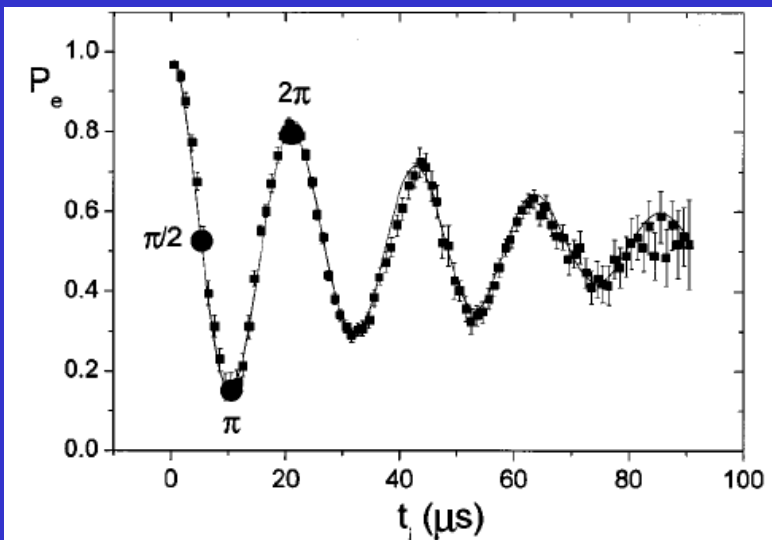


FIG. 3. Vacuum Rabi oscillations. The atom in state e enters

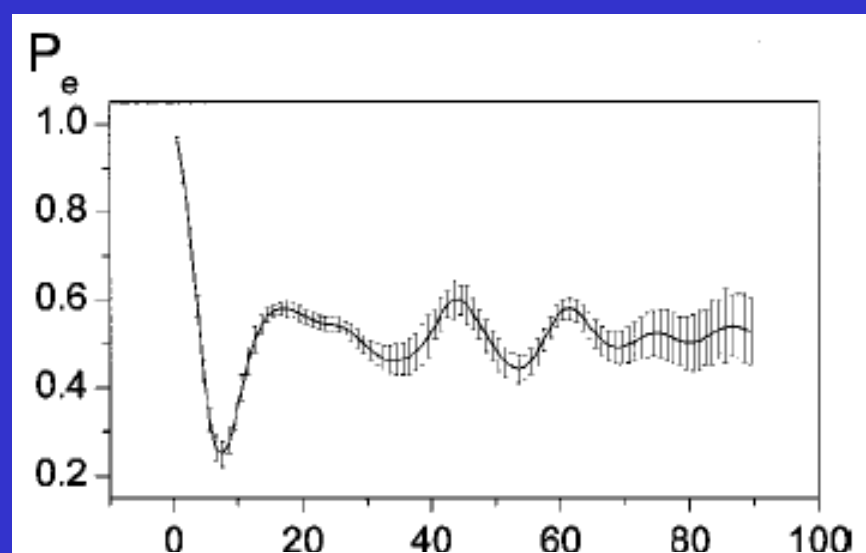
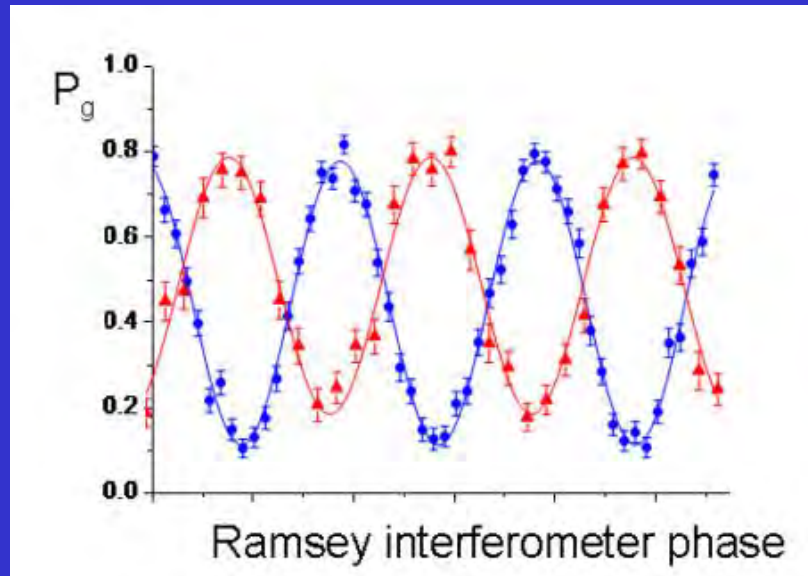
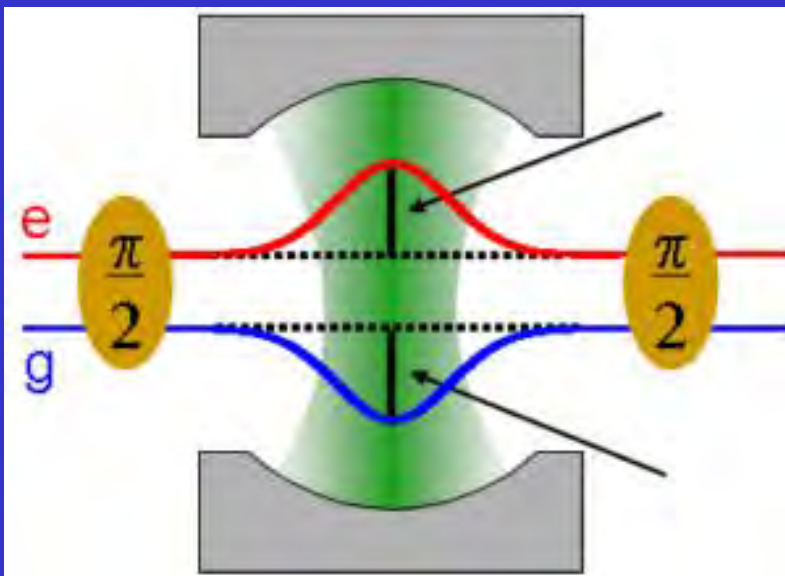


FIG. 5. Quantum Rabi oscillation in a coherent field.



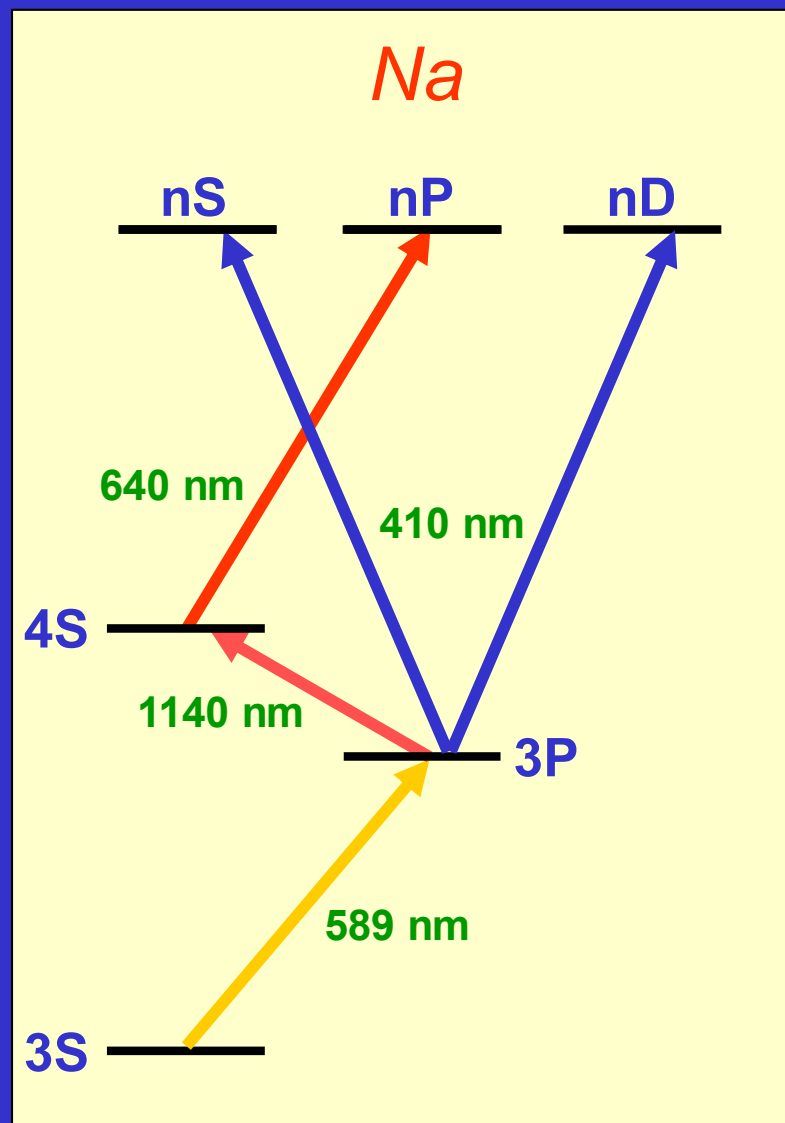
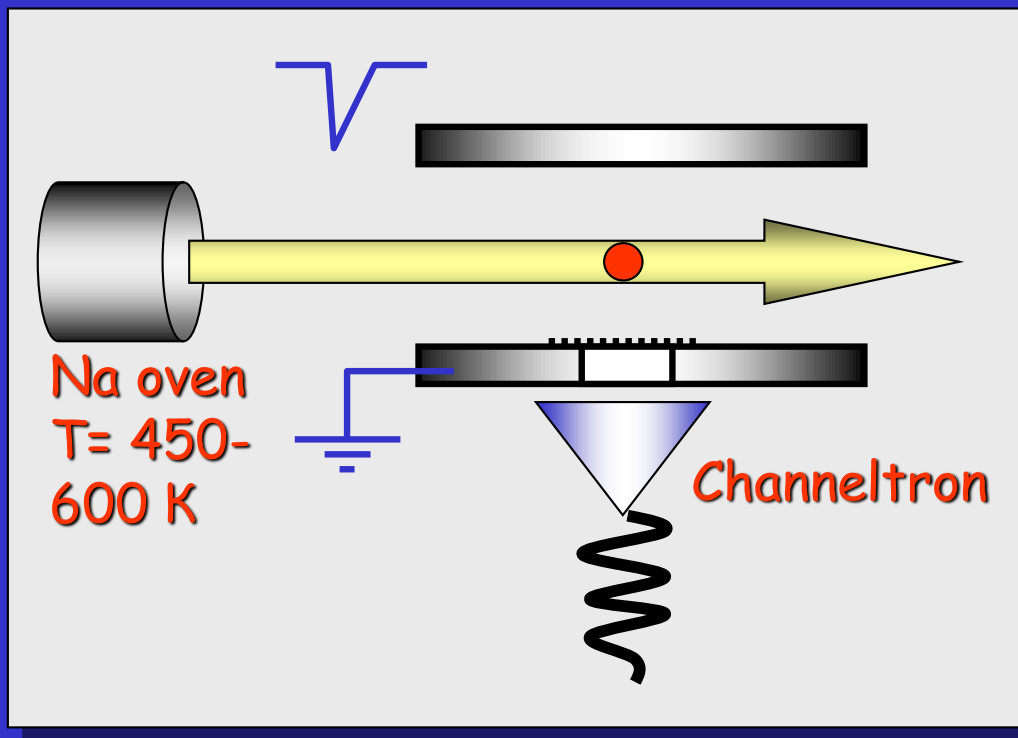


Veniamin Chebotaev
(1938-1992)

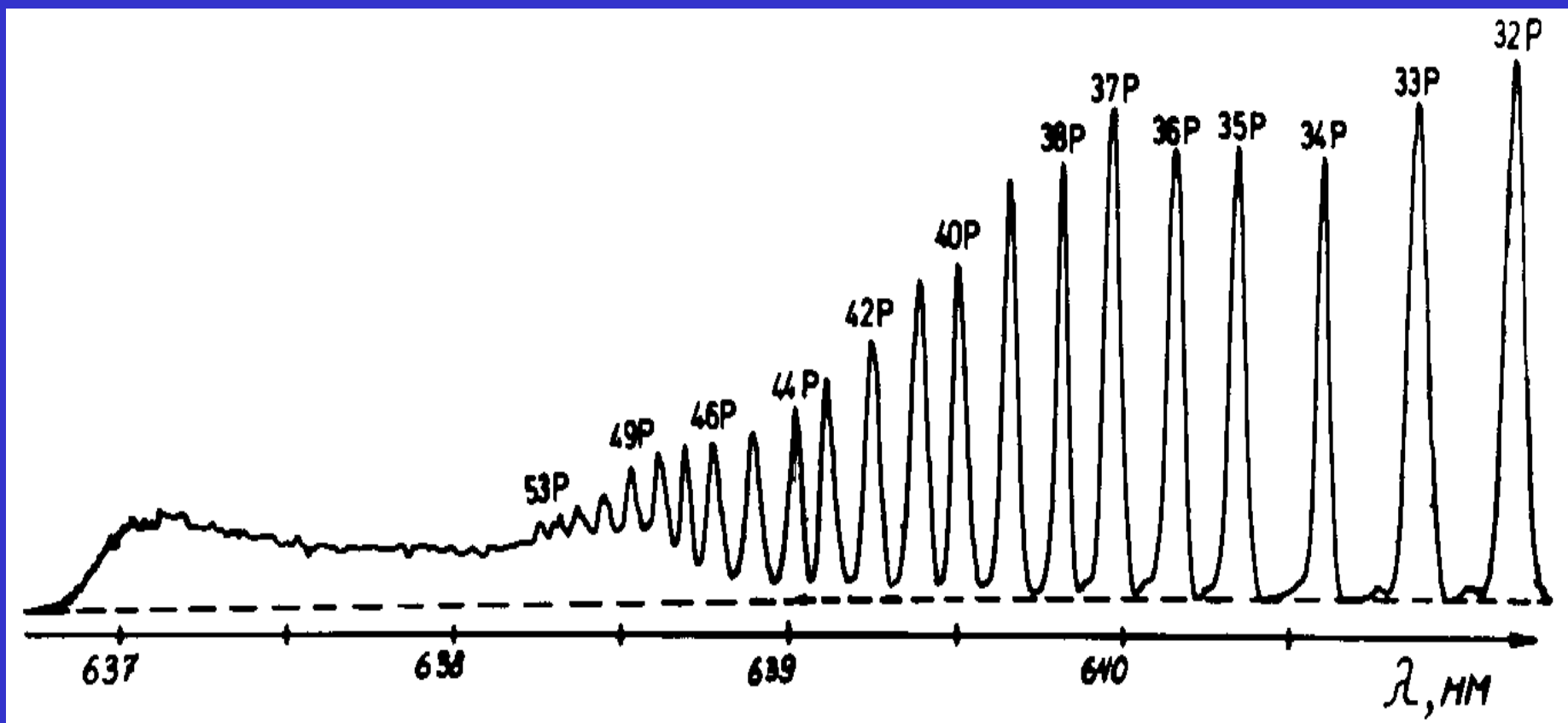


Igor Beterov
(1942-1999)

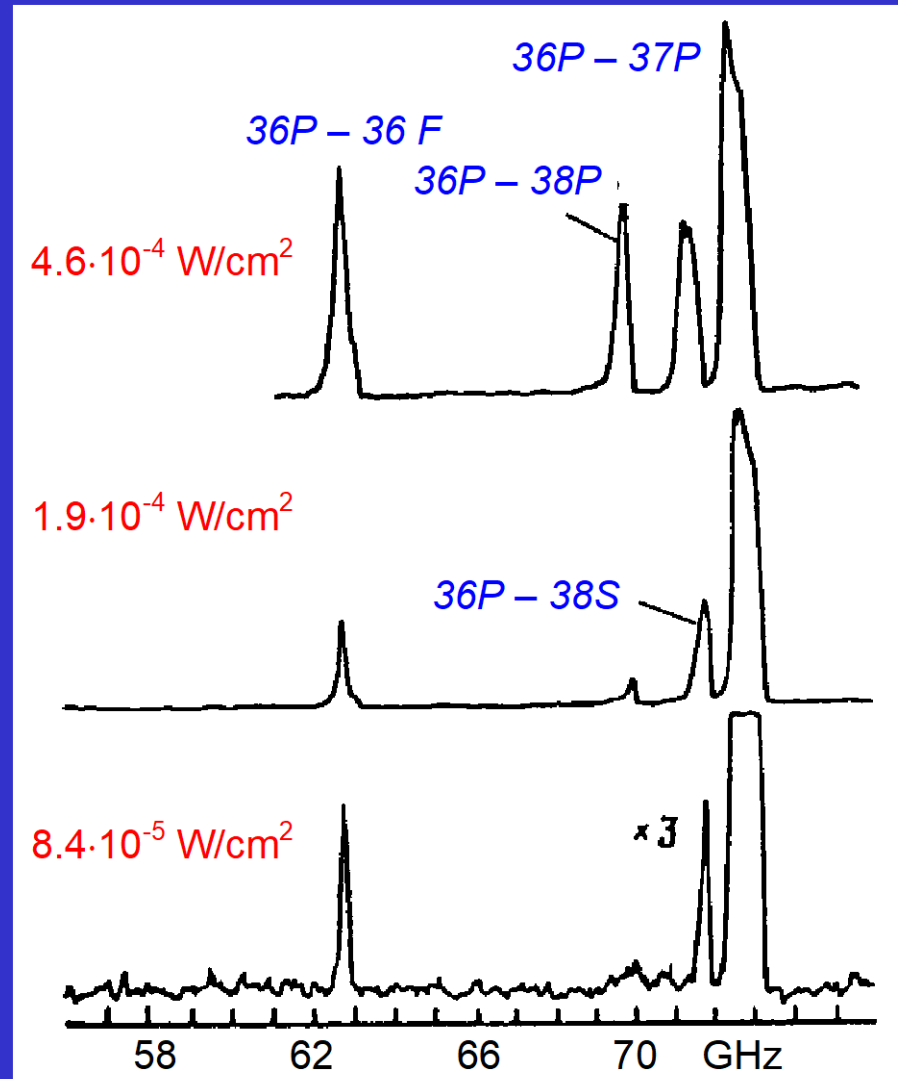
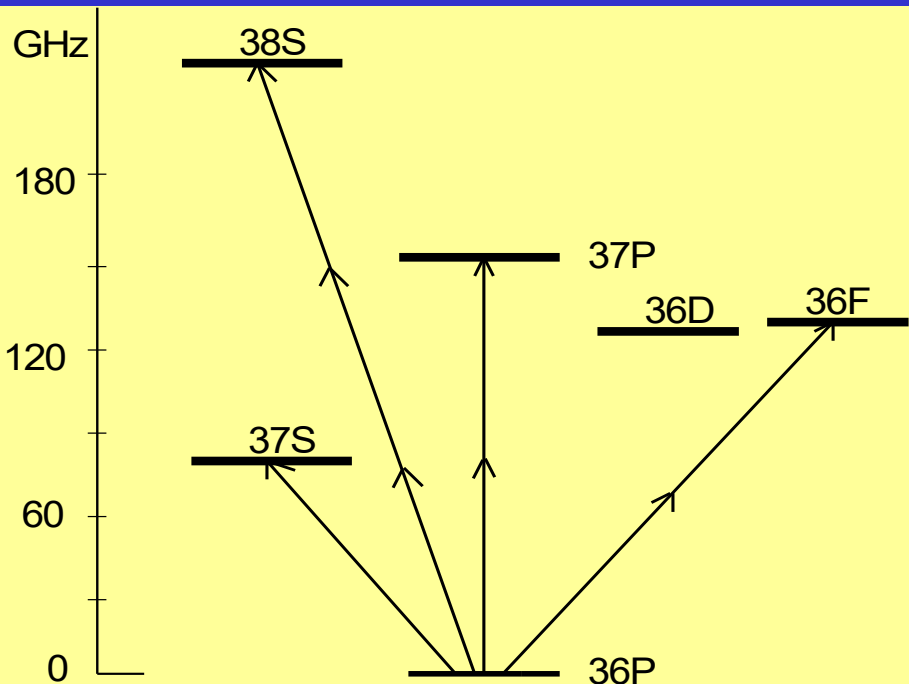
Experiments with Na atomic beam



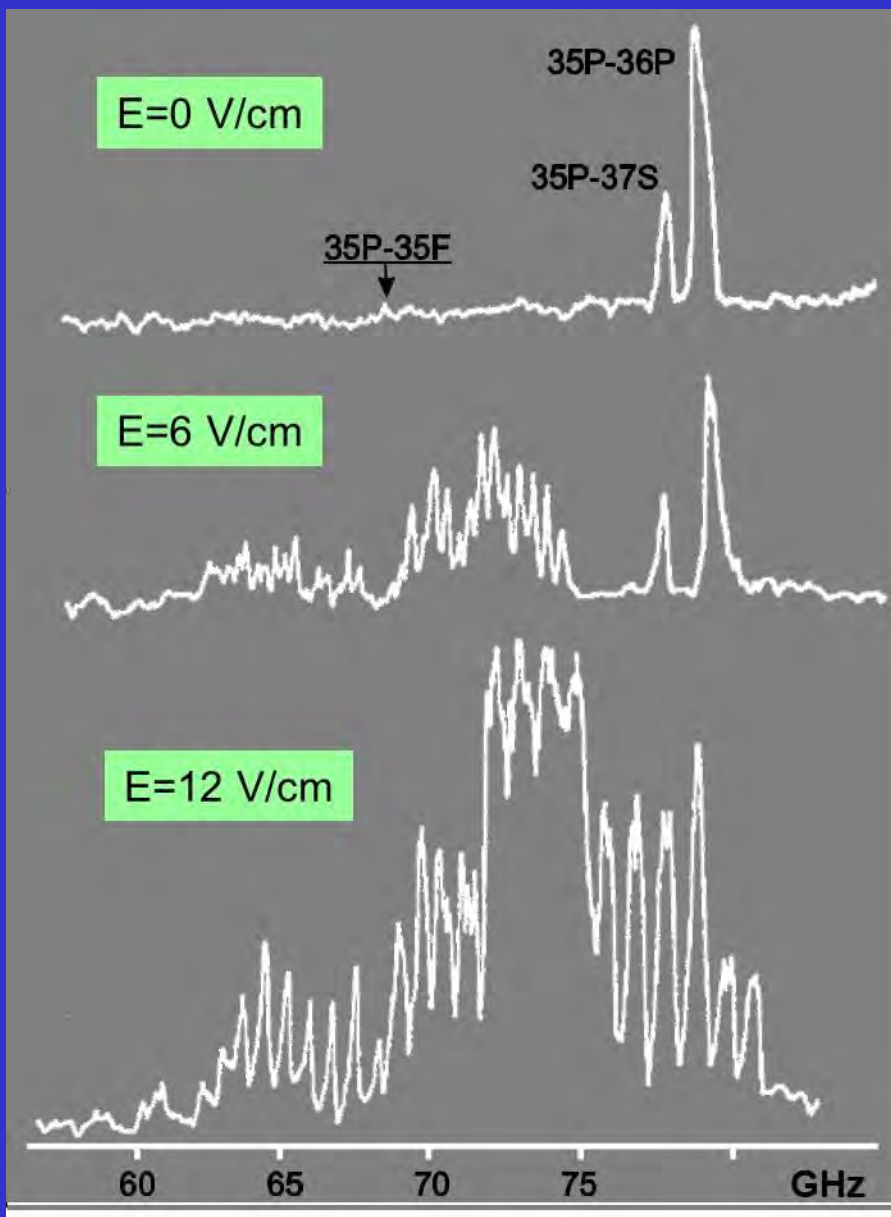
Three-photon laser excitation spectrum of nP Rydberg states in Na atoms



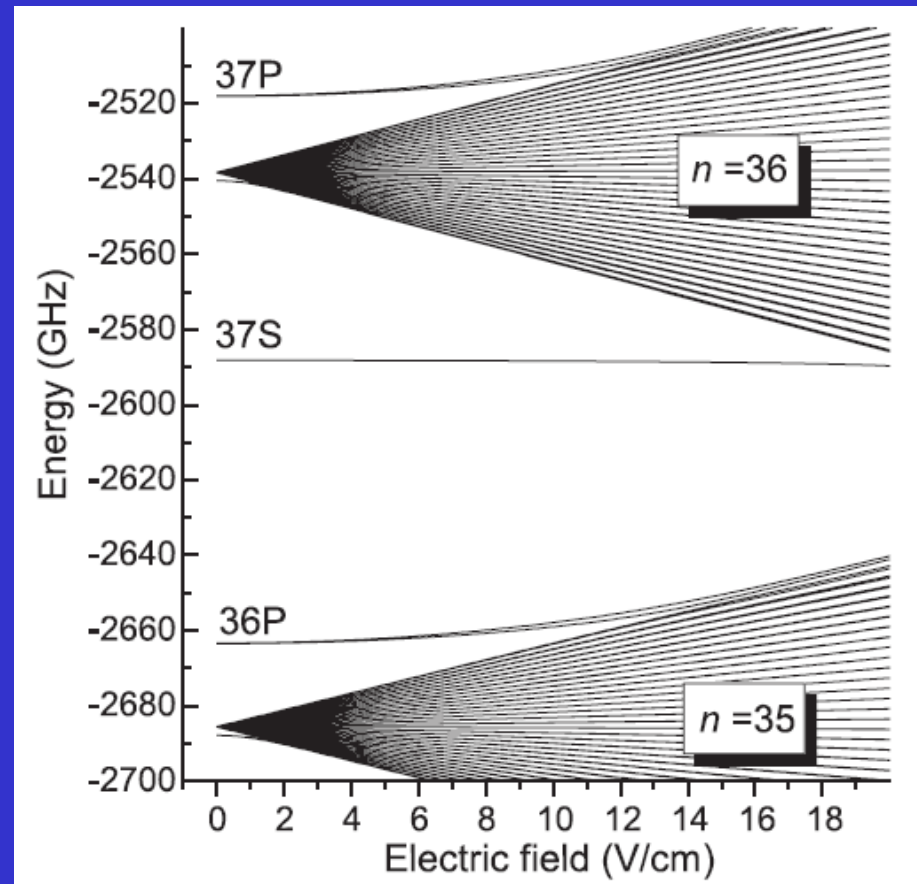
Multiphoton microwave transitions from the 36P state



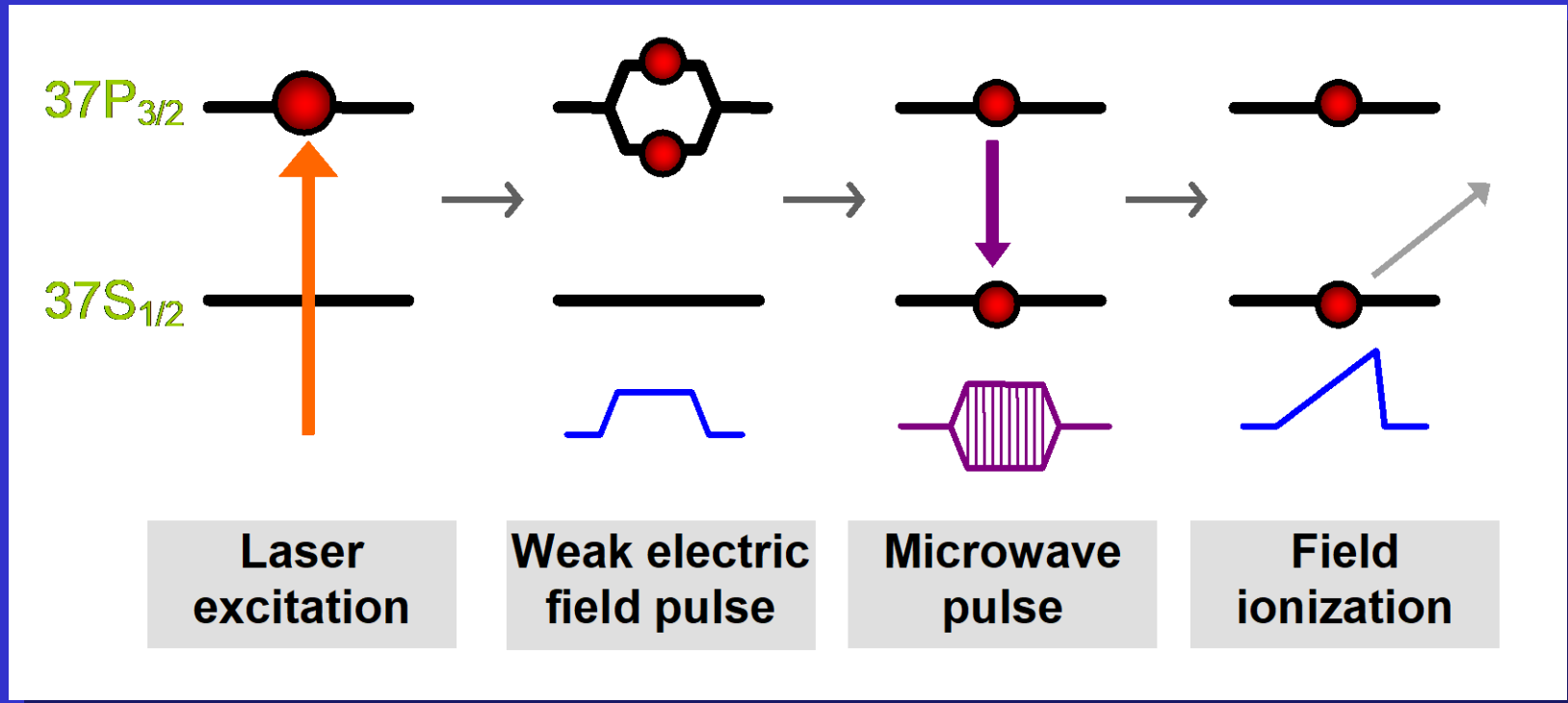
dc Stark effect on microwave transitions from 35P state



Stark map of Na Rydberg states



Quantum interferometry of degenerate Rydberg states



Phase shift from the electric-field pulse

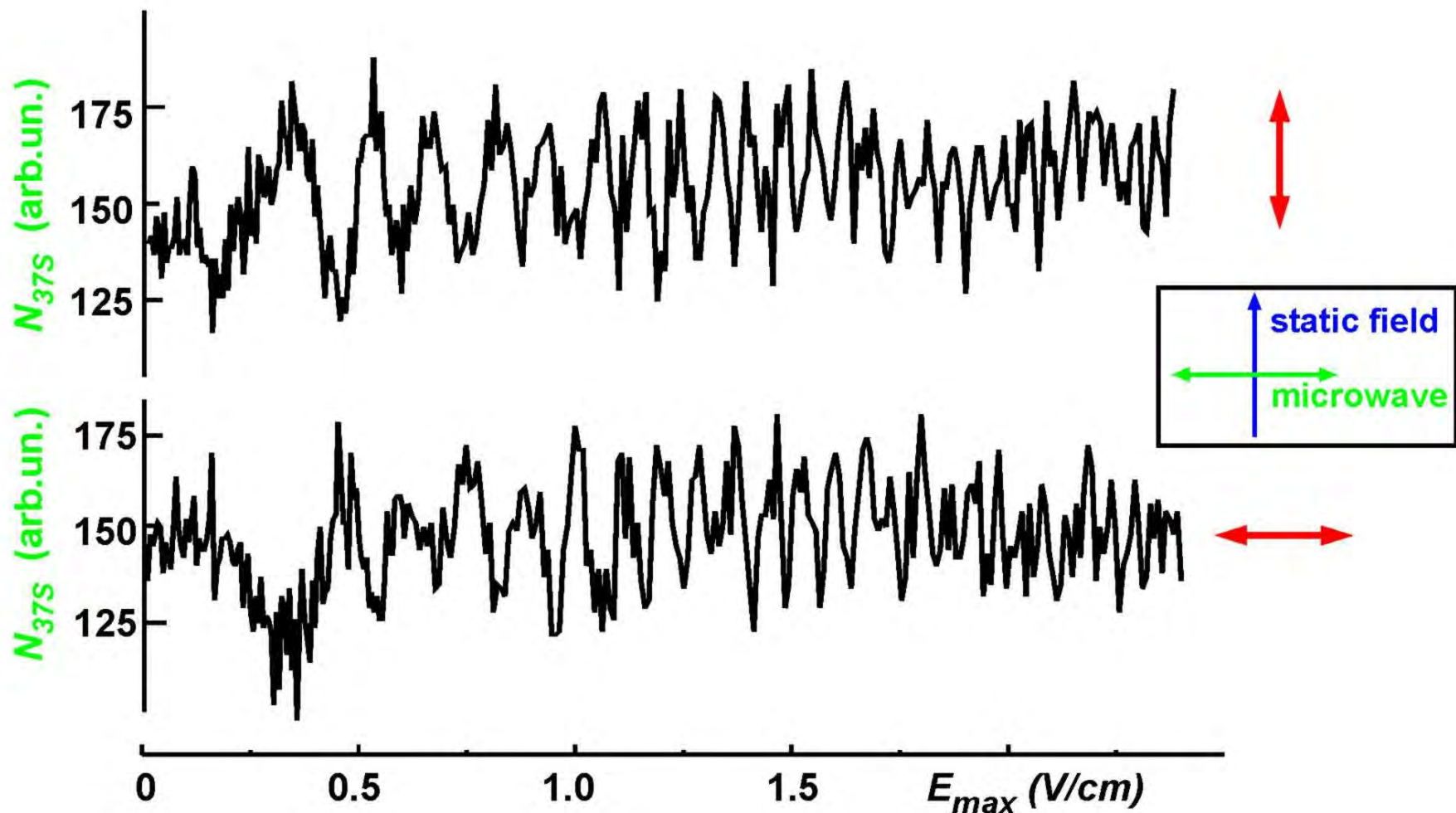
$$\varphi = 2\pi\alpha_2 \int_0^{\infty} E^2(t) dt$$

Population of the final state

$$N(37S) \sim 5 + 3 \cos \varphi$$

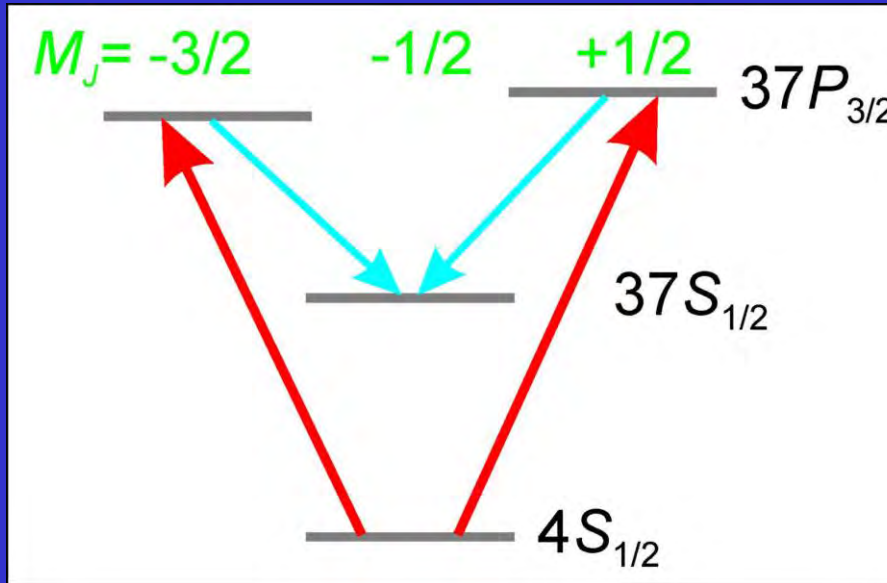
I.I.Ryabtsev and I.M.Beterov, Phys. Rev. A **61**, 063414 (2000)

Quantum interferometry of degenerate Rydberg states



I.I.Ryabtsev and I.M.Beterov, Phys. Rev. A 61, 063414 (2000)

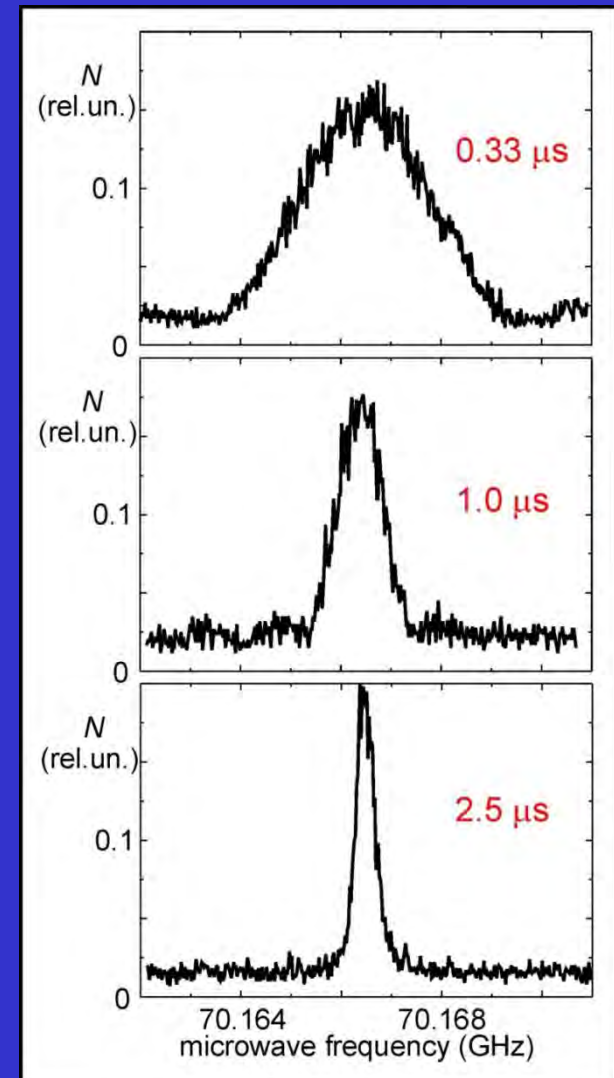
Microwave Hanle effect for degenerate Rydberg states



Population of the final state

$$N(37S) \sim 5 + 3 \cos\left(\frac{8}{3} \frac{\mu_B B}{\hbar} t_0\right)$$

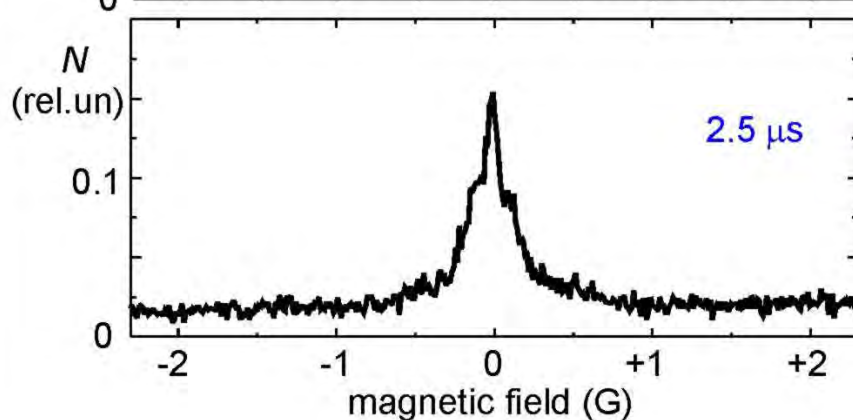
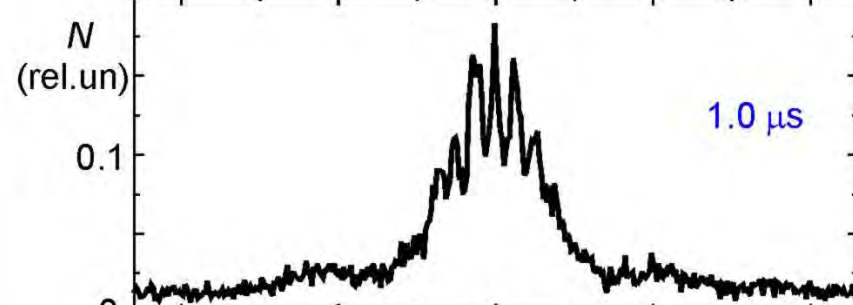
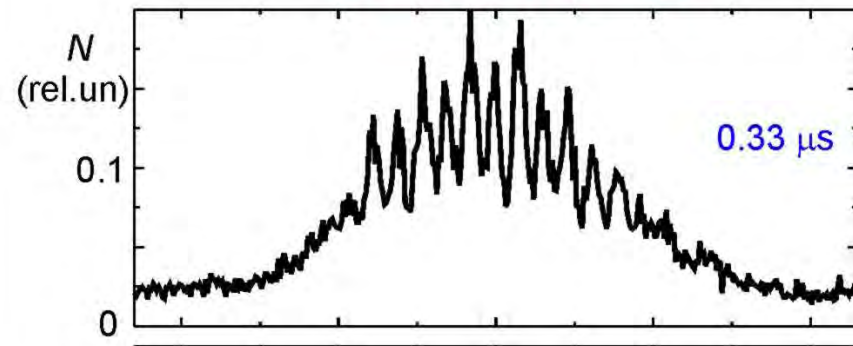
Spectra without magnetic field



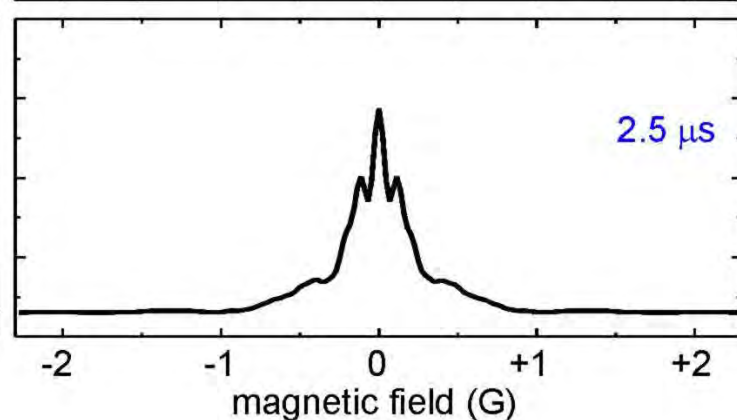
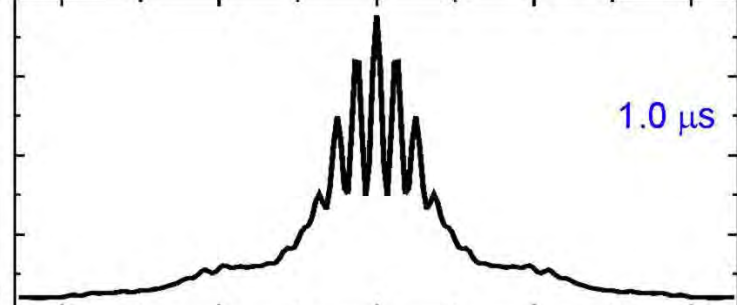
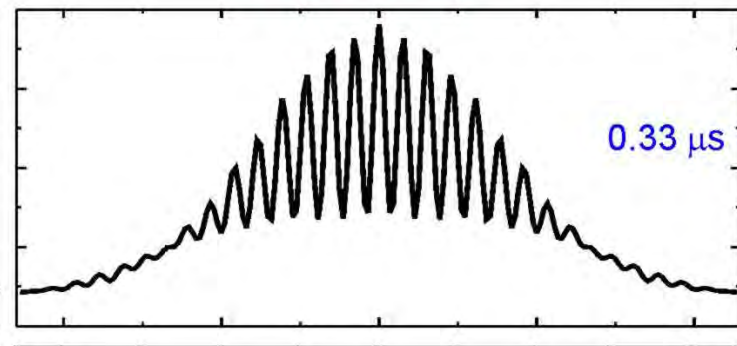
I.I.Ryabtsev and D.B.Tretyakov,
Phys. Rev. A **64**, 033413 (2001)

Microwave Hanle effect

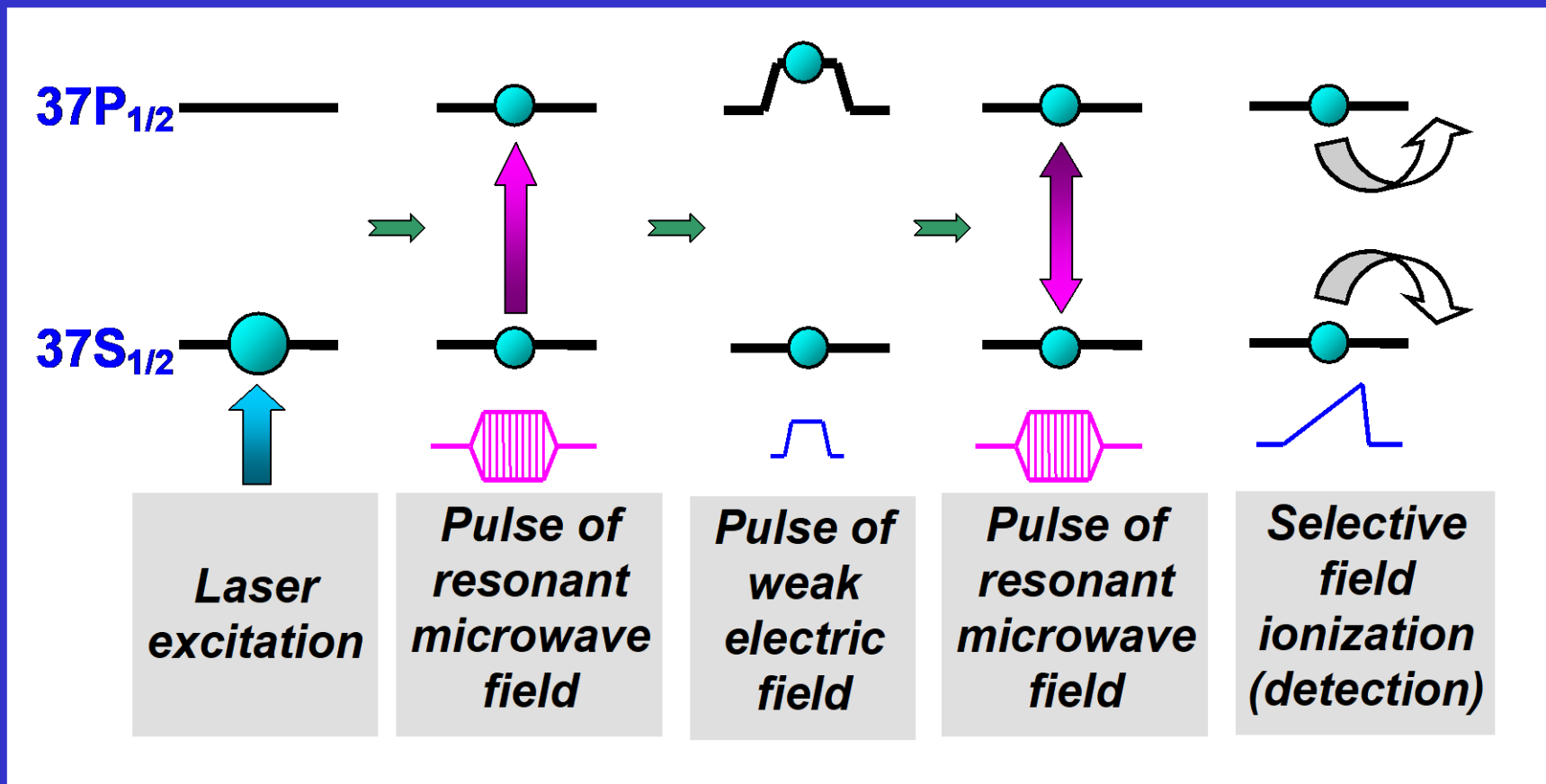
EXPERIMENT



THEORY



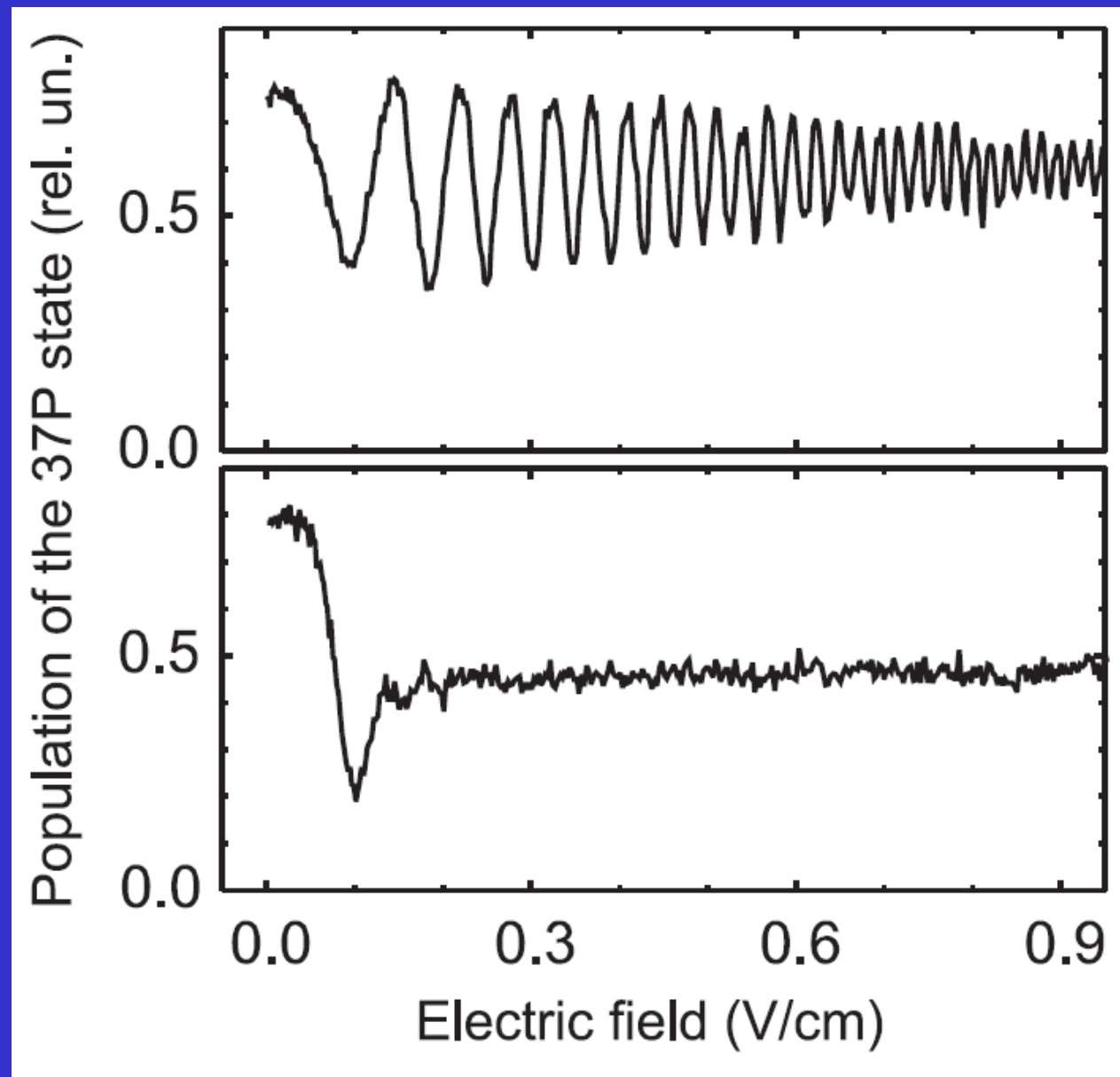
Stark-switched interferometer for non-degenerate states



*Phase shift from
the electric-field
pulse*

$$\varphi = \pi \int_{-\infty}^{+\infty} (\alpha_P - \alpha_S) E(t)^2 dt = \pi(\alpha_P - \alpha_S) E_{\max}^2 \tau_{\text{eff}}$$

Stark-switched Ramsey interferometer



Two
interactions

One
interaction

Decoherence of Rydberg states

Photoionization

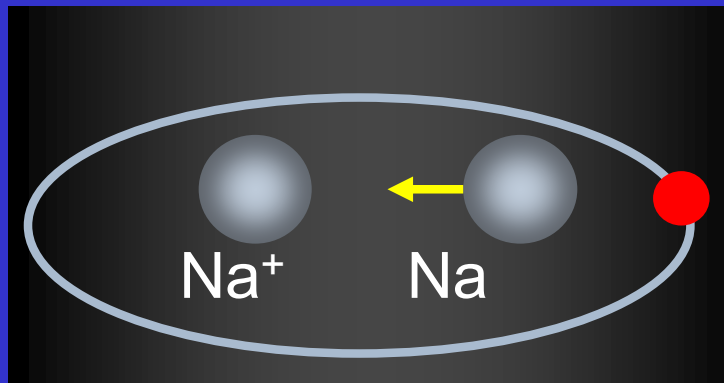
Opt. Sectr. 1989, v.66, p.36

JETP Lett. 1992, v.55, p.431

Opt. Spectr. 1993, v.75, p.531

Opt Spectr. 1996, v.81, p.383

Collisional ionization

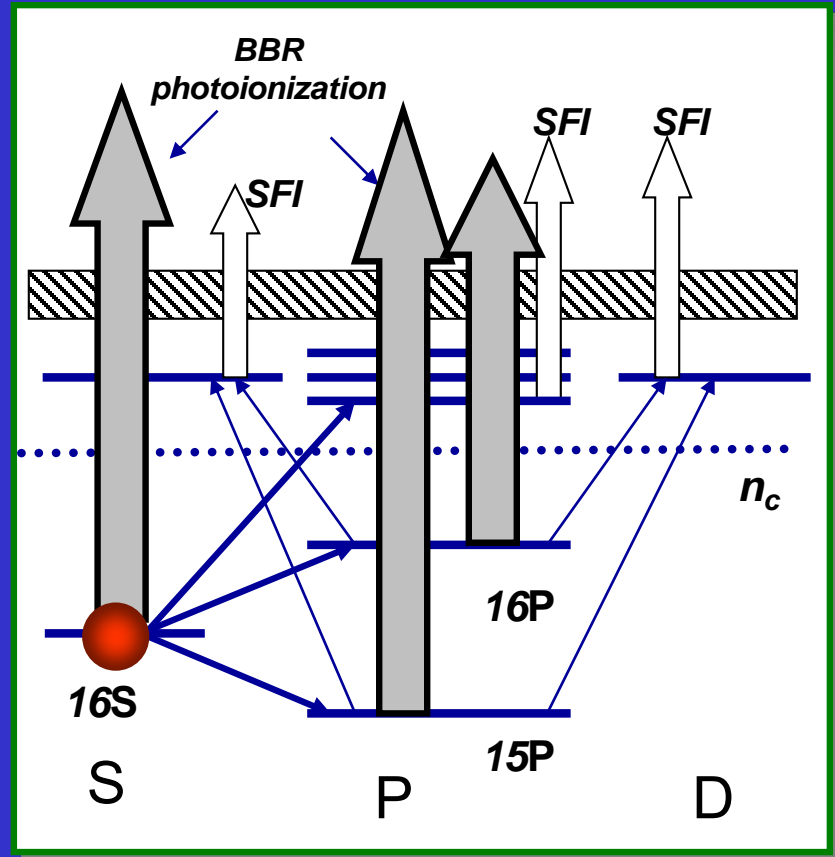


J. Phys. B 2005, v.38, p.S17

J. Phys. B 2005, v.38, p.1811

J. Phys. B 2005, v.38, p.4349

Interaction with blackbody radiation



Phys. Rev. A 2007, v.75, p.052720

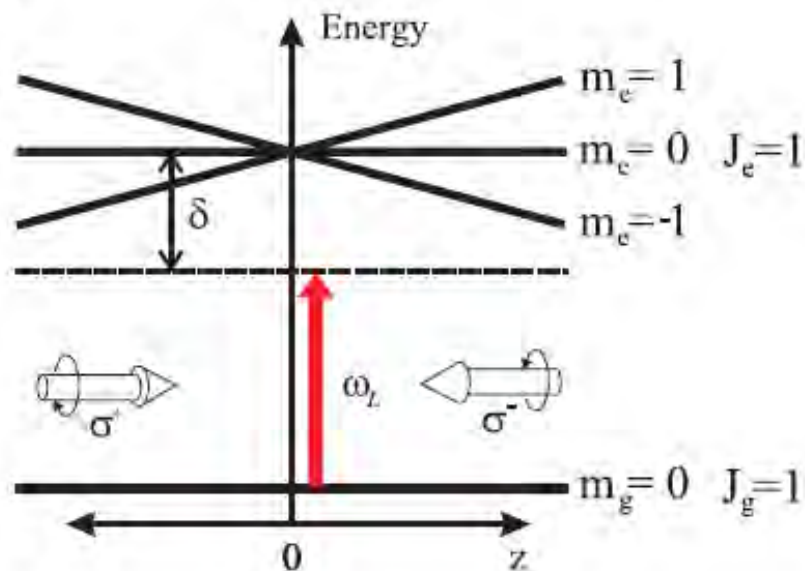
JETP 2008, v.107, p.20

New J. Phys. 2009, v.11, p.013052

Phys. Rev. A 2009, v.79, p.052504

Magneto-optical trap

a.



b.

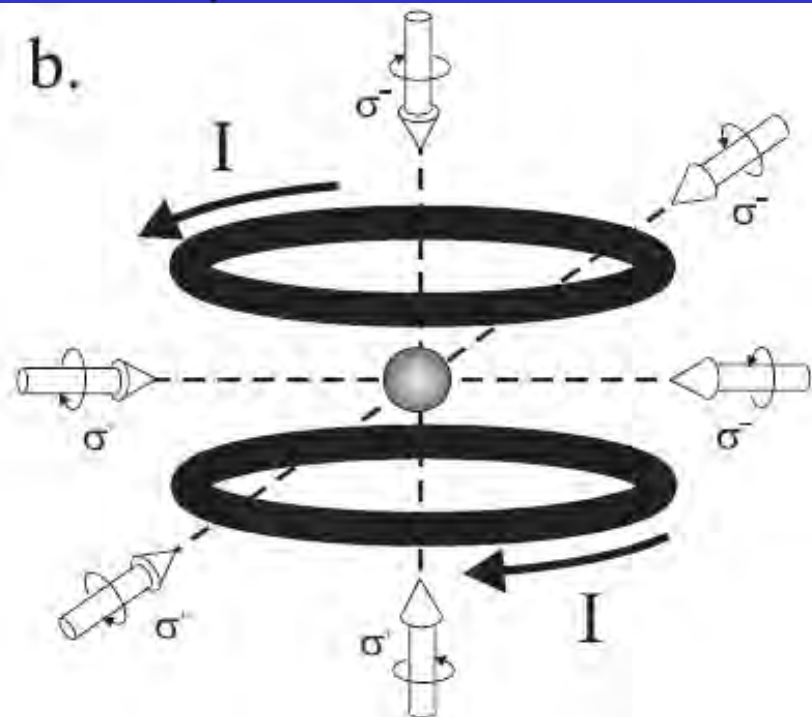


Схема переходов

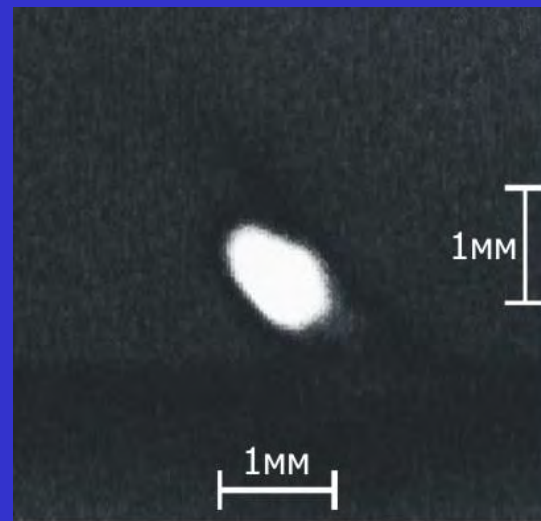
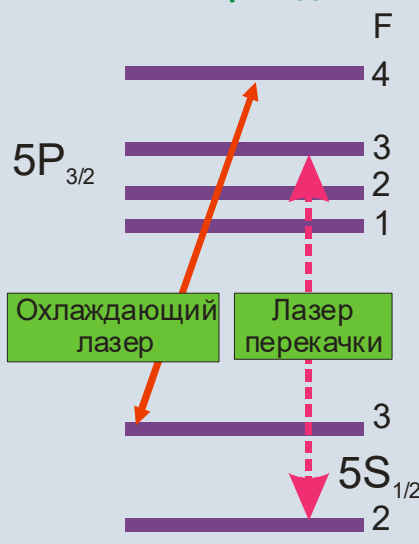
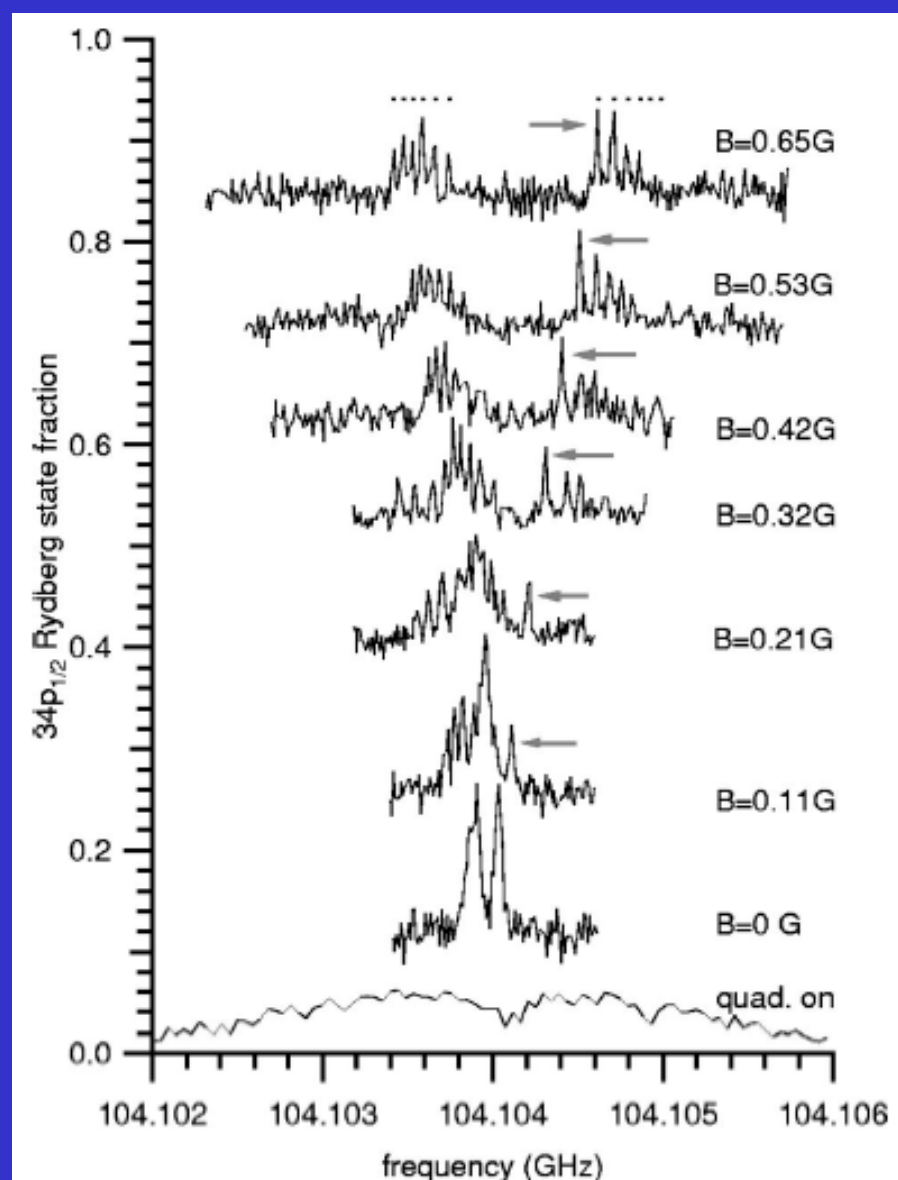
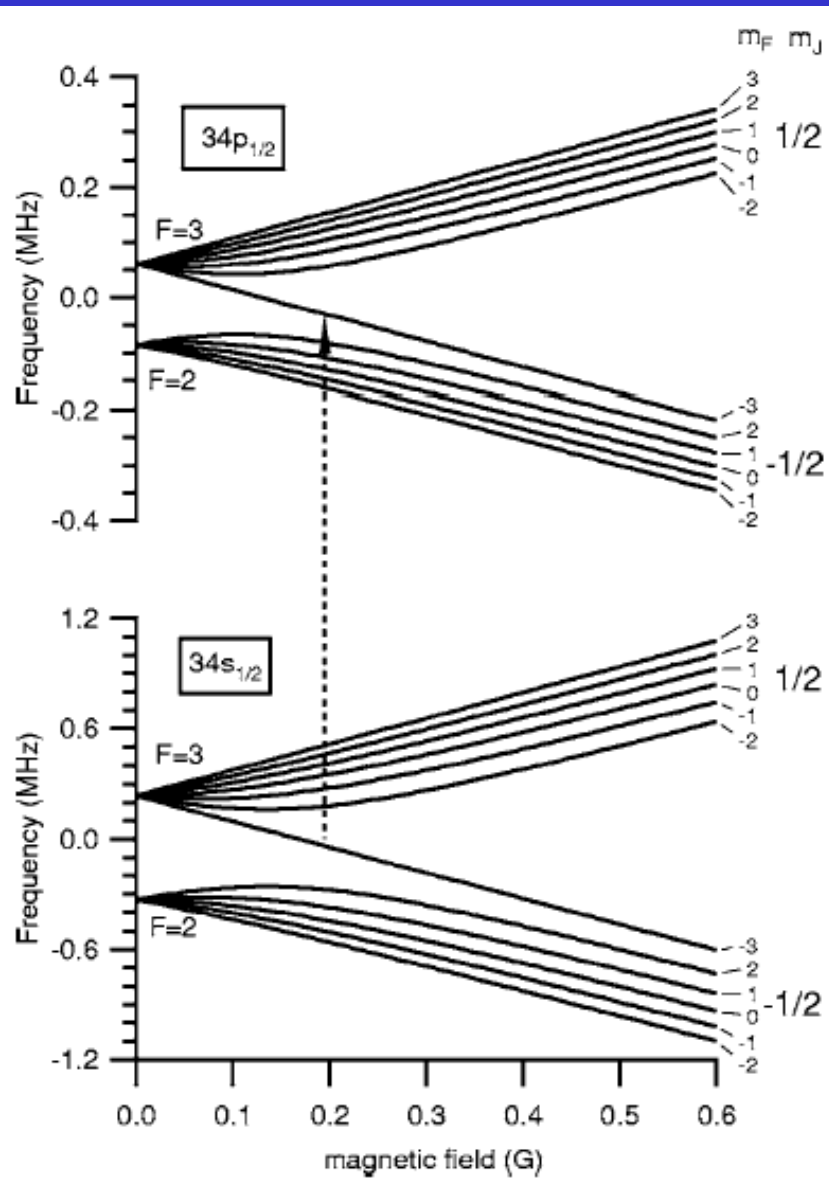
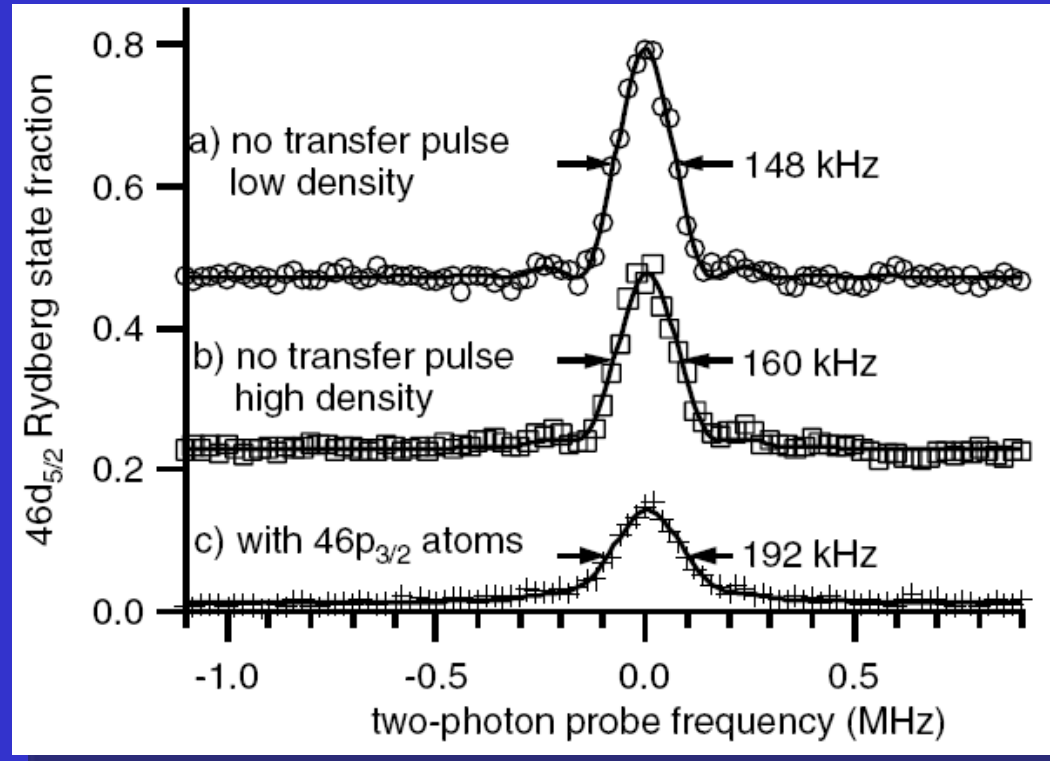


Image of a cloud
of cold Rb atoms
obtained with a
CCD camera

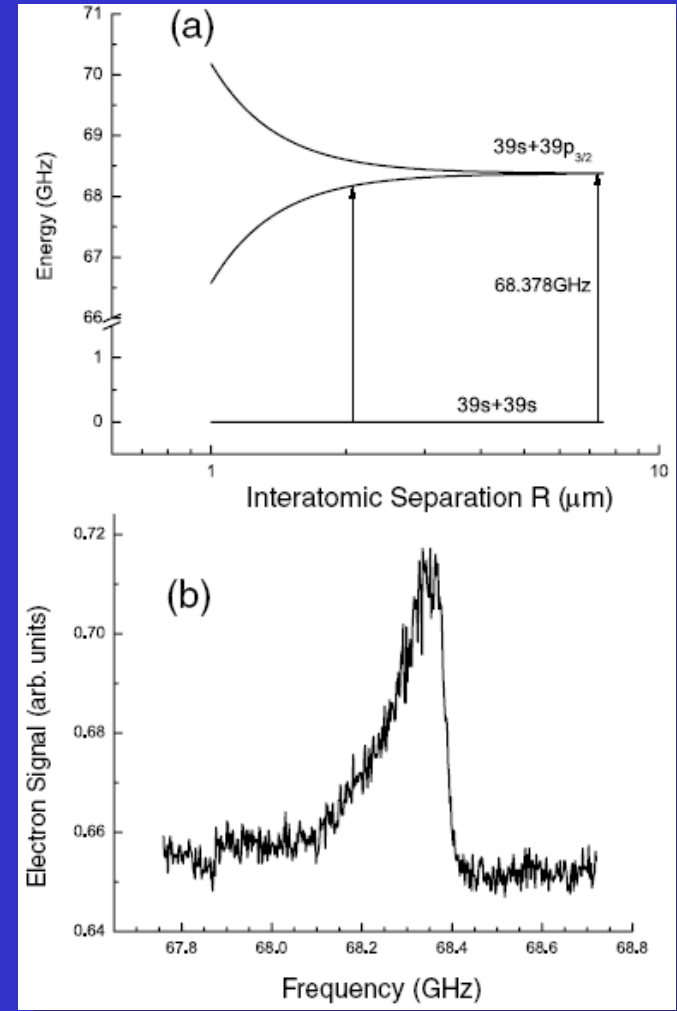
Spectroscopy of microwave transitions



Microwave spectroscopy of long-range interactions

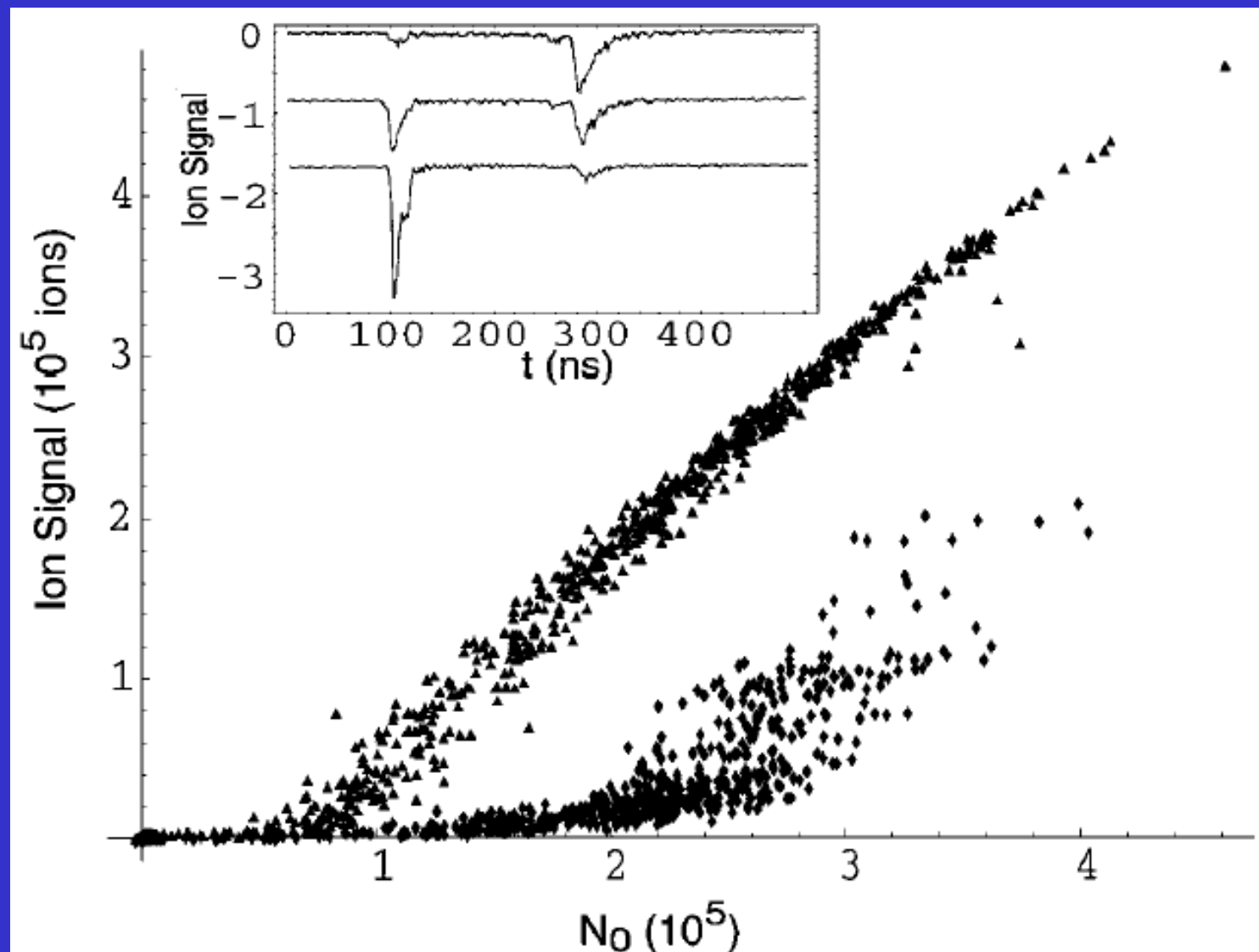


K. Afrousheh et al.
PRL 93 (2004) 233001

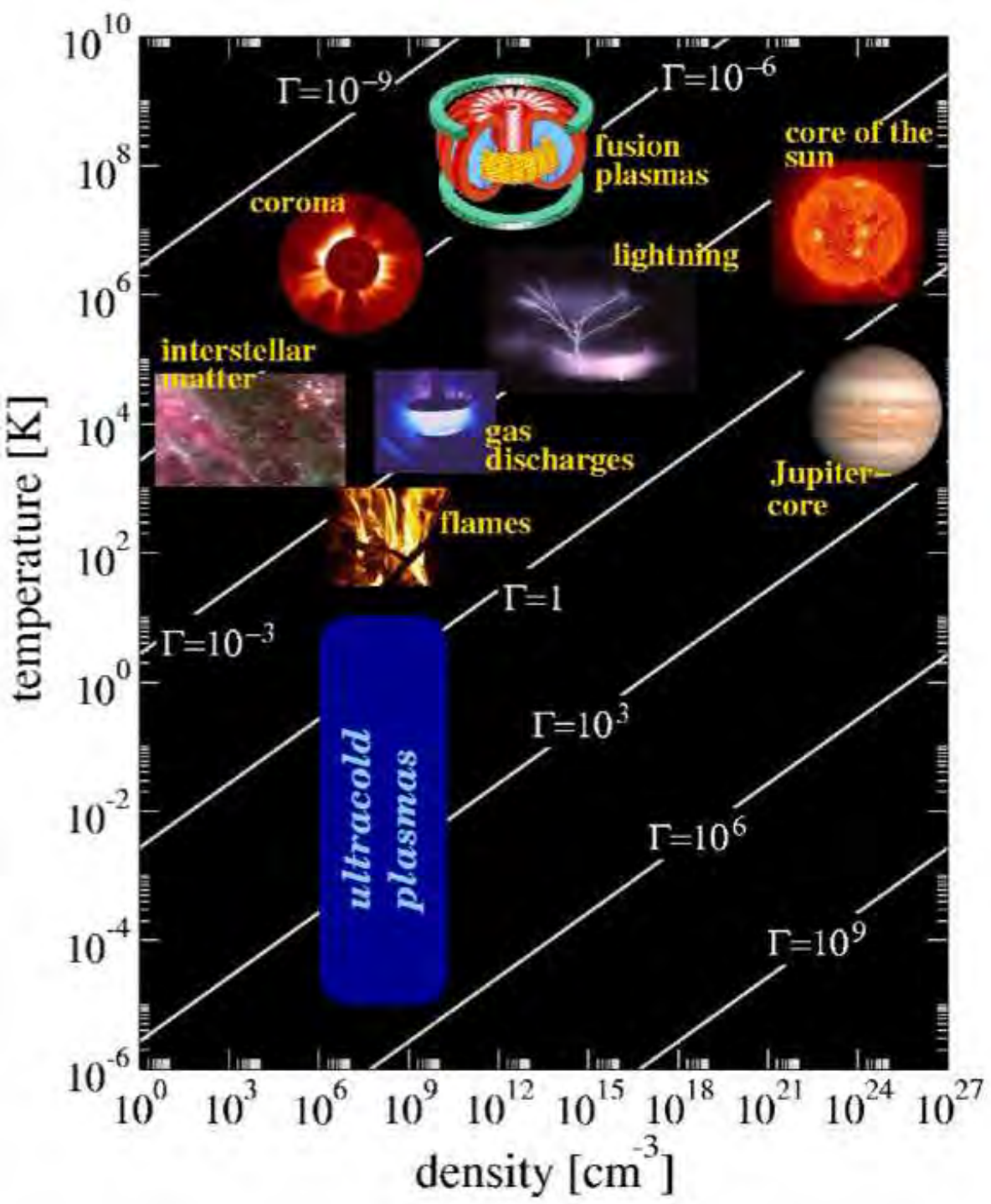


W. Li et al. PRL 94 (2005) 173001

Ultracold plasma formation



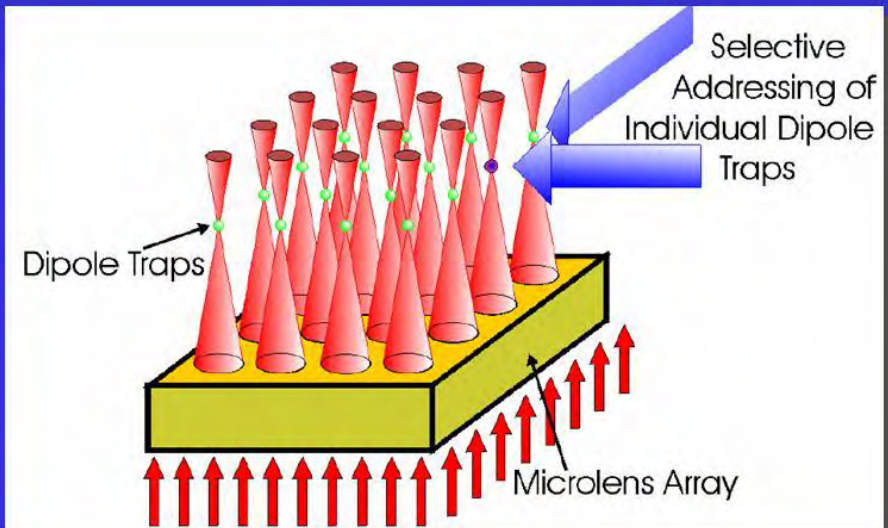
M. Robinson et al. PRL 85 (2000) 4466



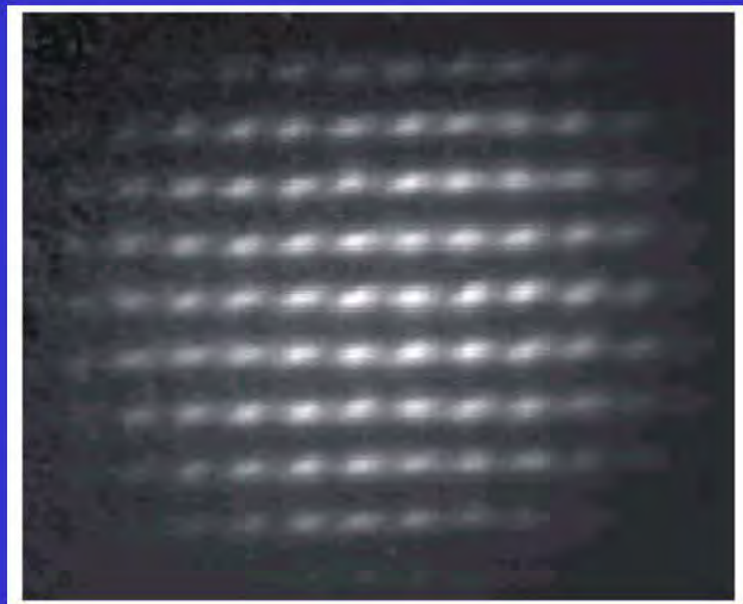
$$\Gamma = e^2 / [4\pi\varepsilon_0 a k_B T]$$

$\Gamma > 1$
**strongly
coupled
plasma**

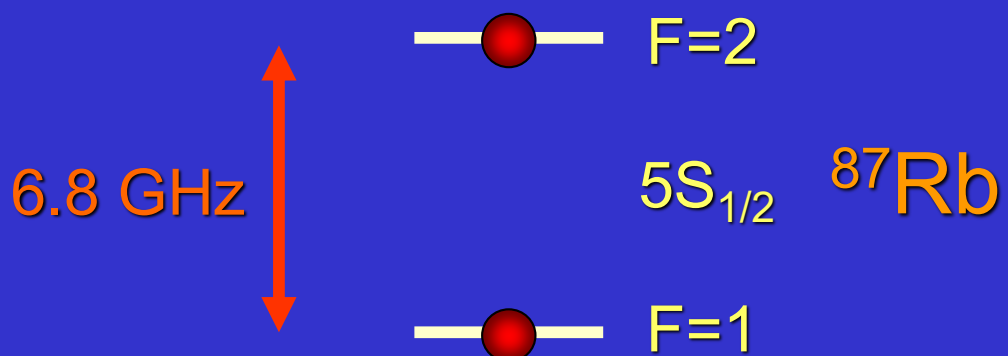
Qubits of a quantum computer – single trapped neutral atoms in optical trap arrays



R. Dumke et al.
PRL 89 (2002) 097903

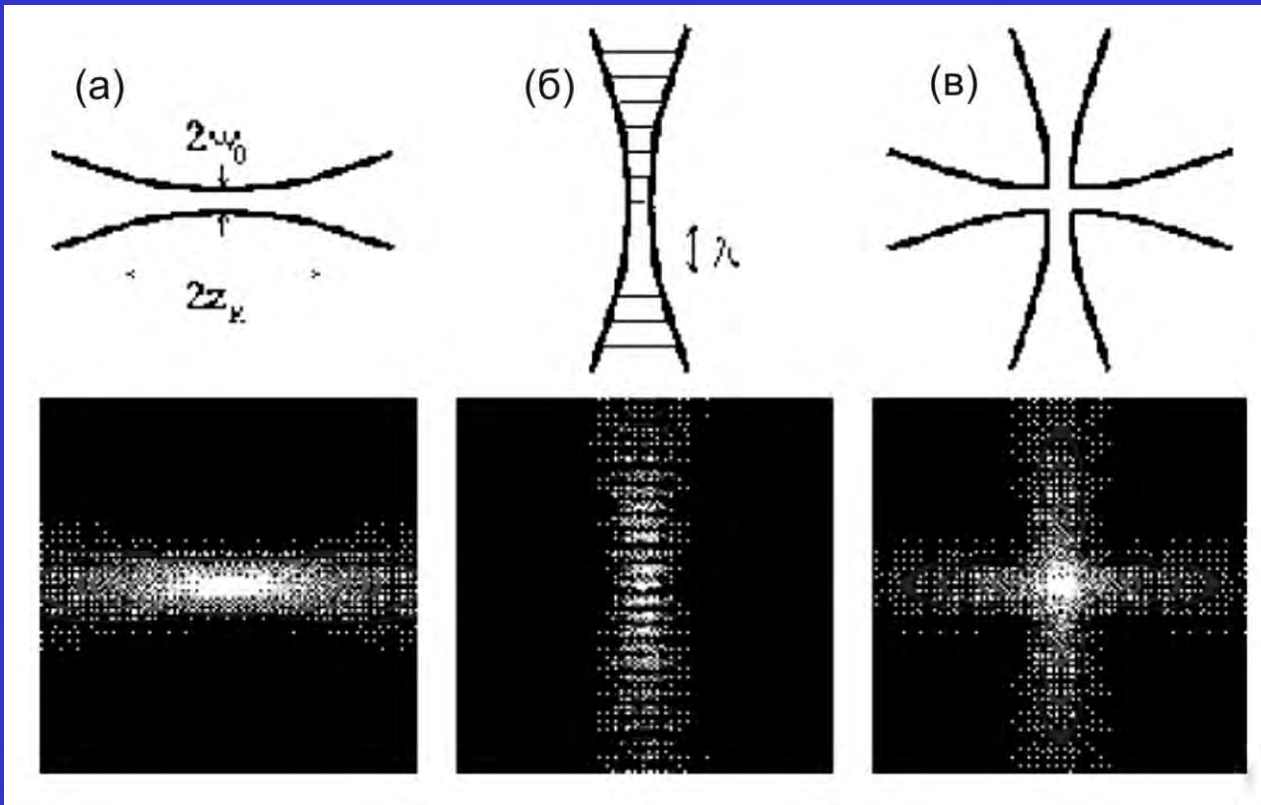


Qubit levels – two hyperfine sublevels of the ground state



Satisfy the DiVincenzo's criteria for qubits of a quantum computer

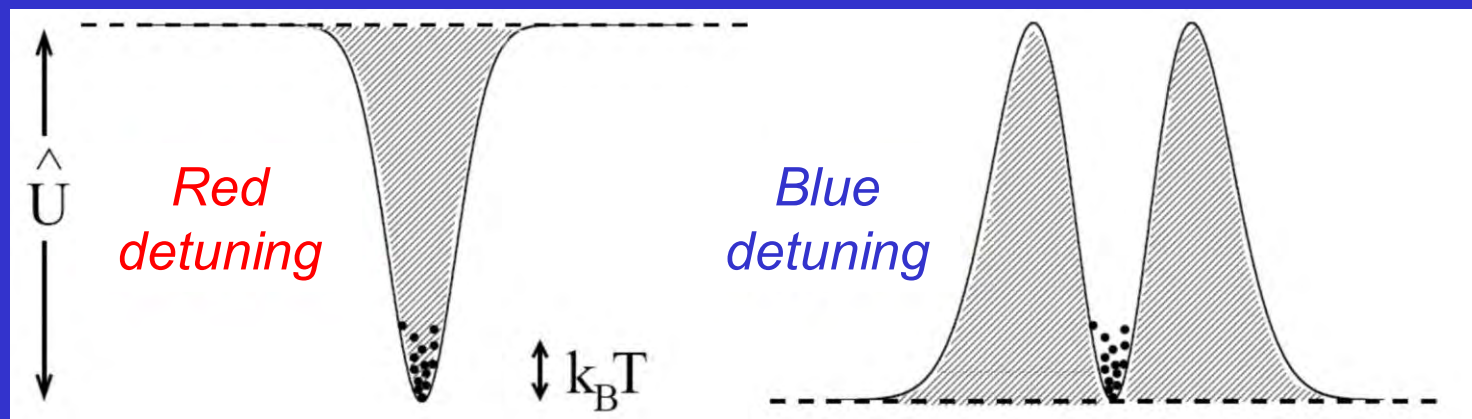
Optical dipole traps and lattices



*Atom potential
in the laser field:*

$$U_{dip}(\mathbf{r}) = \pm \frac{3\pi c^2}{2\omega_0^3} \left(\frac{\Gamma}{\Delta} \right) I(\mathbf{r})$$

*Atoms are trapped
in the maxima or
minima of tightly
focused laser field
or standing light
wave, and can be
readily scaled to
large arrays.*



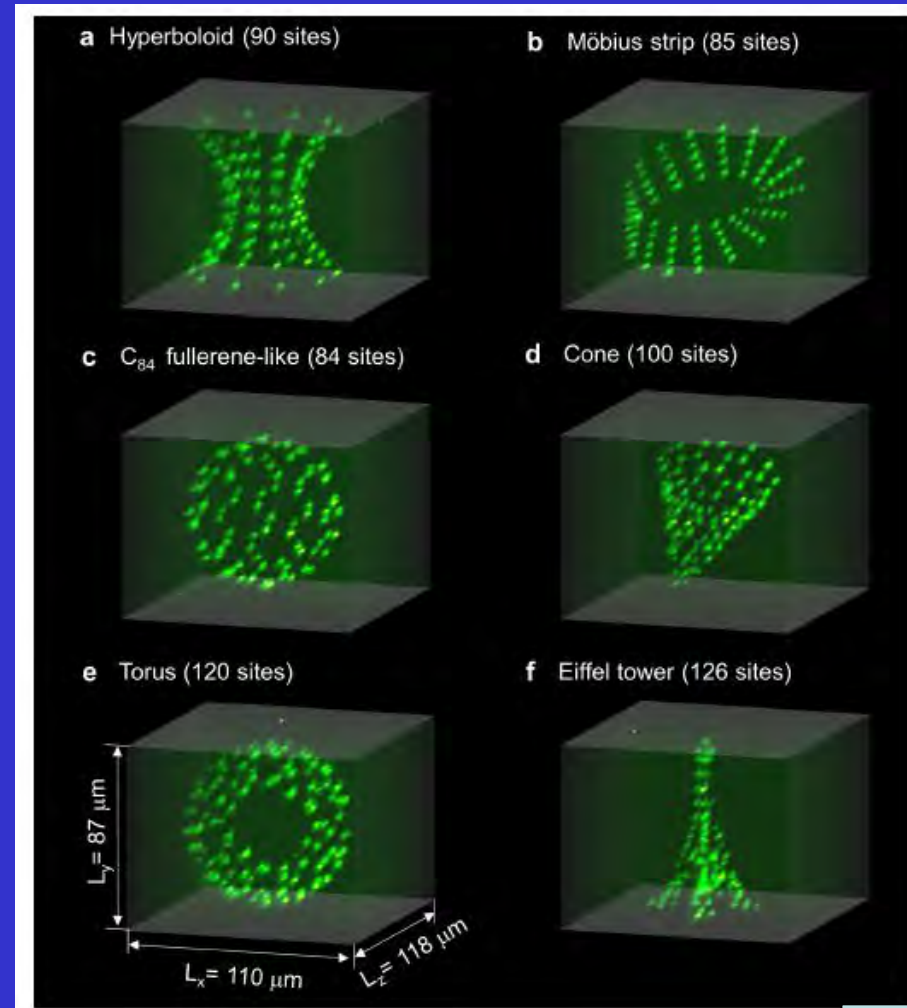
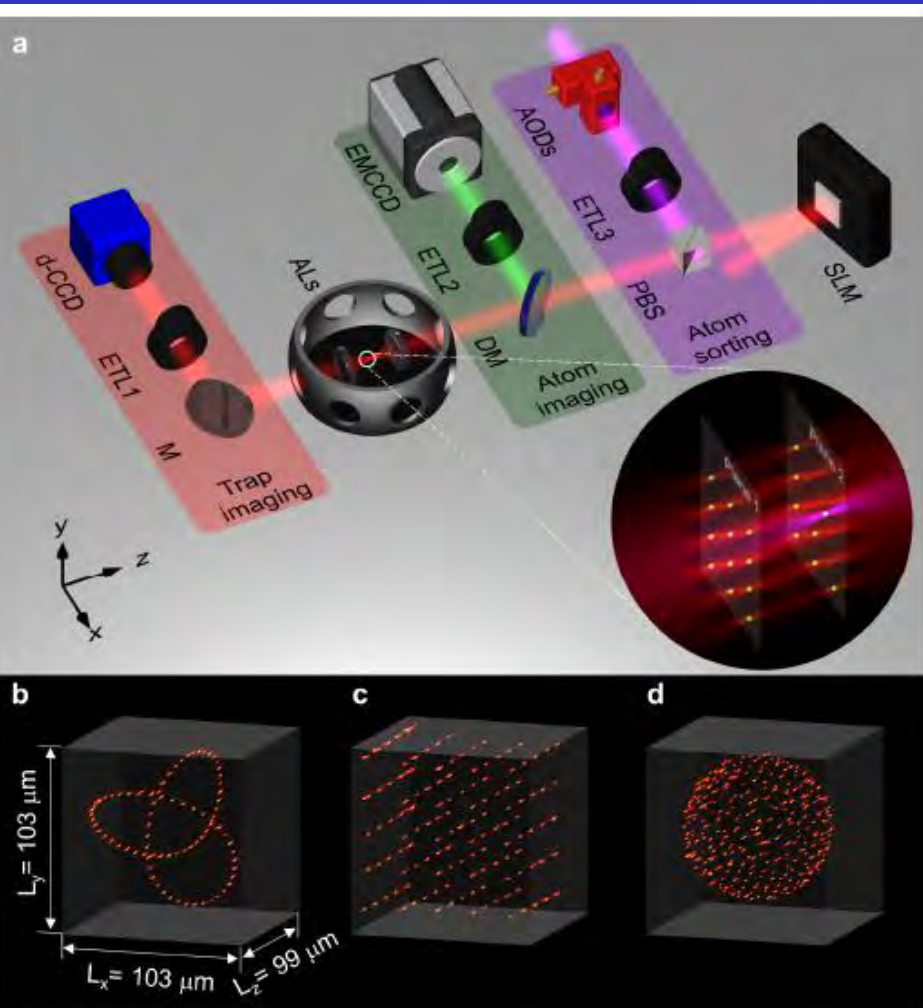
Synthetic three-dimensional atomic structures assembled atom by atom

Daniel Barredo*, Vincent Lienhard*, Sylvain de Léséleuc*, Thierry Lahaye, and Antoine Browaeys

Laboratoire Charles Fabry, Institut d'Optique Graduate School, CNRS,

Université Paris-Saclay, F-91127 Palaiseau Cedex, France

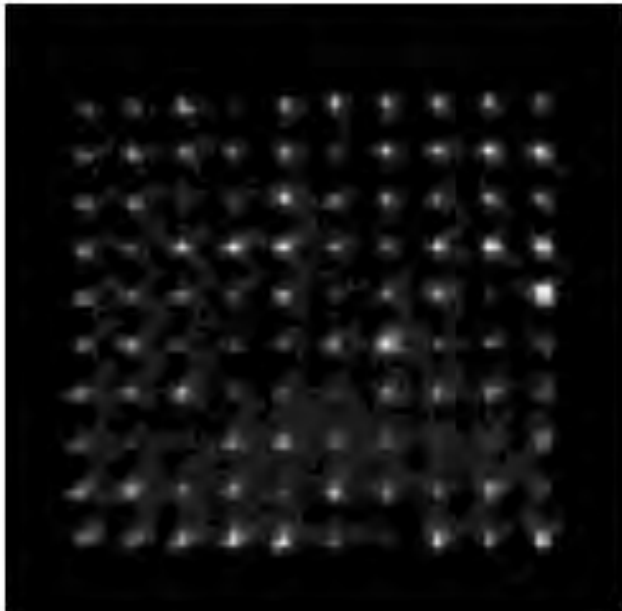
(Dated: December 8, 2017)



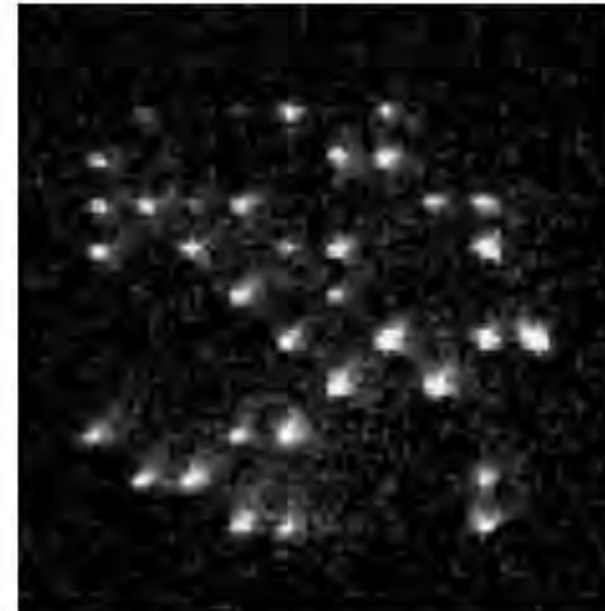
Experiments of Moscow State University on trapping Rb Atoms in large trap arrays

Fluorescence image of single Rb atoms
in a 10x10 trap array

Averaging over 100 shots



Single-shot image



Universal quantum gates

$$\begin{pmatrix} \cos\theta & i\sin\theta \\ i\sin\theta & \cos\theta \end{pmatrix}$$

One-qubit rotation

$$\begin{pmatrix} 1 & 0 & 0 & 0 \\ 0 & 1 & 0 & 0 \\ 0 & 0 & \cos\theta & i\sin\theta \\ 0 & 0 & i\sin\theta & \cos\theta \end{pmatrix}$$

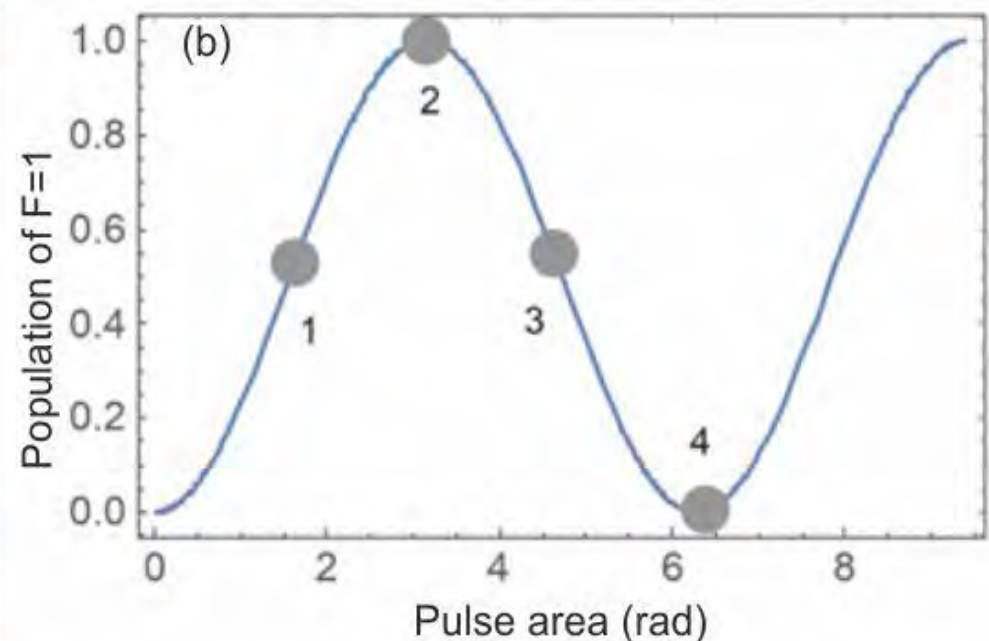
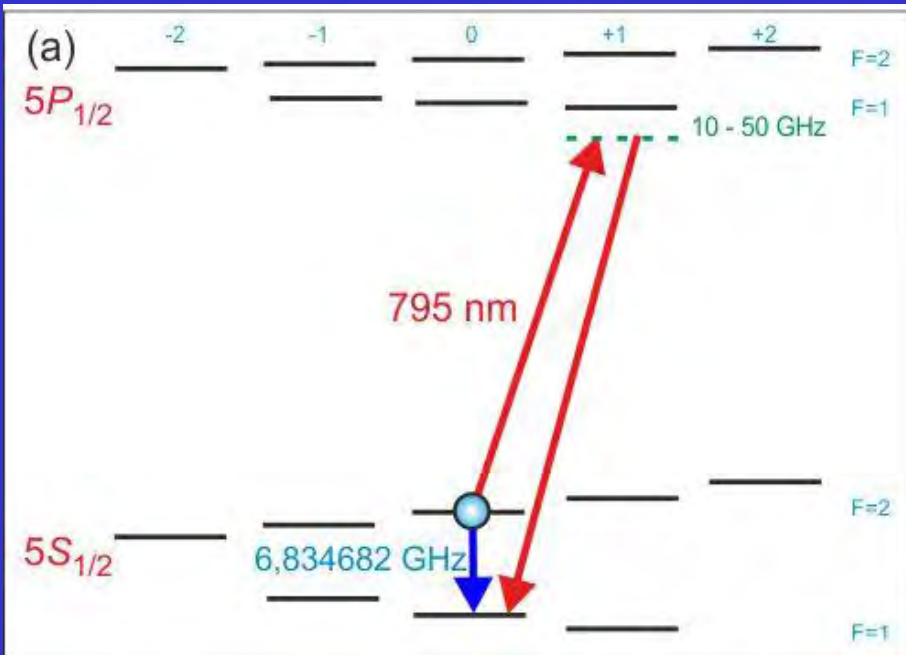
Two-qubit
quantum
phase gate

Conditional quantum phase gate $|a b\rangle \rightarrow \exp(i \theta \delta_{a1} \delta_{b1}) |a b\rangle$

One-qubit gate: a rotation by arbitrary angle

$\uparrow \uparrow \uparrow \uparrow \uparrow \downarrow \uparrow \uparrow \uparrow \uparrow \uparrow$ NOT

Raman or microwave transition between qubit levels

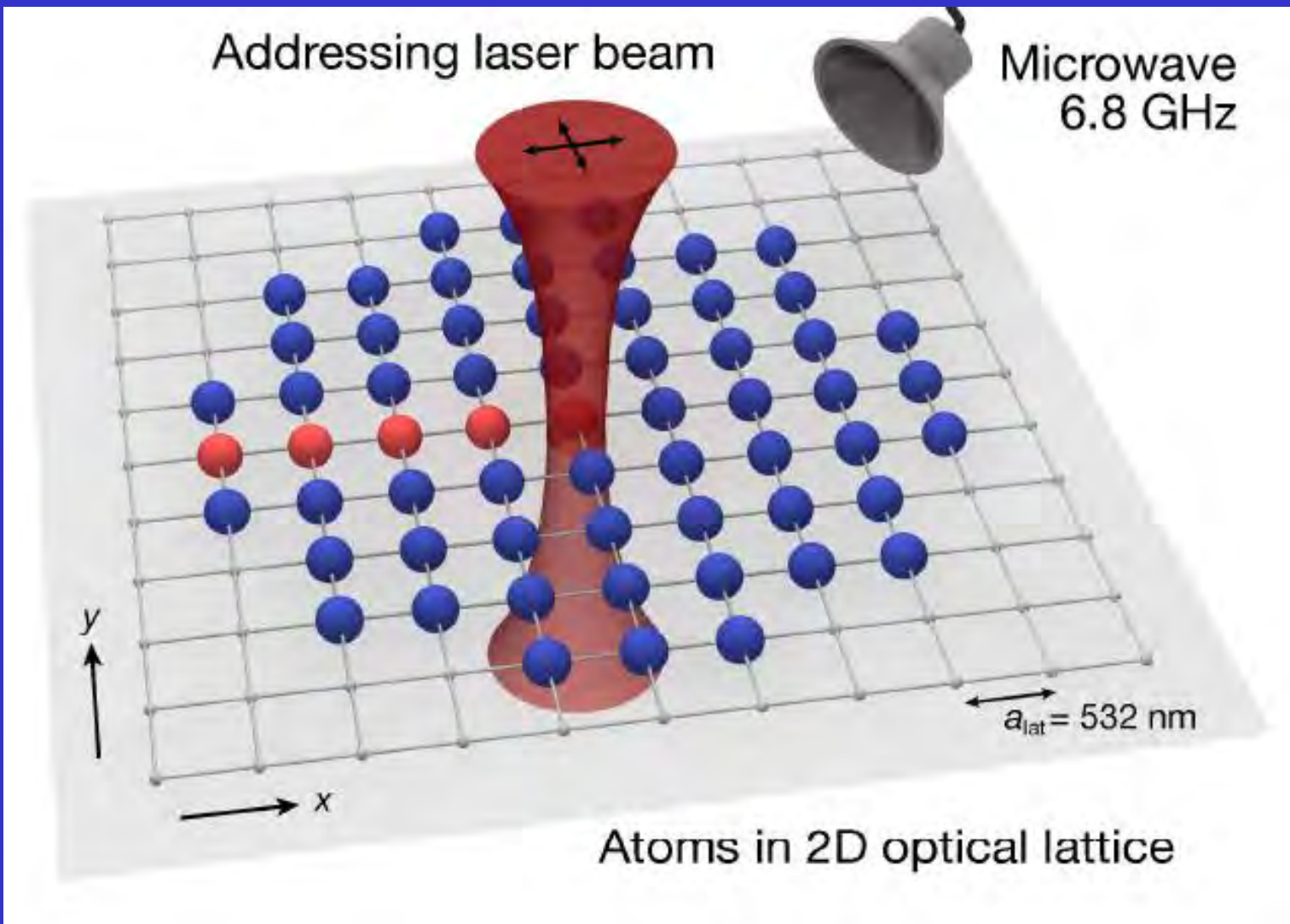


Rabi population oscillations at various phases correspond to various one-qubit gates.

Single-spin addressing in an atomic Mott insulator

17 MARCH 2011 | VOL 471 | NATURE | 319

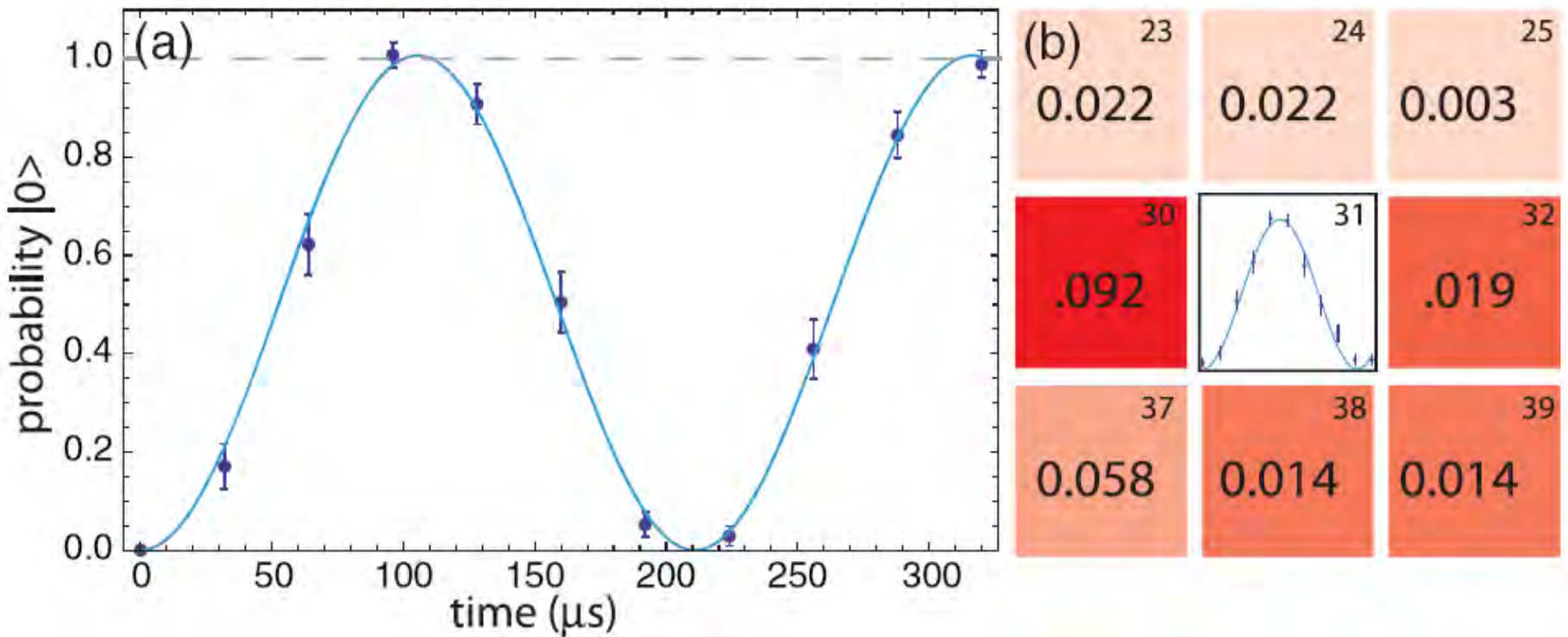
Christof Weitenberg¹, Manuel Endres¹, Jacob F. Sherson^{1†}, Marc Cheneau¹, Peter Schauß¹, Takeshi Fukuhara¹, Immanuel Bloch^{1,2}
& Stefan Kuhr¹





Randomized Benchmarking of Single-Qubit Gates in a 2D Array of Neutral-Atom Qubits

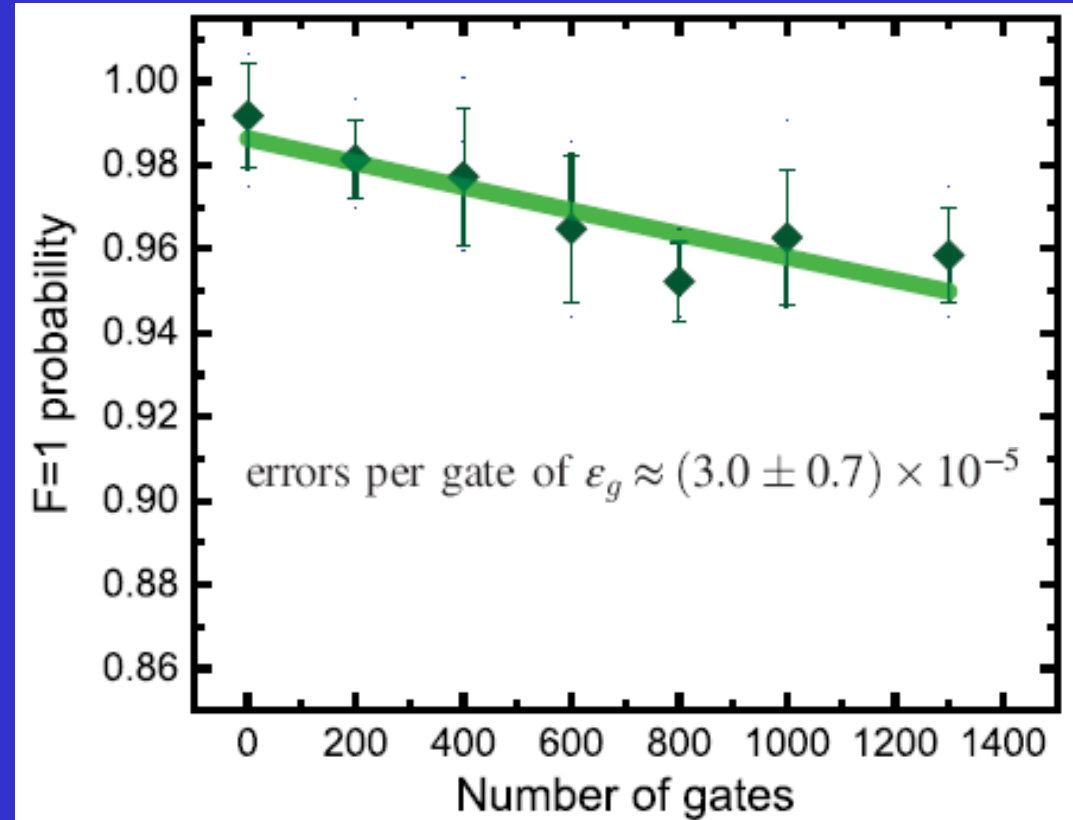
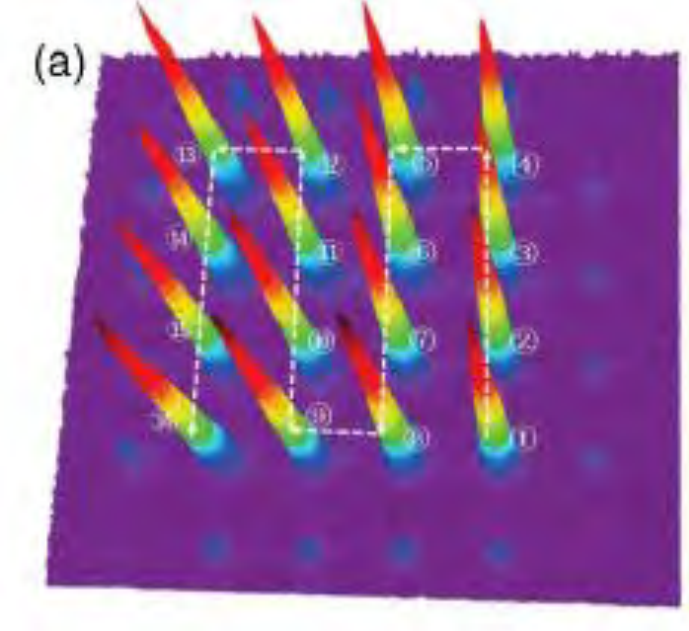
T. Xia, M. Lichtman, K. Maller, A. W. Carr, M. J. Piotrowicz, L. Isenhower, and M. Saffman



Addressing single Cs atoms by focused beam at 459 nm, producing the light shift of 33 kHz. For one trap the average one-qubit fidelity is $F = 0.9923$, and the crosstalk is 1-5%. The main error sources are finite atom temperature (5-10 μK), magnetic field noise and repumping at blowing-away.

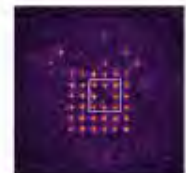
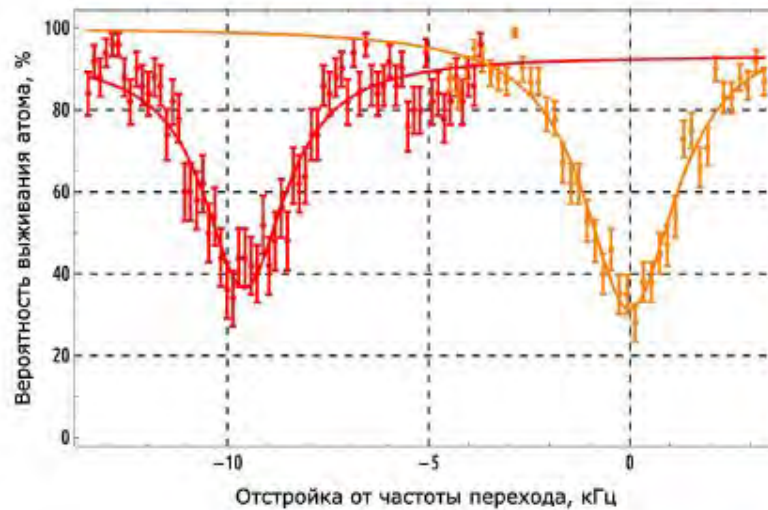
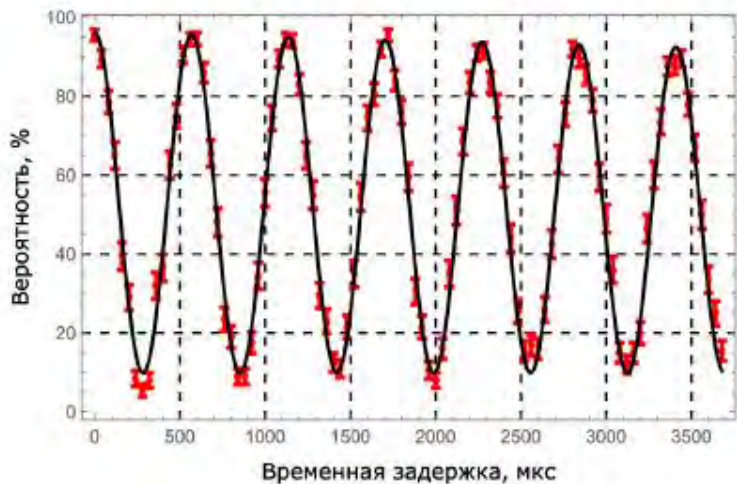
High-Fidelity Single-Qubit Gates on Neutral Atoms in a Two-Dimensional Magic-Intensity Optical Dipole Trap Array

Cheng Sheng,^{1,2,3} Xiaodong He,^{1,3,*} Peng Xu,^{1,3} Ruijun Guo,^{1,2,3} Kunpeng Wang,^{1,2,3}
Zongyuan Xiong,^{1,3} Min Liu,^{1,3} Jin Wang,^{1,3} and Mingsheng Zhan^{1,3,†}



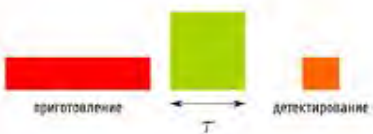
An array 4×4 of optical dipole traps for Rb atoms. The average error per gate for Clifford gate sequence is 3×10^{-5} due to compensation of DLS at circular laser polarization and active magnetic field stabilization below 1 mG.

Индивидуальная адресация

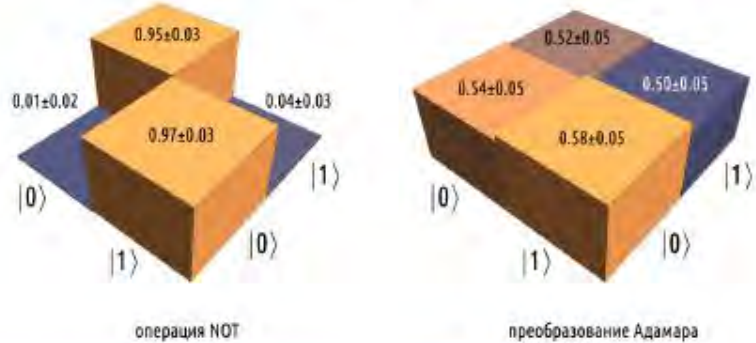


0.95	0.94	0.95
0.97	0.91	0.95
0.96	0.94	0.94

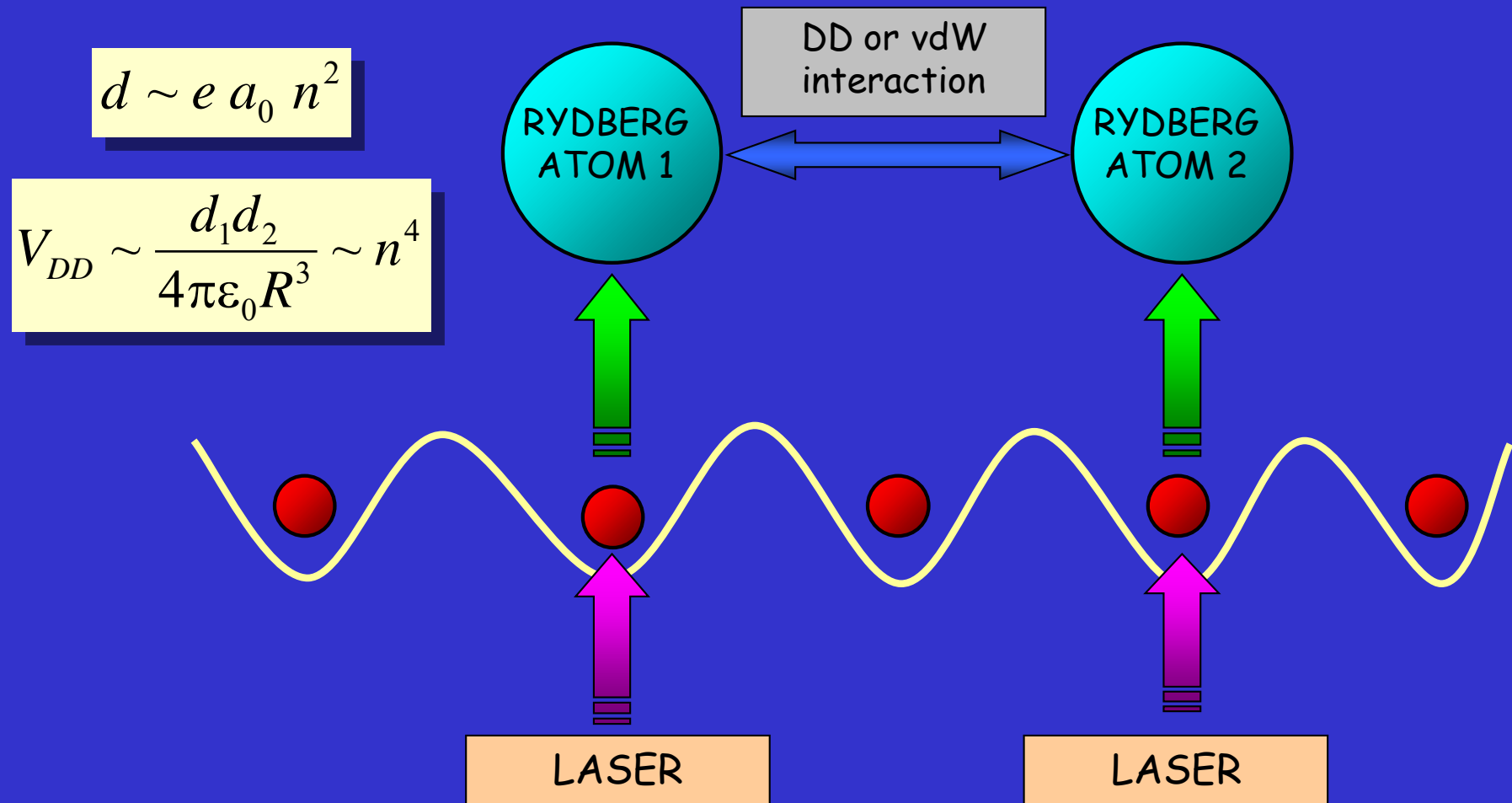
кросс-корреляции
при с-импульсе
в центральном узле



$$V \simeq 90\% \\ \bar{V} = 96.0 \pm 1.6\%$$



Two-qubit gates based on laser excitation of neutral atoms to Rydberg states and their interaction

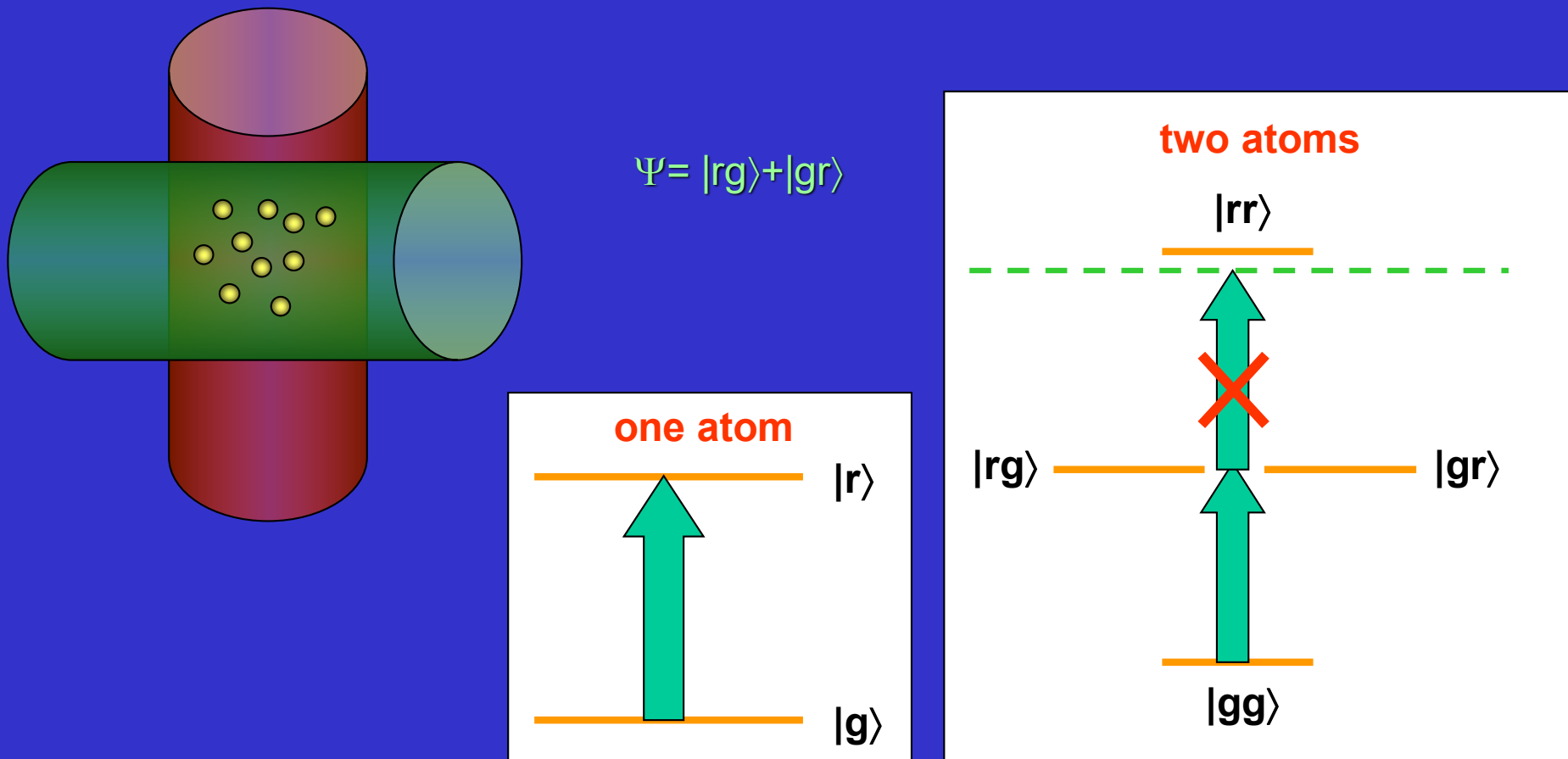


D. Jaksch et al. PRL 85 (2000) 2208; M. Lukin et al. PRL 87 (2001) 037901

$V \sim 100 \text{ MHz}$ at $n = 100, R \approx 5 \mu\text{m}$

Dipole blockade in mesoscopic ensembles

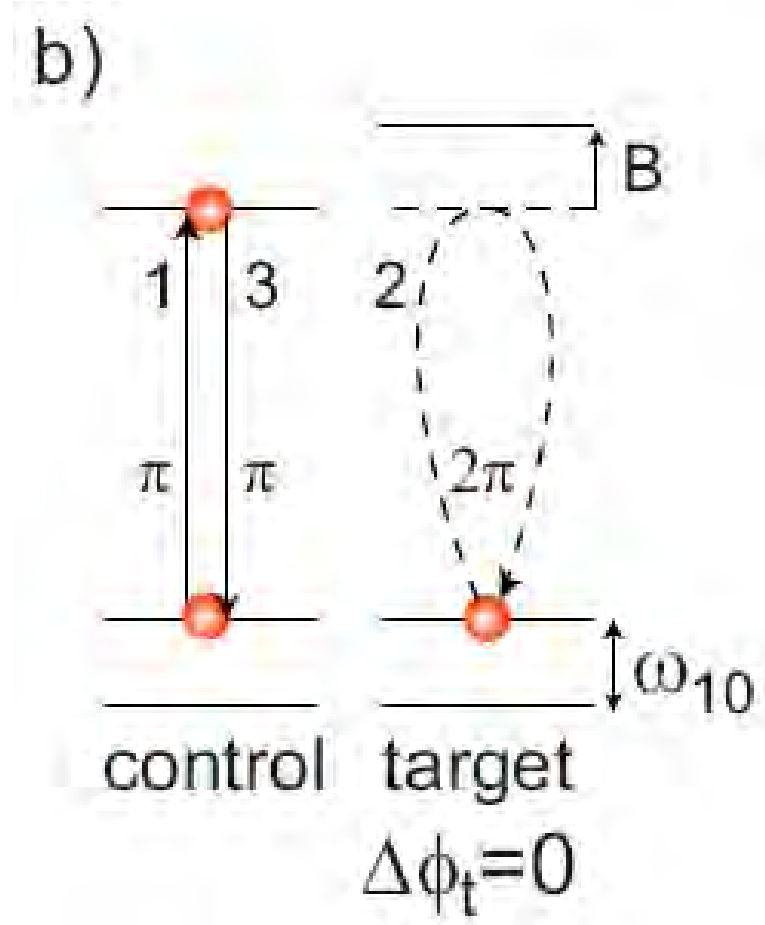
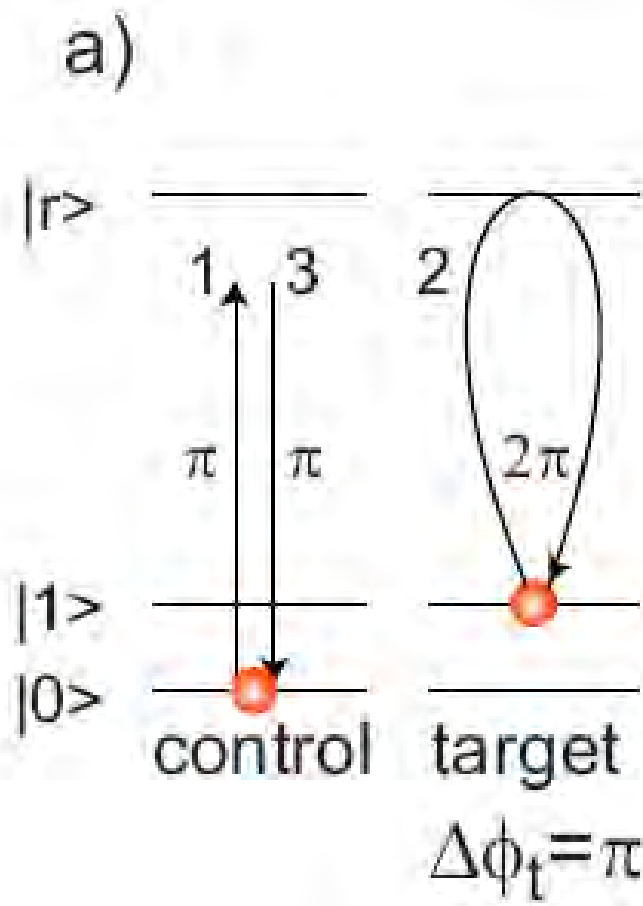
M. Lukin et al. PRL 87 (2001) 037901



M. Saffman et al., Rev. Mod. Phys. **82**, 2313 (2010)

D. Comparat et al., J. Opt. Soc. Am. B **27**, A208 (2010)

CZ quantum gate with dipole blockade



M.D.Lukin et al., Phys. Rev. Lett., 2001, v.87, p.037901

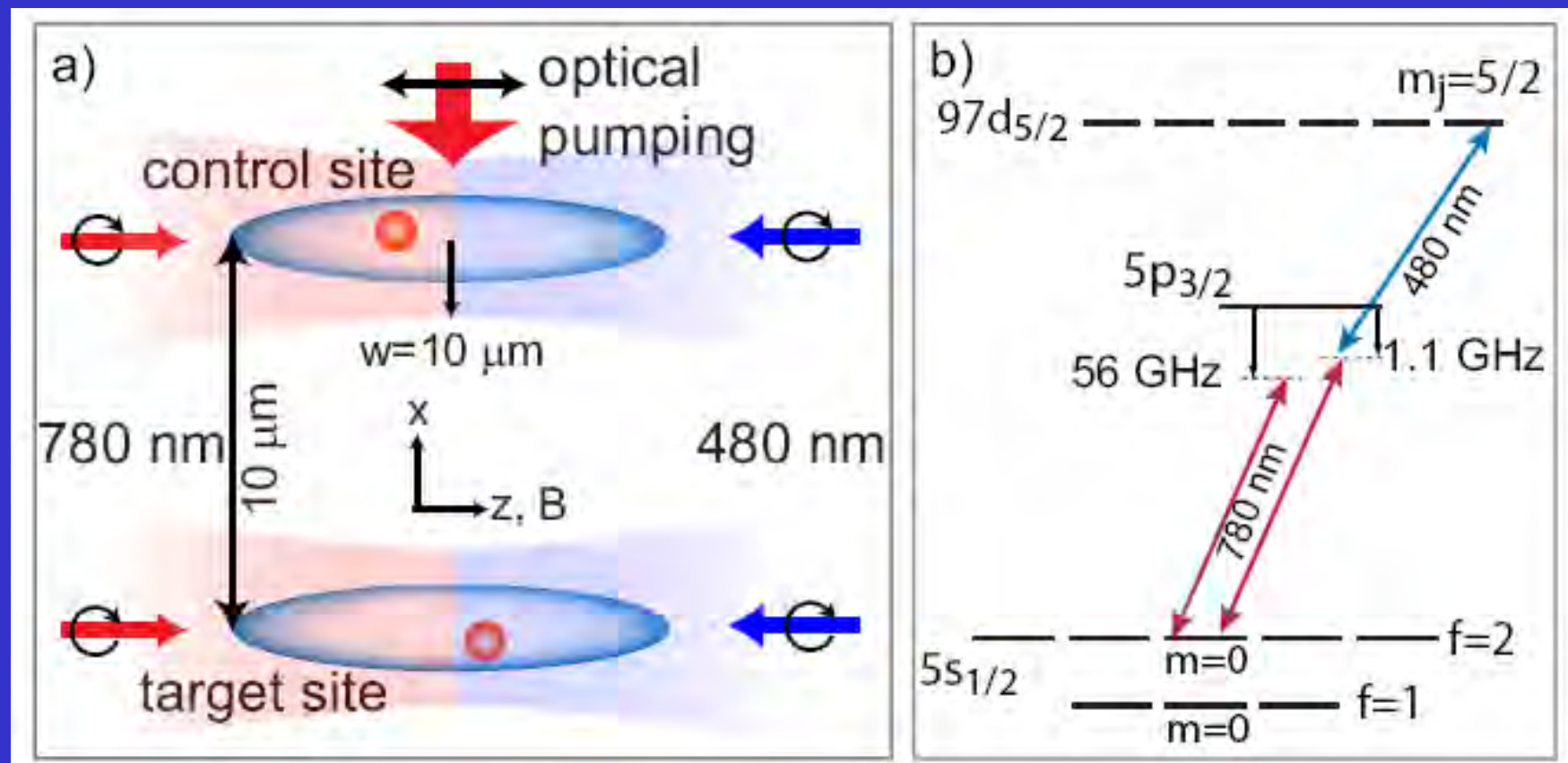


Demonstration of a Neutral Atom Controlled-NOT Quantum Gate

L. Isenhower, E. Urban, X. L. Zhang, A. T. Gill, T. Henage, T. A. Johnson,* T. G. Walker, and M. Saffman

Department of Physics, University of Wisconsin, 1150 University Avenue, Madison, Wisconsin 53706 USA

(Received 5 August 2009; published 8 January 2010)



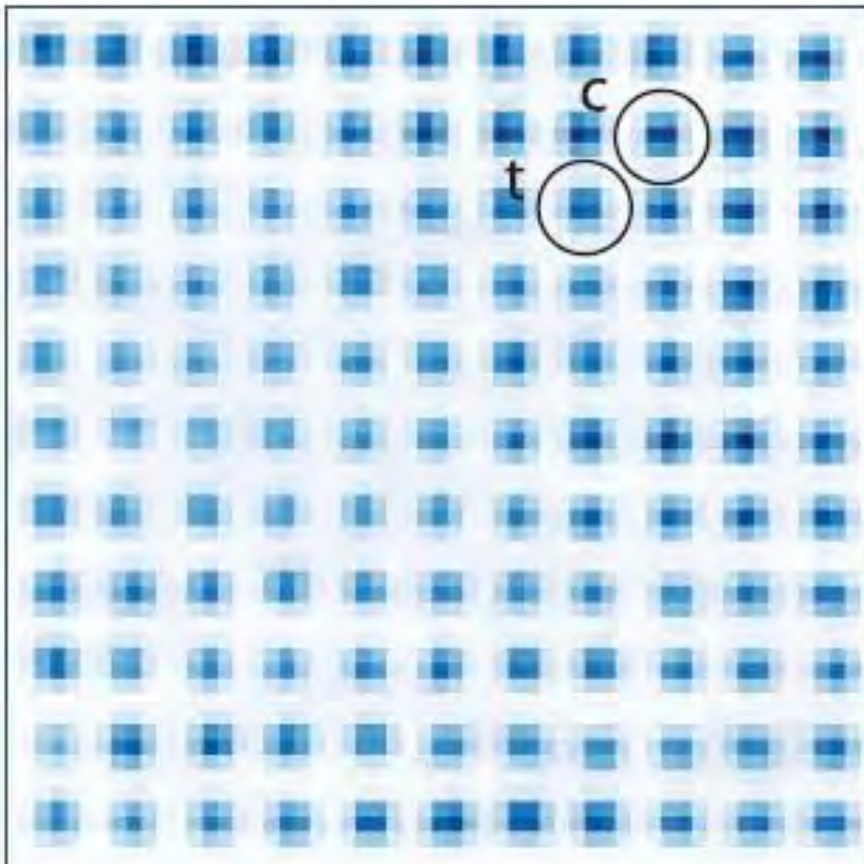
Fidelity of two-qubit gates $F \sim 80\%$.

Rydberg-Mediated Entanglement in a Two-Dimensional Neutral Atom Qubit Array

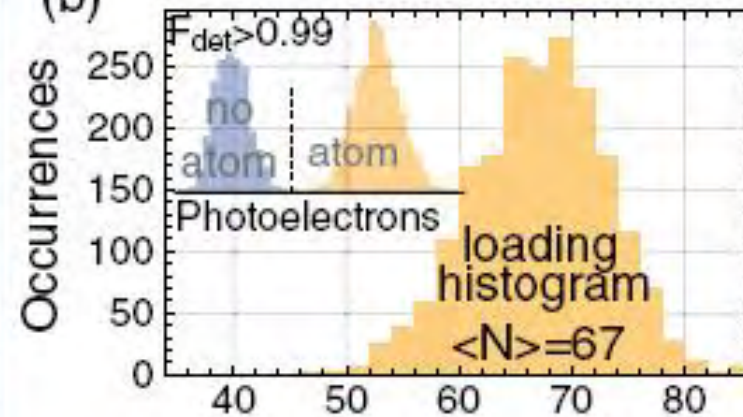
T. M. Graham, M. Kwon^{DOI}, B. Grinkemeyer^{DOI}, Z. Marra, X. Jiang, M. T. Lichtman^{DOI},^{*}
Y. Sun,[†] M. Ebert^{DOI},[‡] and M. Saffman^{DOI},[‡]

Department of Physics, University of Wisconsin-Madison, 1150 University Avenue, Madison, Wisconsin 53706, USA

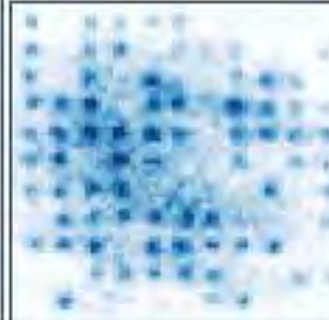
(a)



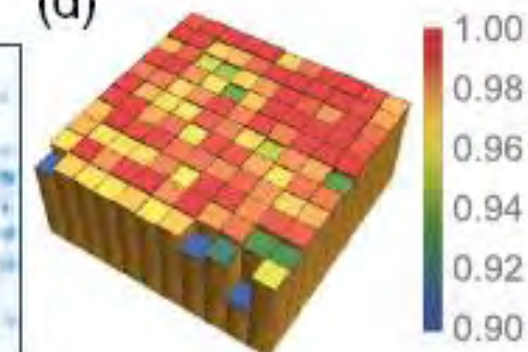
(b)



(c)



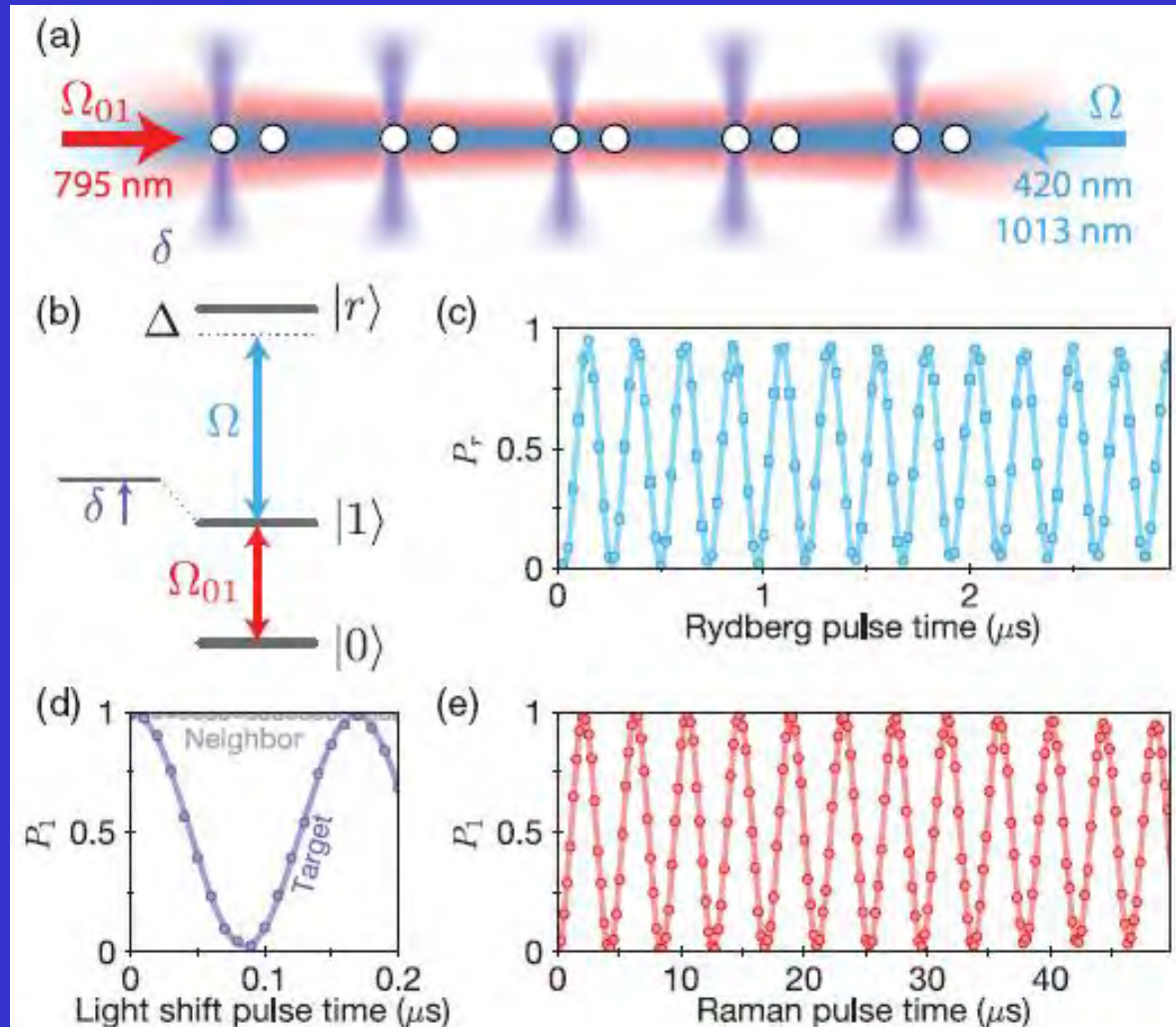
(d)



Fidelity of two-qubit gates for neighboring qubits $F \sim 90\%$.

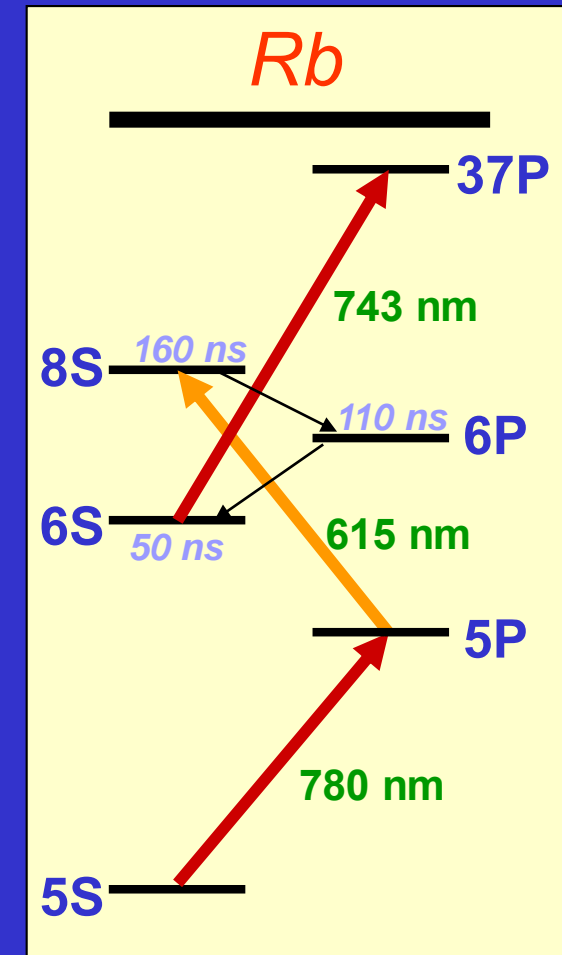
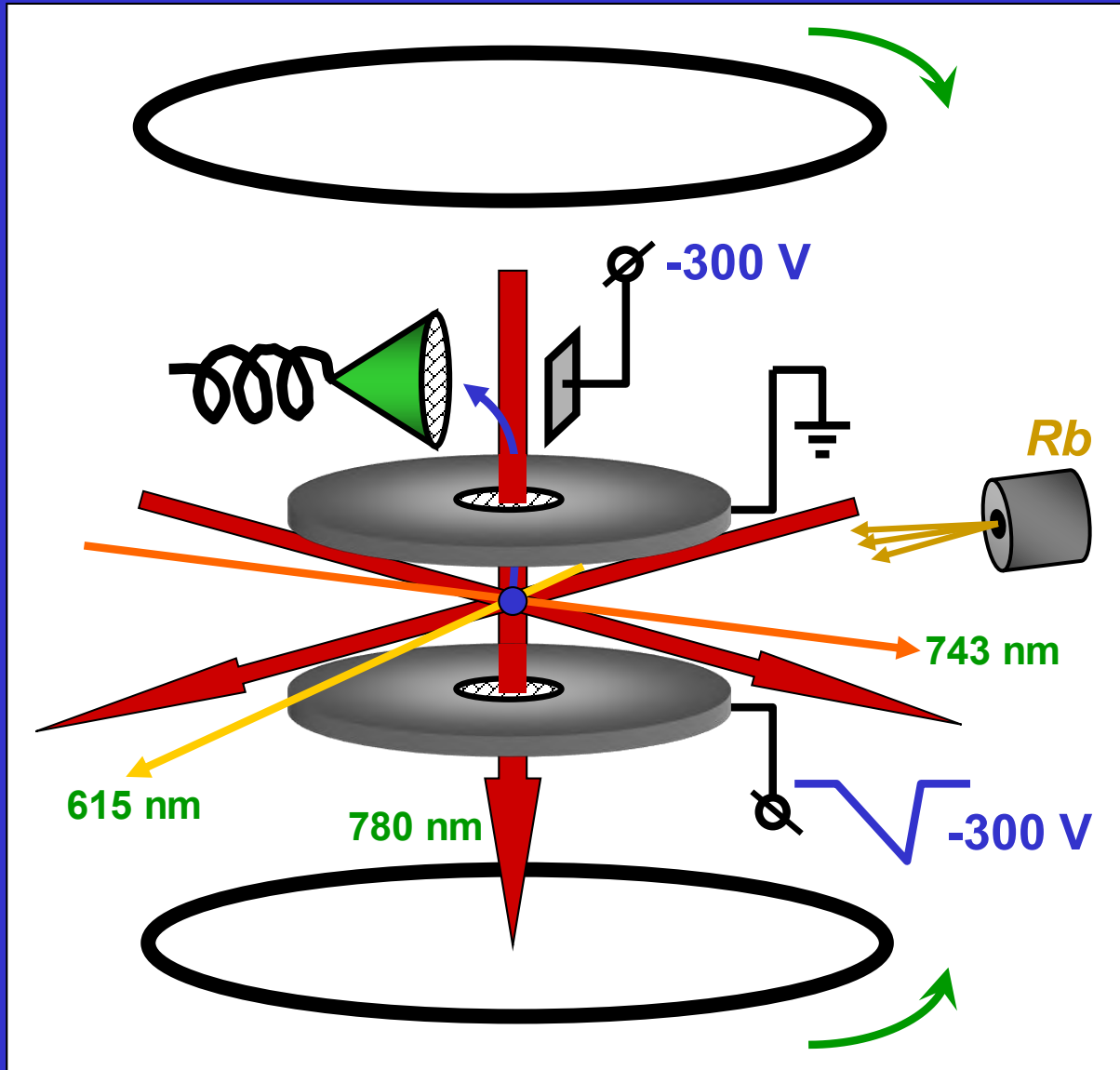
Parallel Implementation of High-Fidelity Multiqubit Gates with Neutral Atoms

Harry Levine^{1,*}, Alexander Keesling¹, Giulia Semeghini¹, Ahmed Omran¹, Tout T. Wang^{1,2}, Sepehr Ebadi,¹ Hannes Bernien,³ Markus Greiner,¹ Vladan Vuletić,⁴ Hannes Pichler,^{1,5} and Mikhail D. Lukin¹

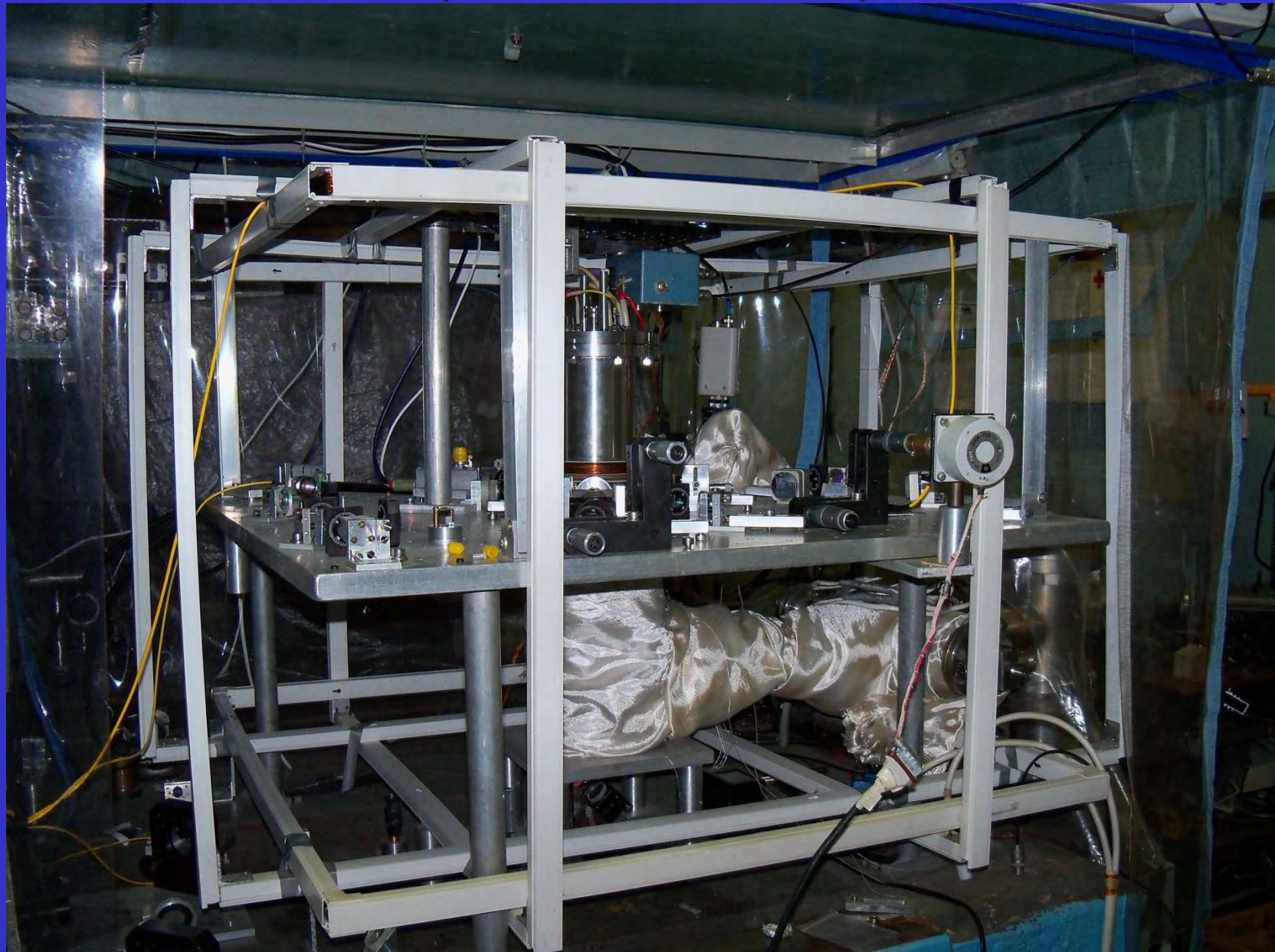


Fidelity of two-qubit gates for neighboring qubits F~97% due to laser phase noise suppression.

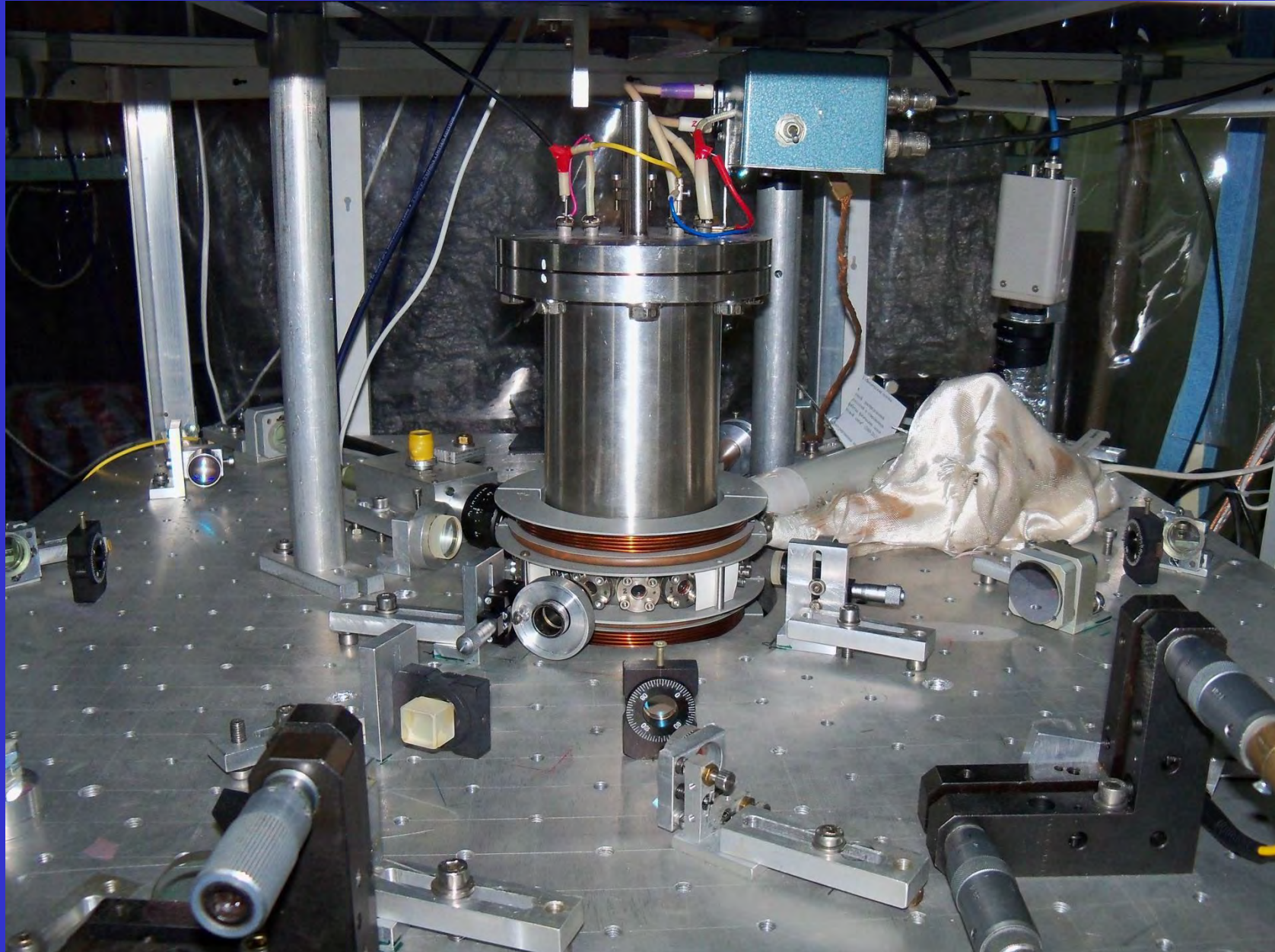
Our Rb magneto-optical trap with detection system for Rydberg atoms



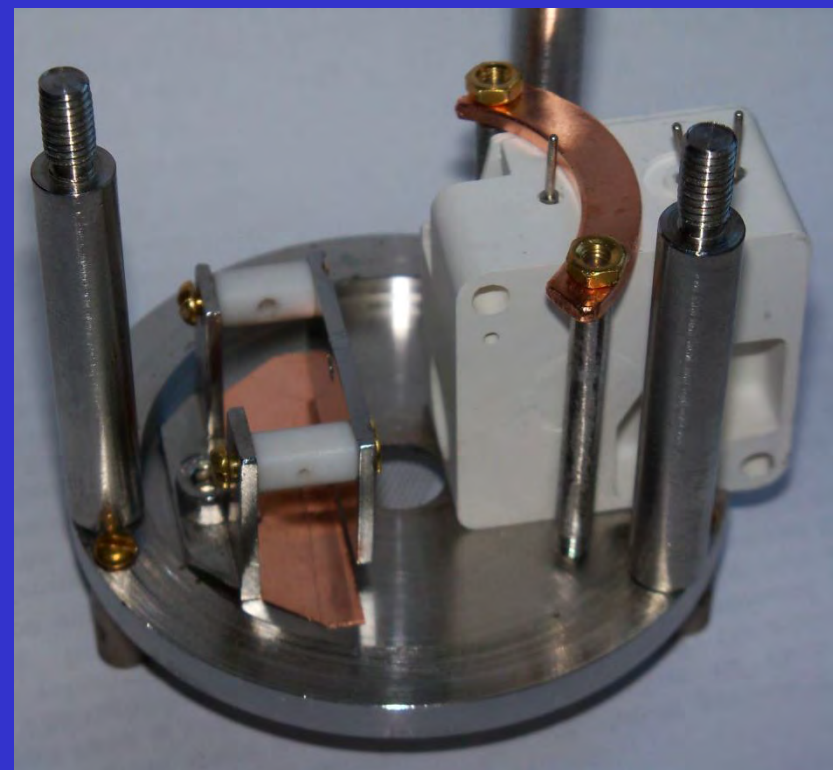
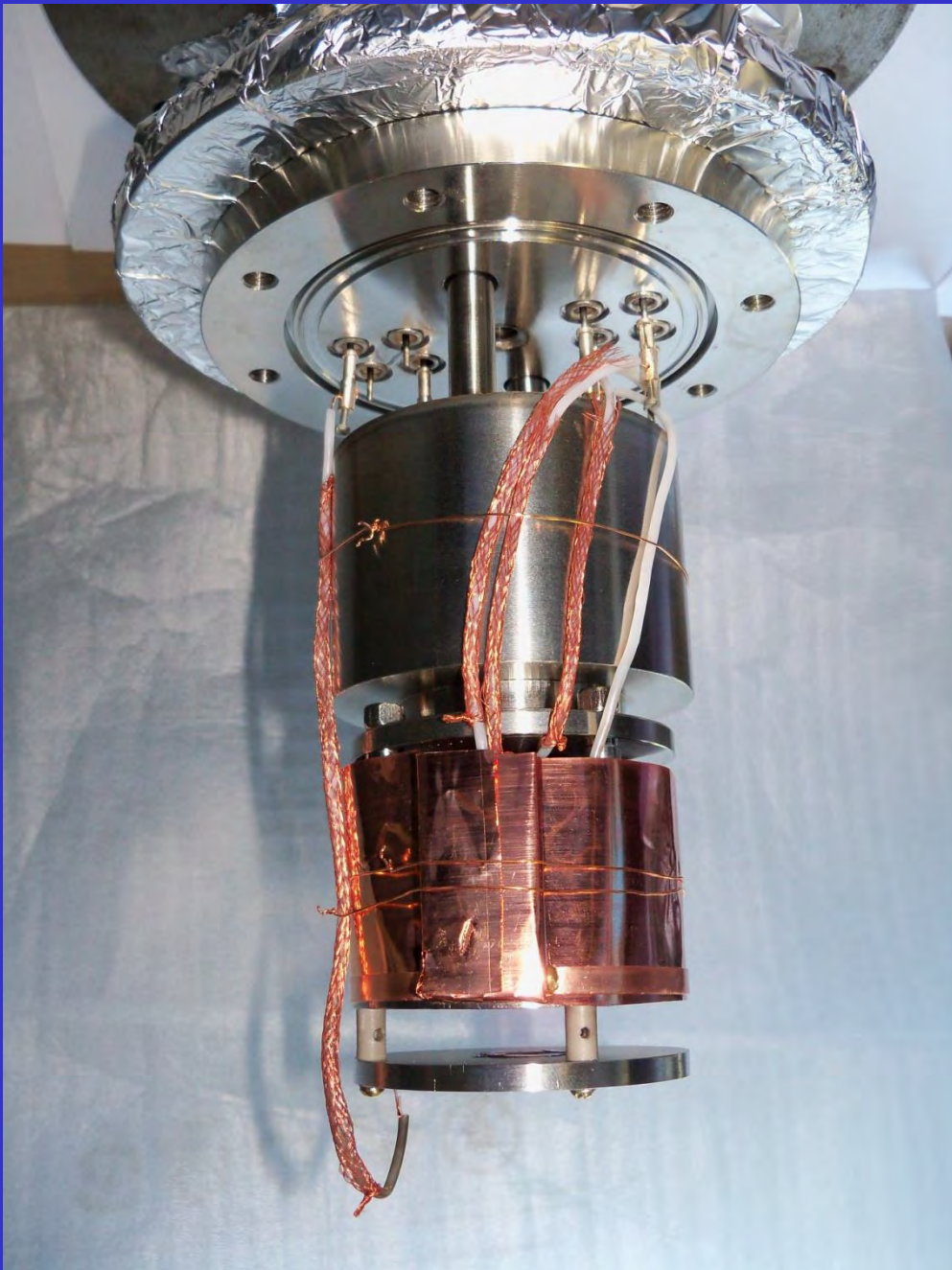
Experimental setup



Experimental setup

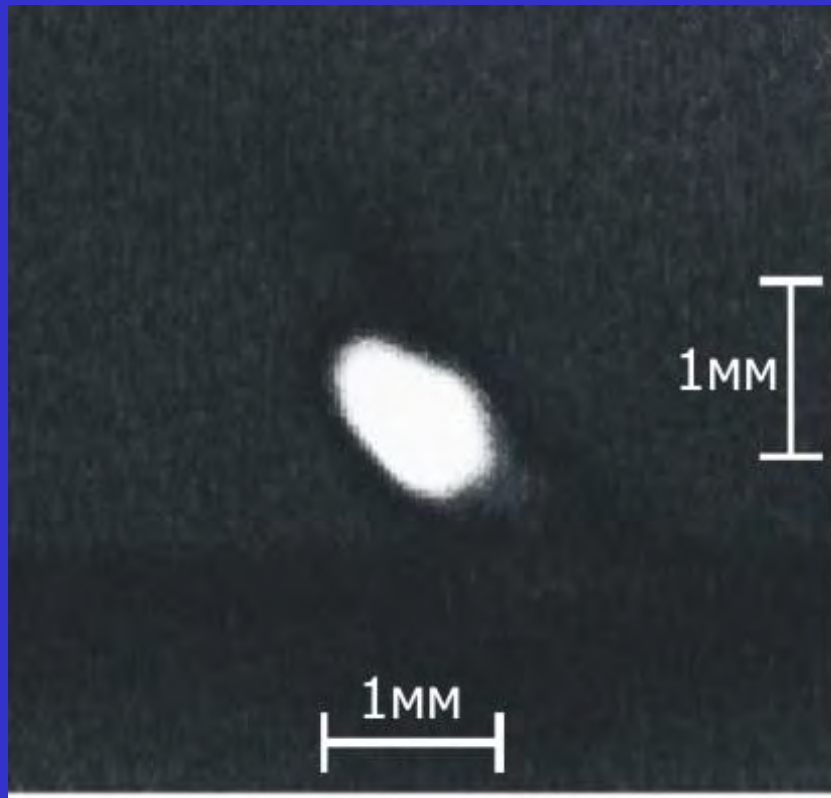


Field ionization detector

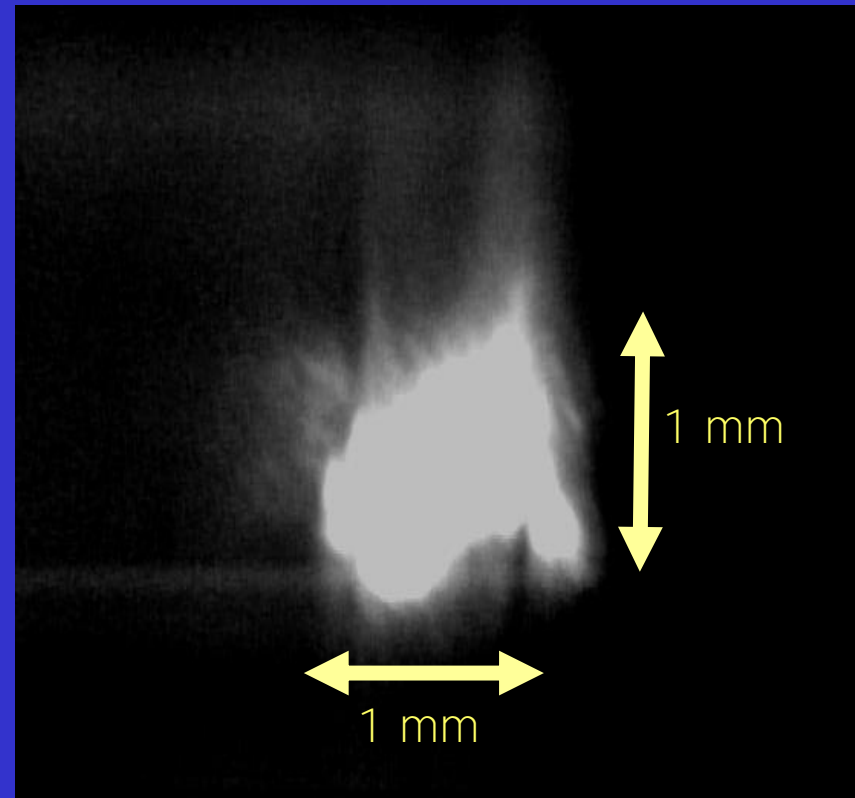


Cold Rb atom cloud

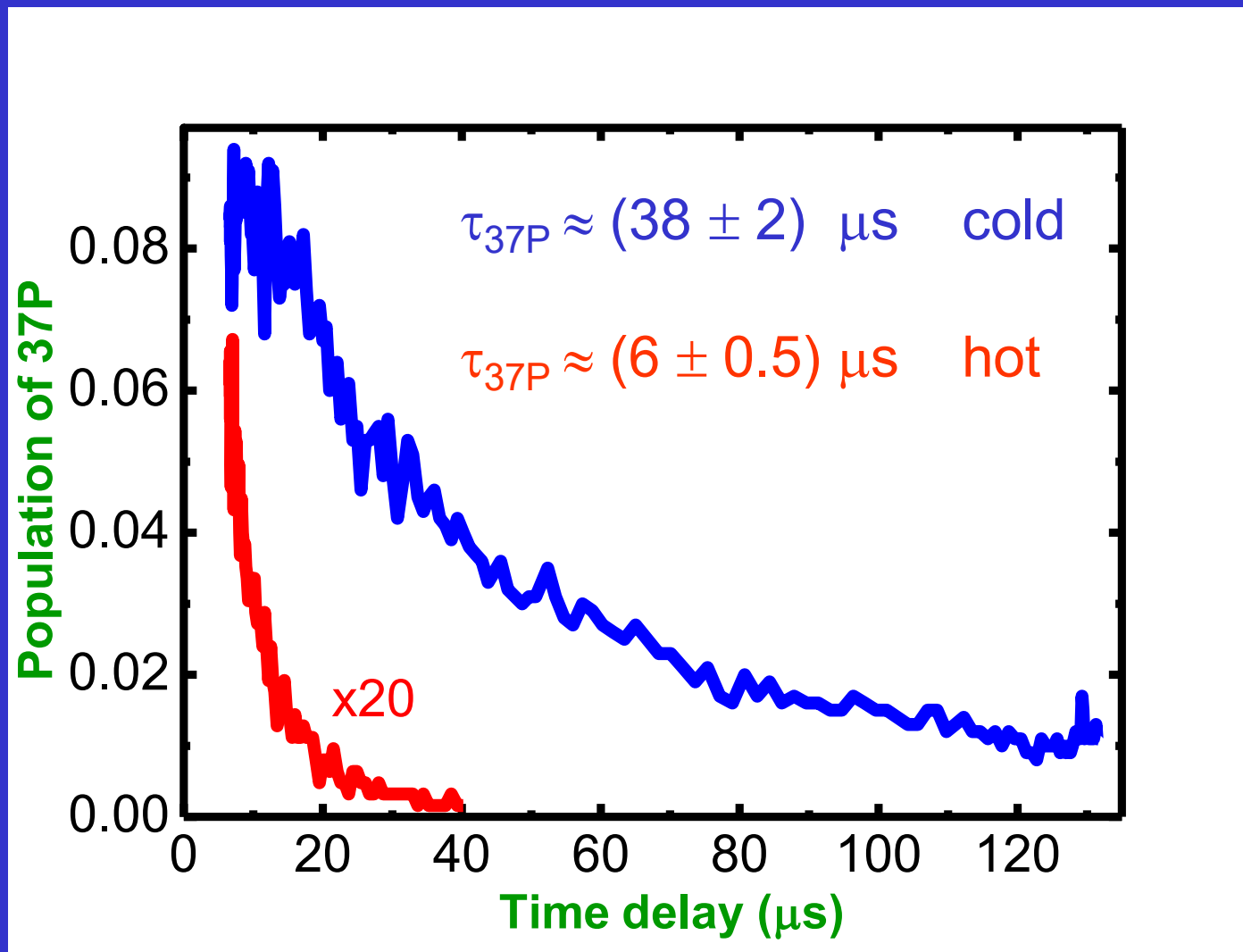
No meshes



With meshes



Lifetime of Rb(37P)



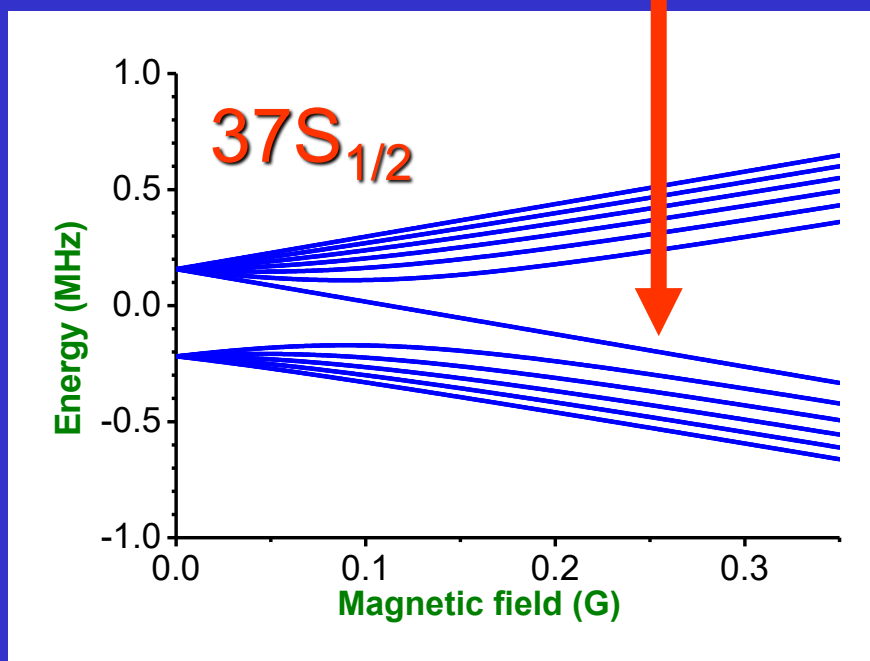
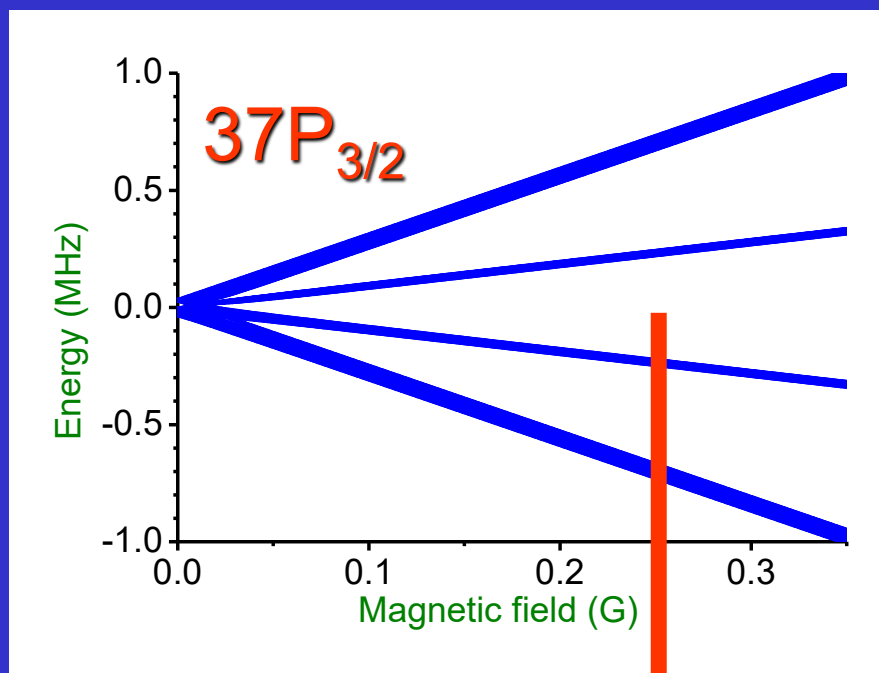
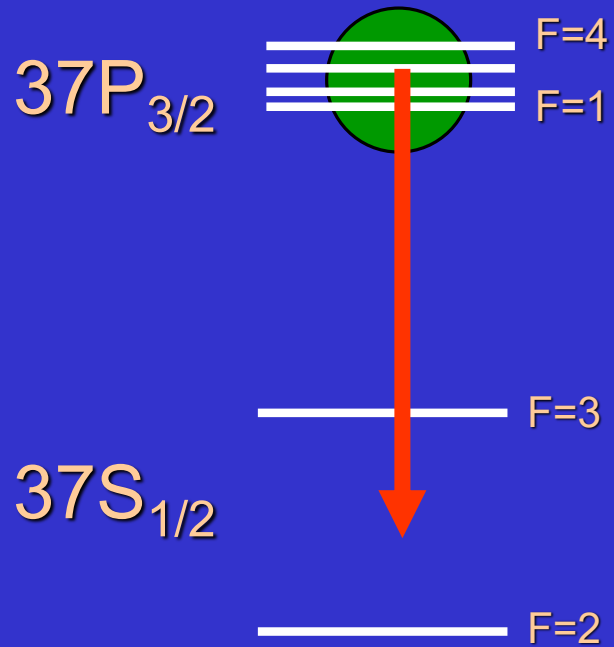
Experiment : Tretyakov et al., JETP 108, 374 (2009)

Theory at 300 K : $\tau_{37P} \approx 43 \mu\text{s}$

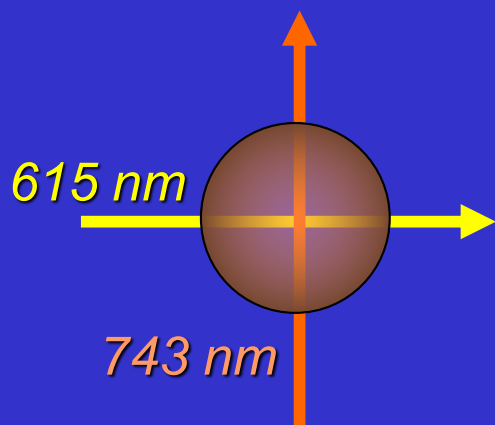
Beterov et al., PRA 79, 052504 (2009)

$37P_{3/2} \rightarrow 37S_{1/2}$ microwave transition

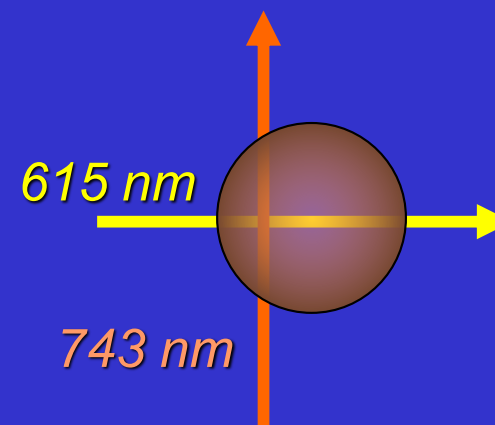
Tretyakov et al., JETP 108, 374 (2009)



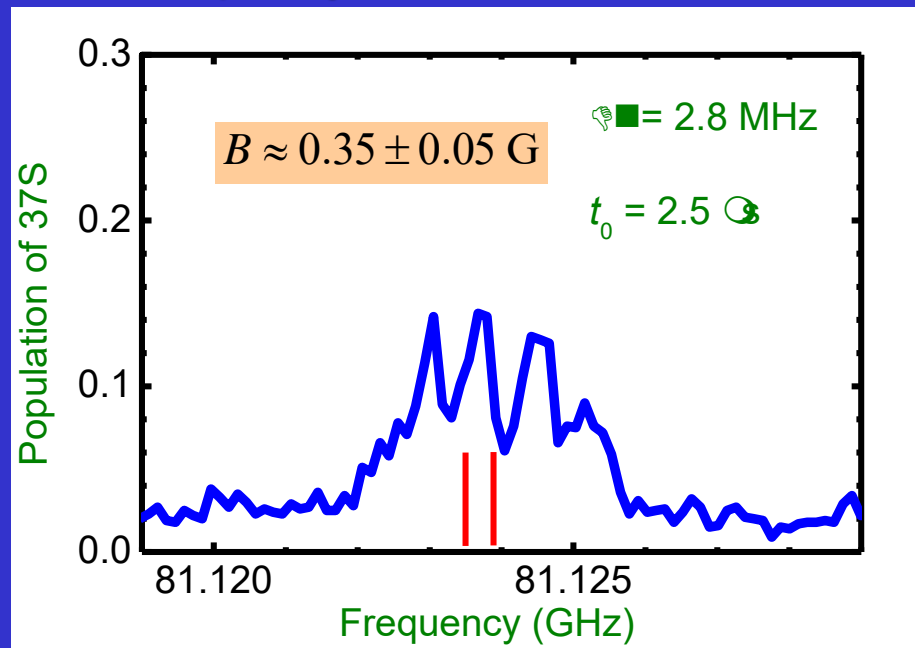
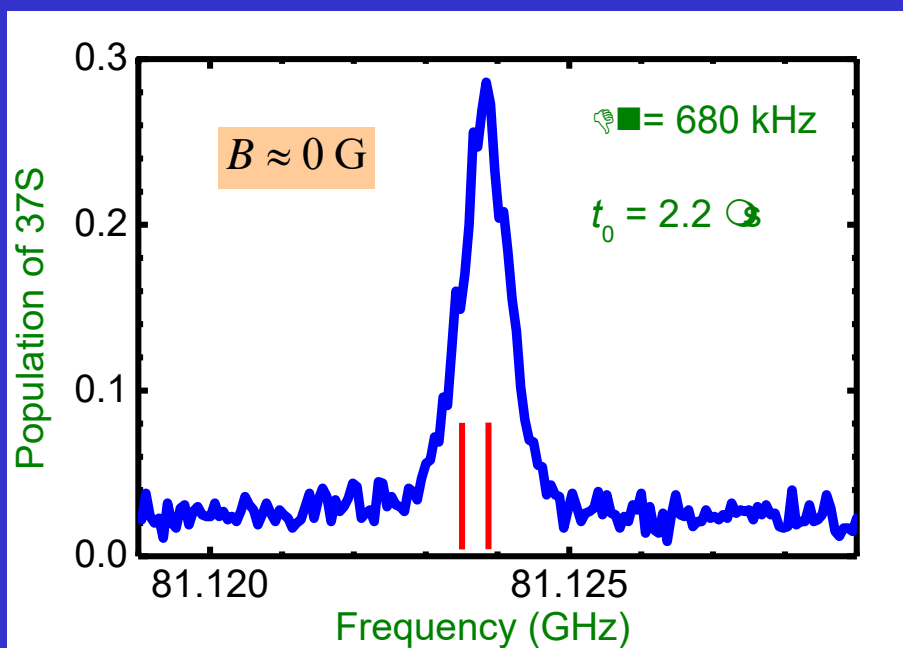
$37P_{3/2} \rightarrow 37S_{1/2}$ microwave transition in a quadrupole magnetic field 15 G/cm



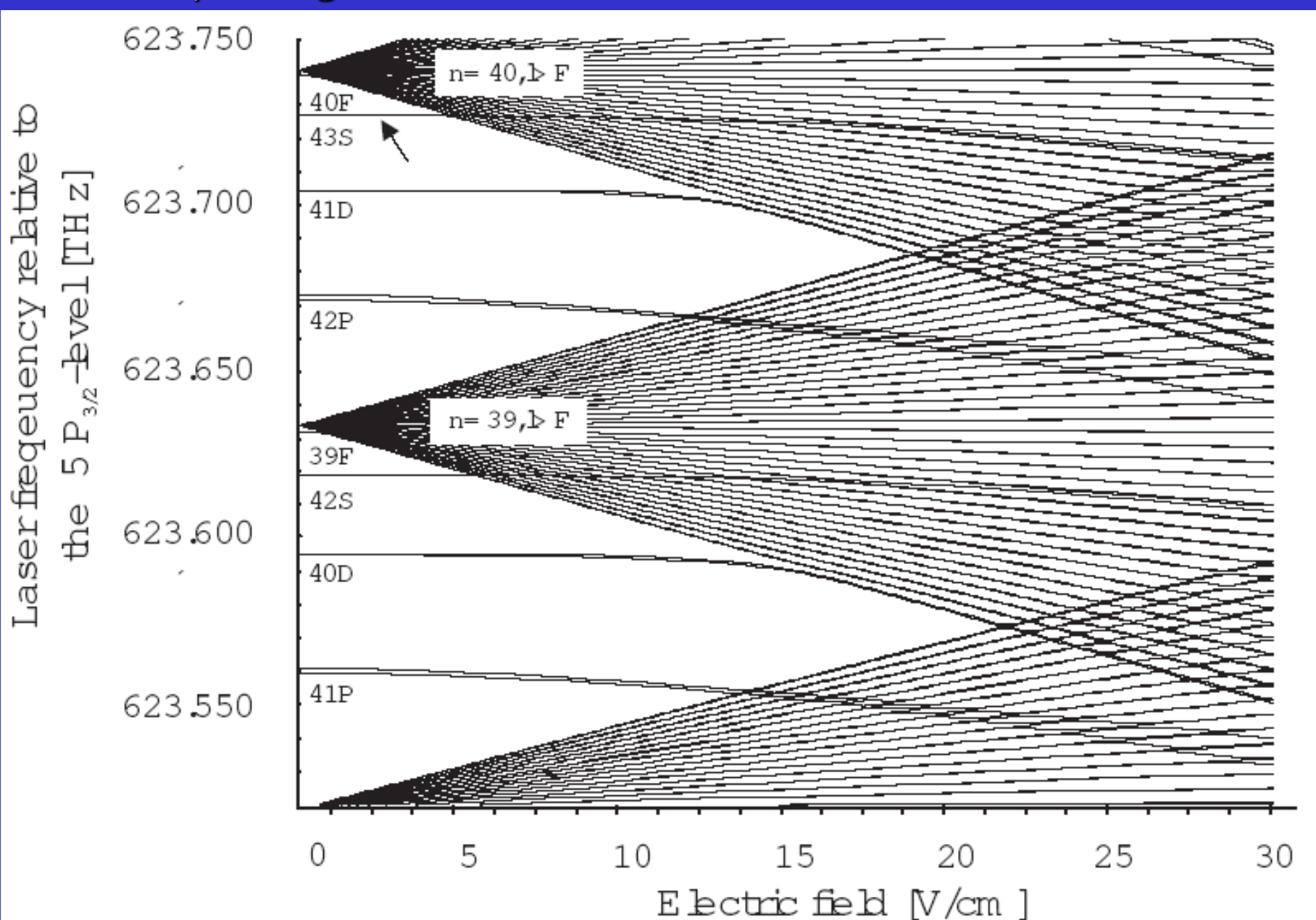
Center of cold atom cloud



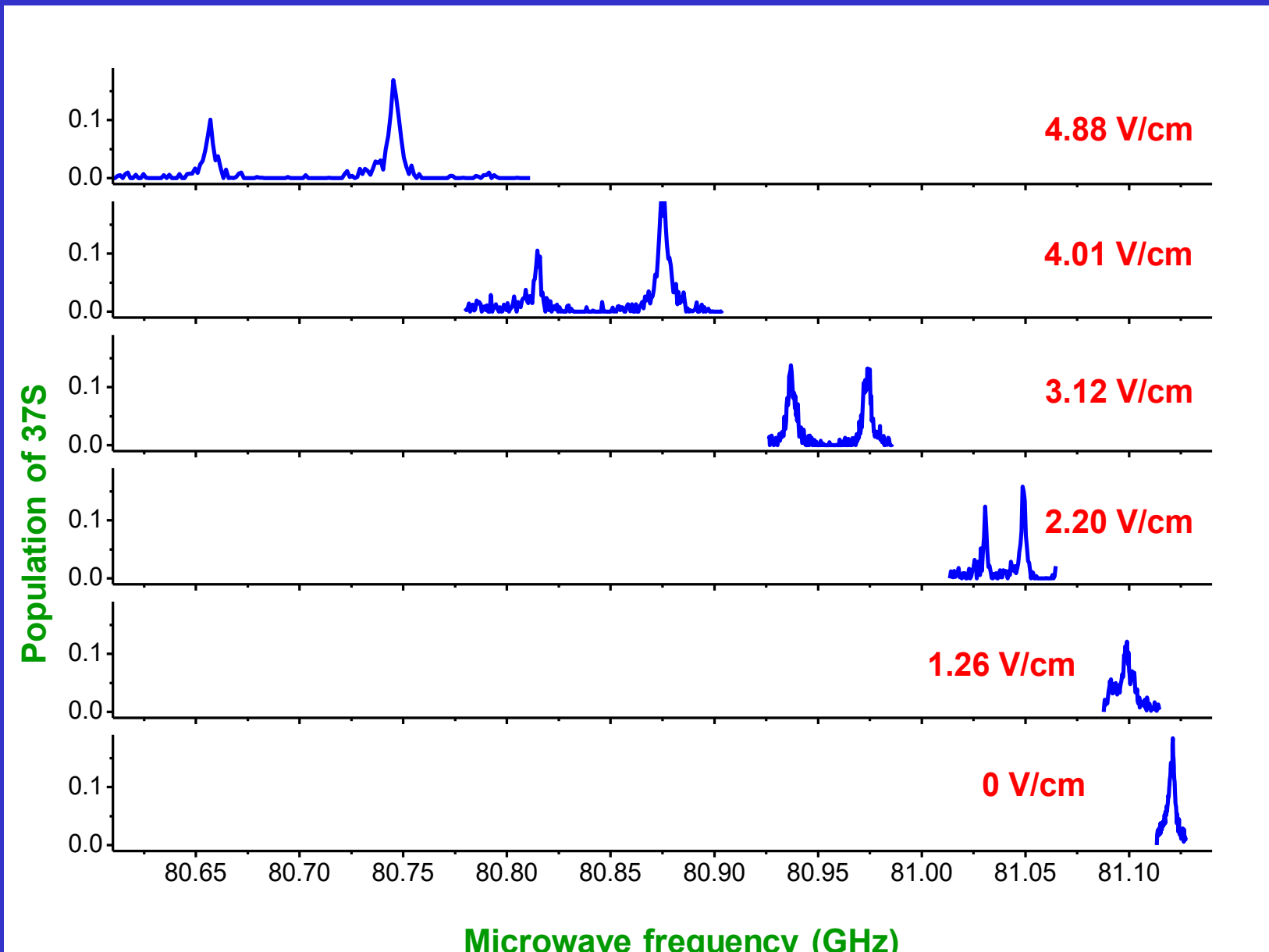
Periphery of cold atom cloud



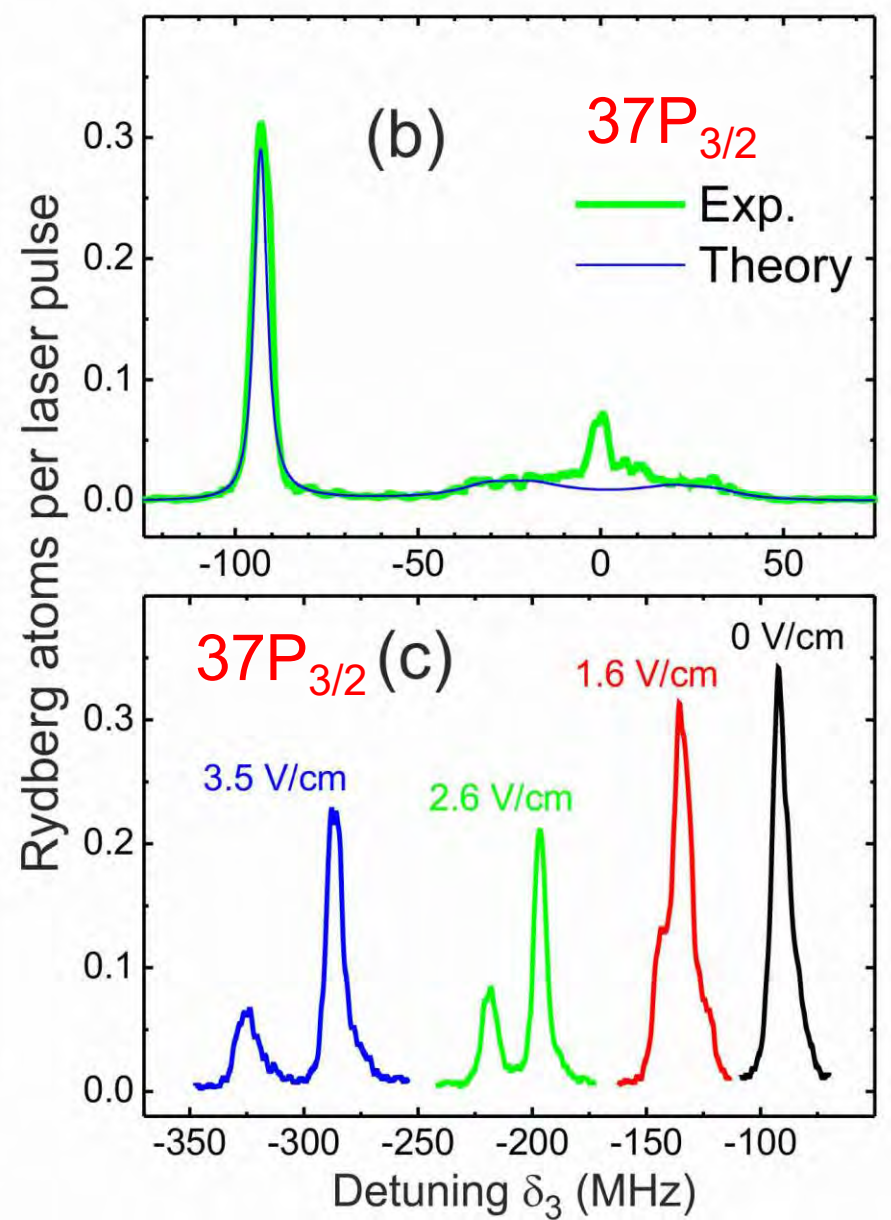
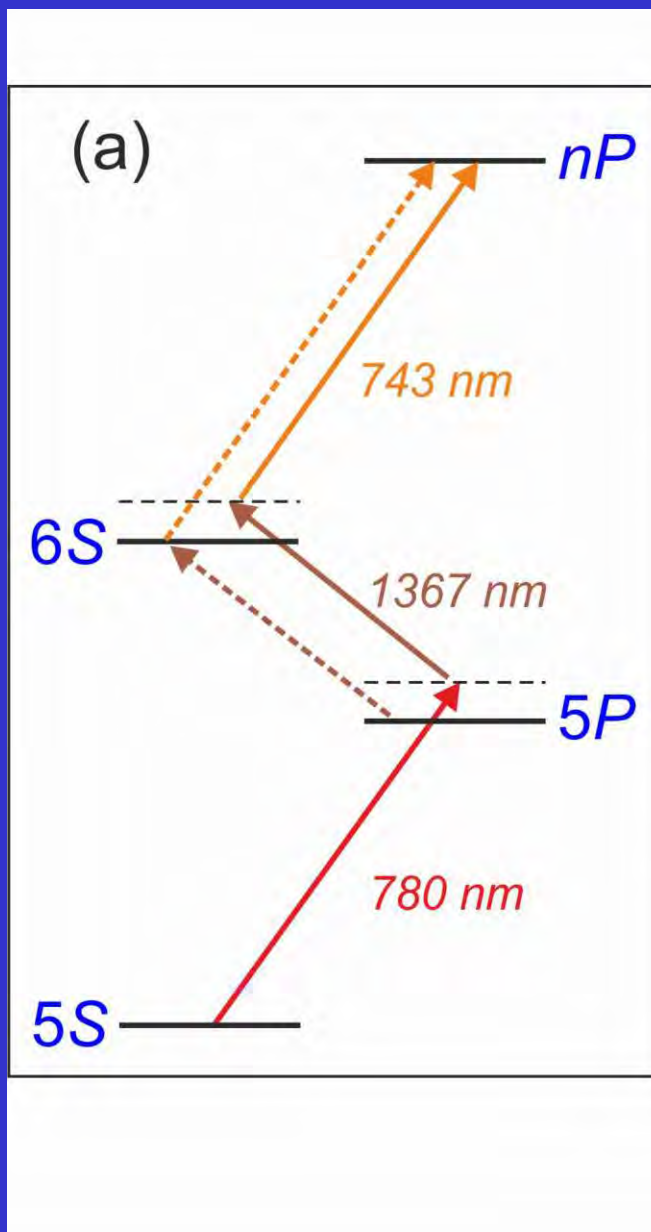
Rydberg states of Rb atoms in the electric field



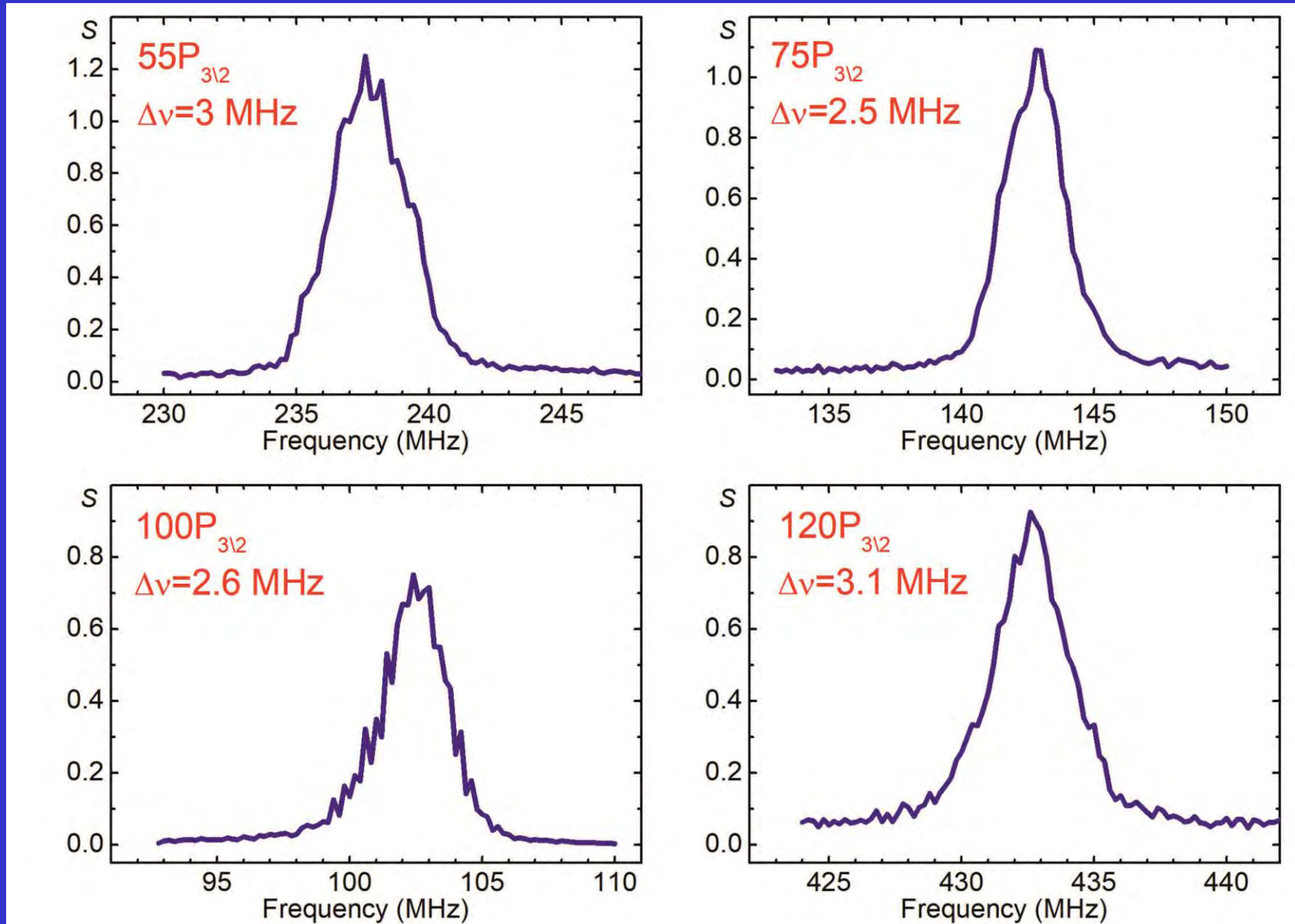
Stark effect on the microwave transition $37P_{3/2} \rightarrow 37S_{1/2}$



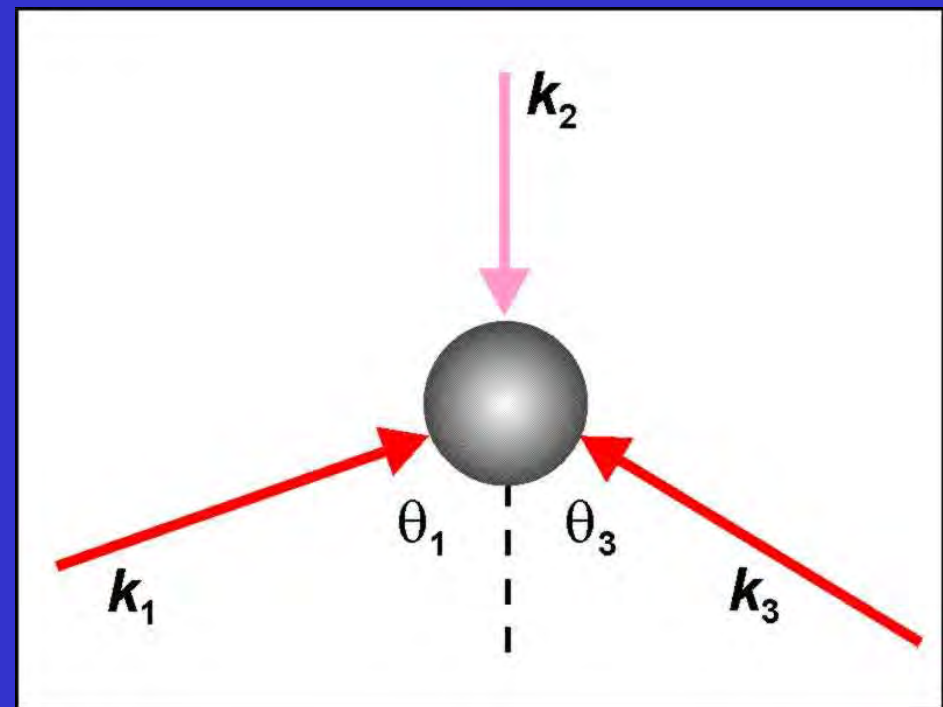
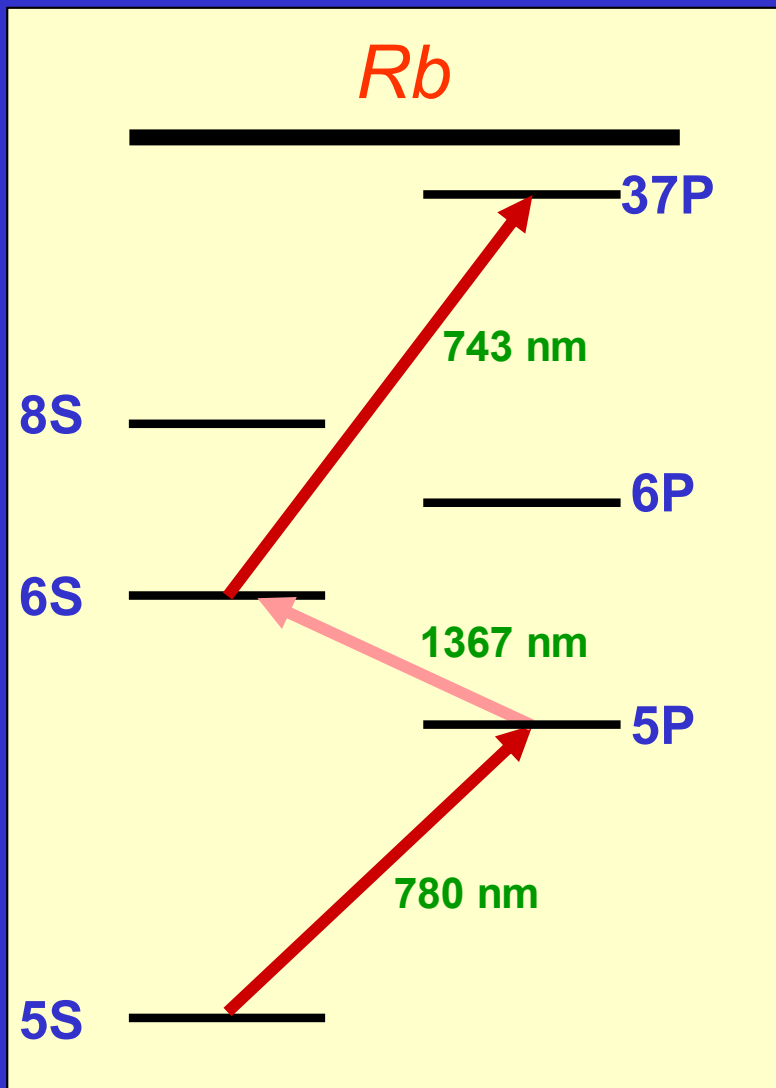
Three-photon laser excitation with cw lasers



Spectra of three-photon laser excitation of high Rydberg nP states in Rb atoms



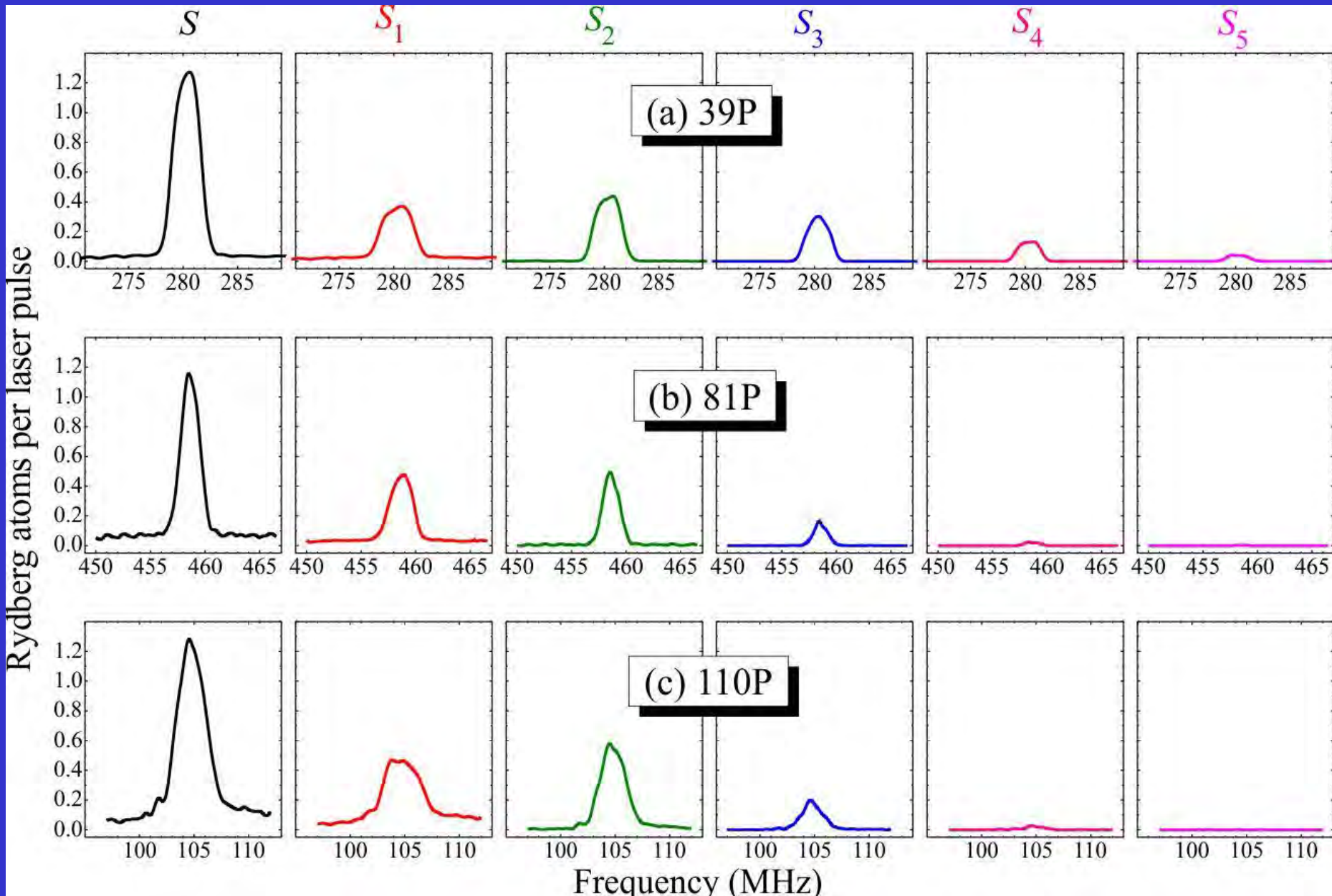
Doppler- and recoil-free laser excitation of Rydberg states via three-photon transitions



$$\vec{k}_1 + \vec{k}_2 + \vec{k}_3 \equiv 0$$

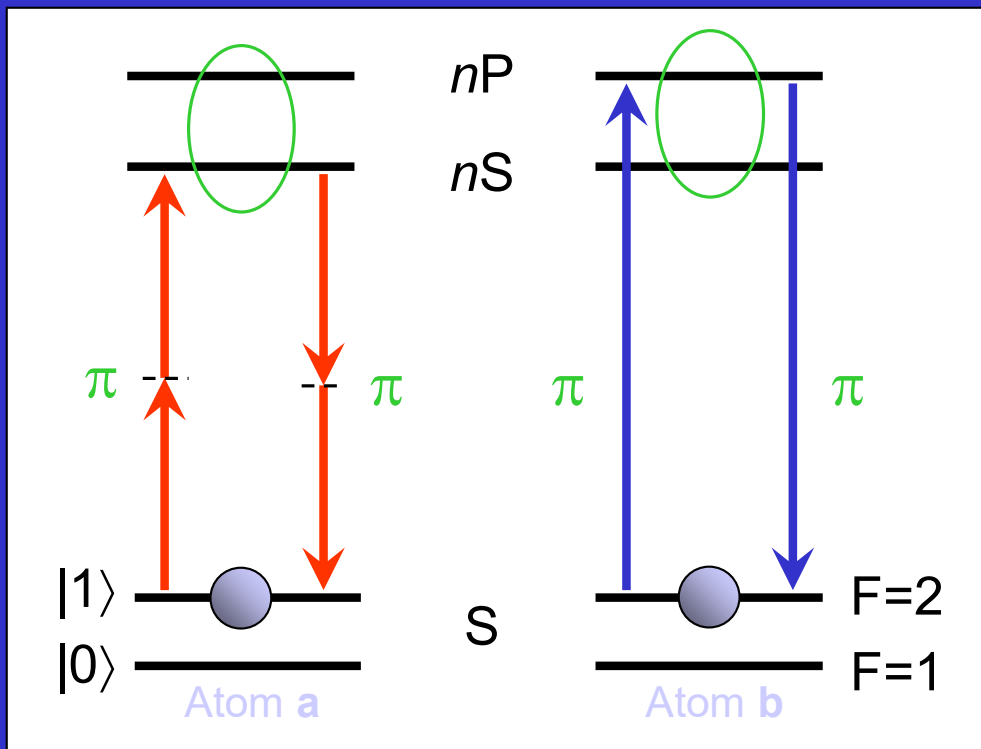
I.I.Ryabtsev et al., Phys. Rev. A,
2011, v.84, p.053409

Observation of partial dipole blockade for $81P_{3/2}$ and $110P_{3/2}$ states



Conditional Quantum Phase Gate

$$|ab\rangle \rightarrow \exp(i\Phi\delta_{a1}\delta_{b1}) |ab\rangle$$



$$V_{DD} \sim \frac{d_1 d_2}{4\pi\epsilon_0 R^3}$$

$$\Psi(t) = |\text{SP}\rangle \cos(V_{dd}t/\hbar) - i|\text{PS}\rangle \sin(V_{dd}t/\hbar)$$

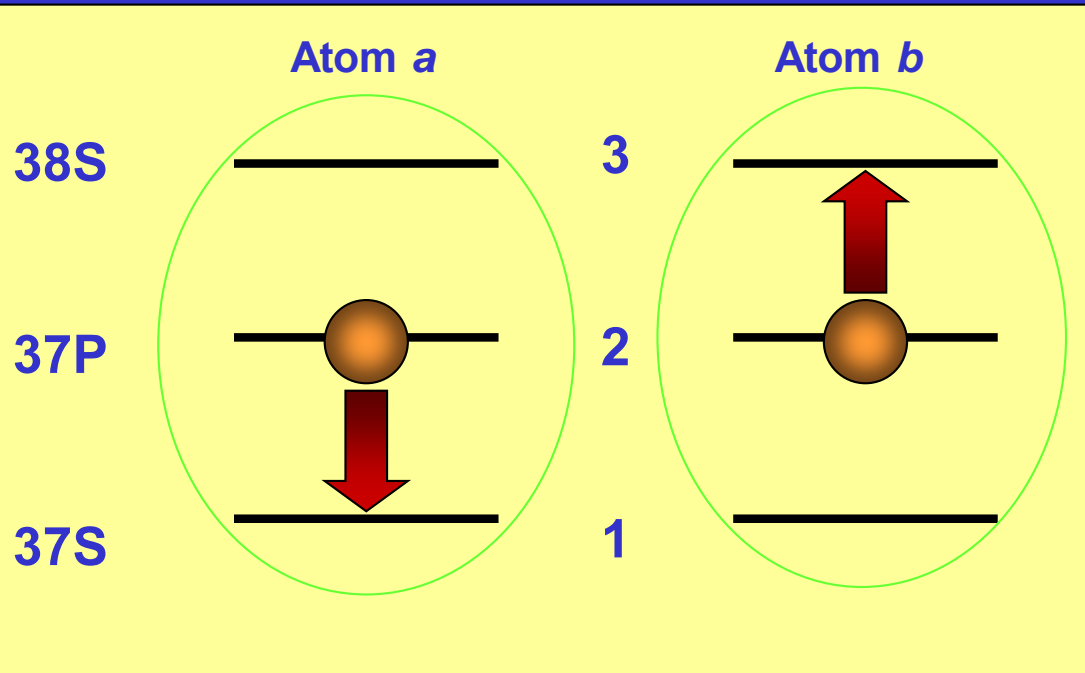
$$\Phi = \pi \quad \text{at} \quad T = \pi\hbar / V_{dd}$$

$$\langle r \rangle \sim 2500 \quad \text{at} \quad n = 50 \\ R \approx 5 \mu\text{m}$$

$$V_{dd}/\hbar \sim 10 \text{ MHz} \quad T \sim 50 \text{ ns}$$

I.I.Ryabtsev, D.B.Tretyakov, and I.I.Beterov, J. Phys. B **38**, S421 (2005)

Förster resonance in Rydberg atoms Rb(37P_{3/2})



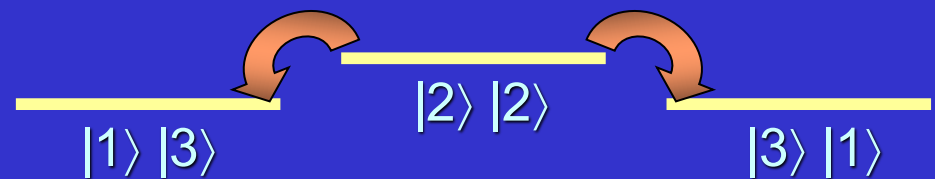
$$\hat{V}_{ab} \sim \frac{\hat{d}_a \hat{d}_b}{R^3}$$

$n = 37, R \approx 10 \mu\text{m}$
 $V_{dd}/h \sim 400 \text{ kHz}$

Collective states:

$$\Psi = A |2\ 2\rangle + a_{13} |1\ 3\rangle + a_{31} |3\ 1\rangle$$

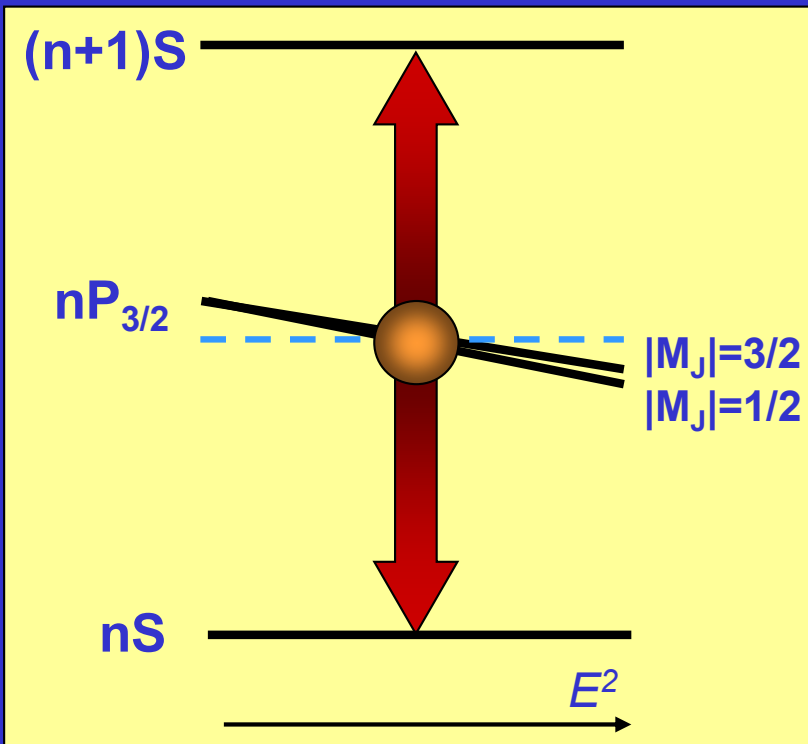
Example of two atoms:



Evolution of populations:

$$\rho_2(t) = \frac{\Omega_{ab}^2}{2\Omega_{ab}^2 + \Delta^2/4} \sin^2 \left(t \sqrt{2\Omega_{ab}^2 + \Delta^2/4} \right)$$

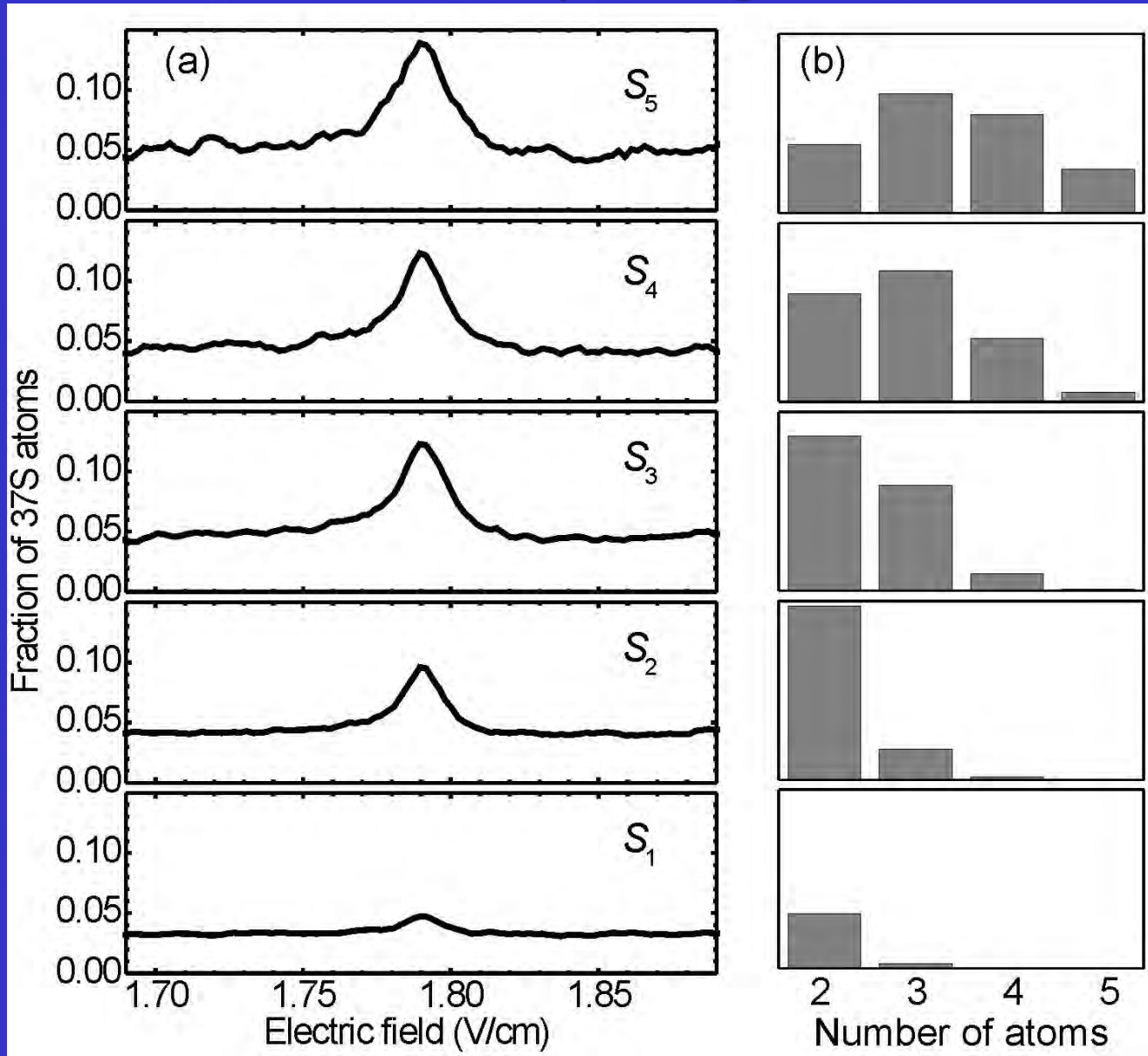
Förster resonance for Rb($nP_{3/2}$) atoms



n	Δ_0 (MHz)	E_{cr} (V/cm)
35	382	4.5
36	228	3.1
37	105	1.9
38	5.6	0.4
39	-73	
40	-136	

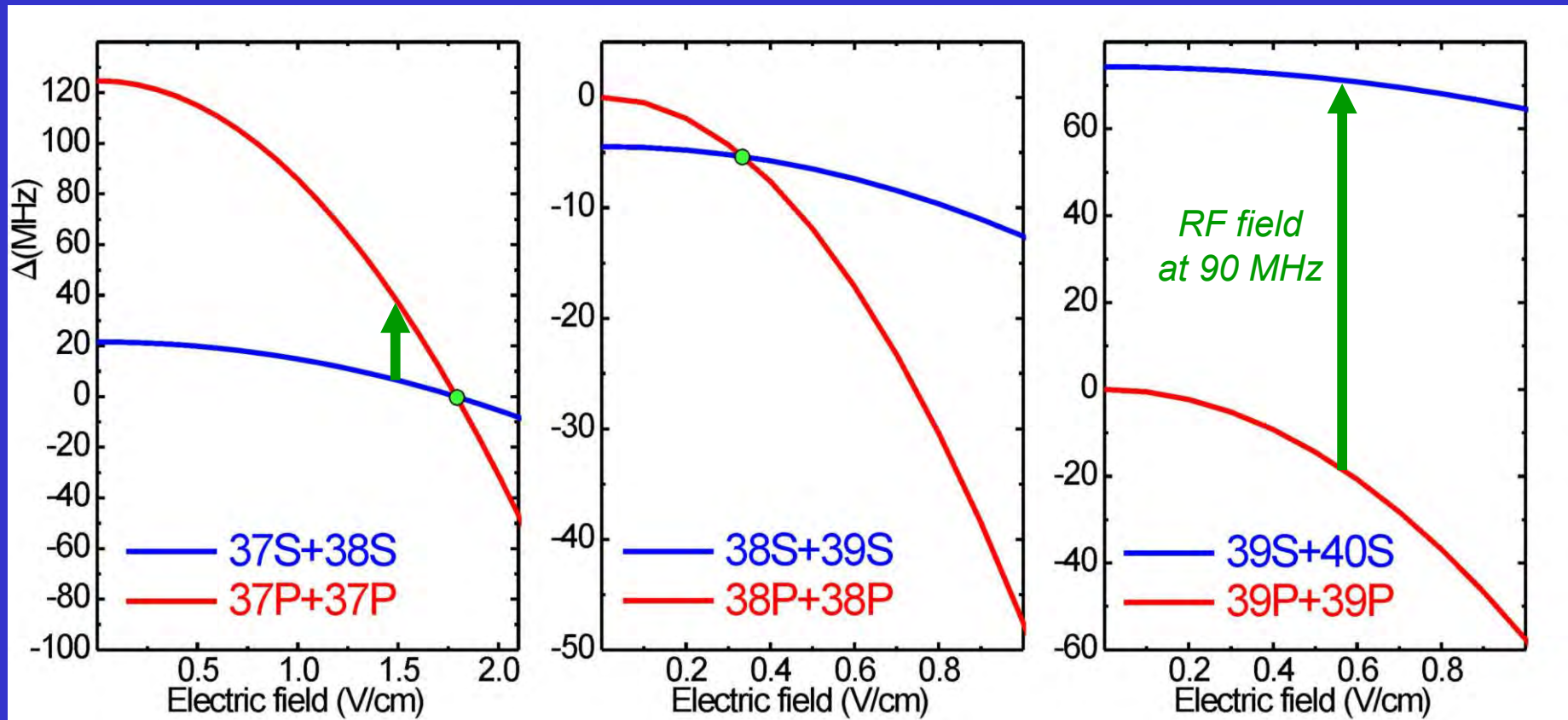
$$S_N = \frac{n_N(37S)}{n_N(37P) + n_N(37S) + n_N(38S)}$$

Förster resonance in Rydberg atoms Rb($37P_{3/2}$)



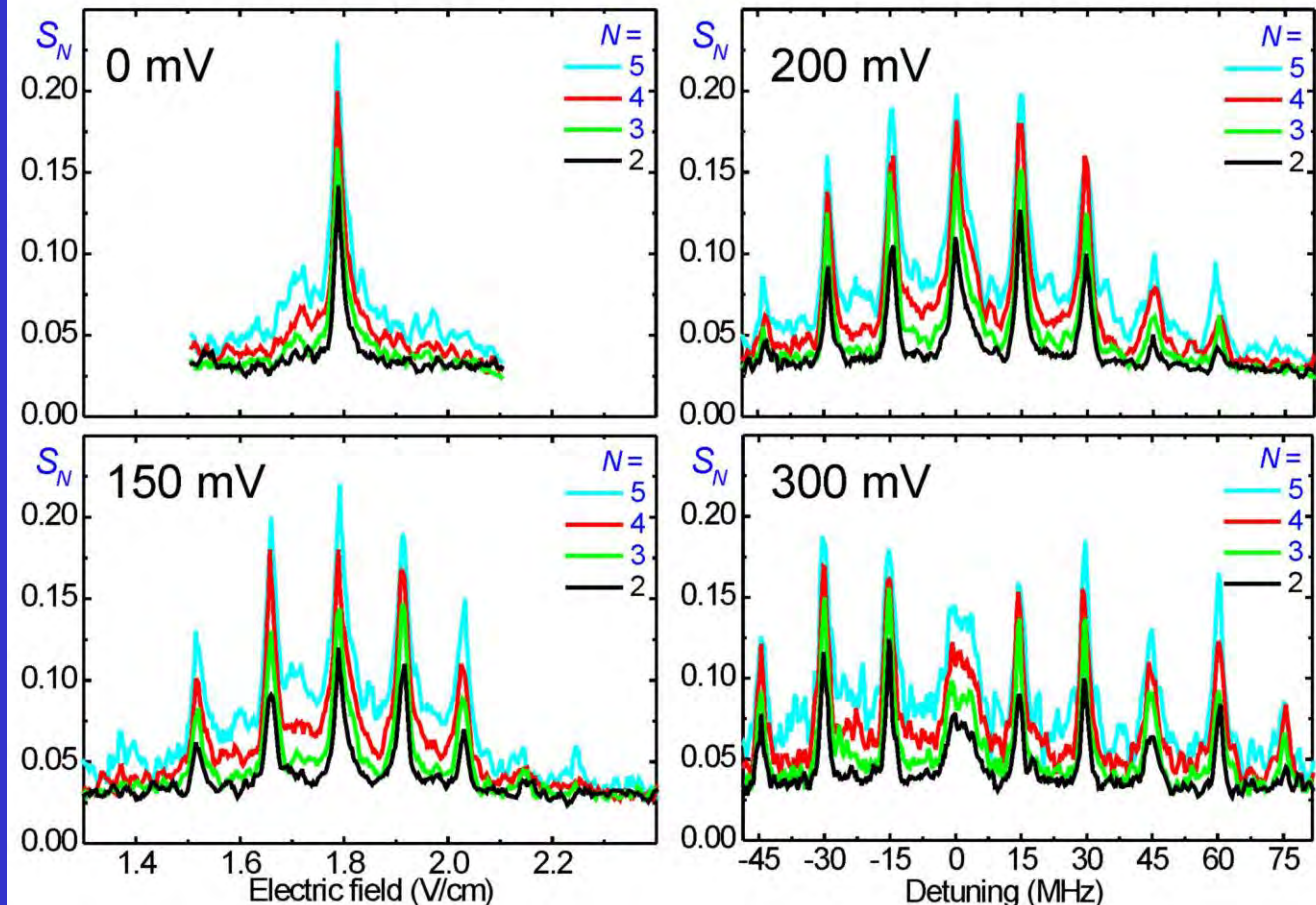
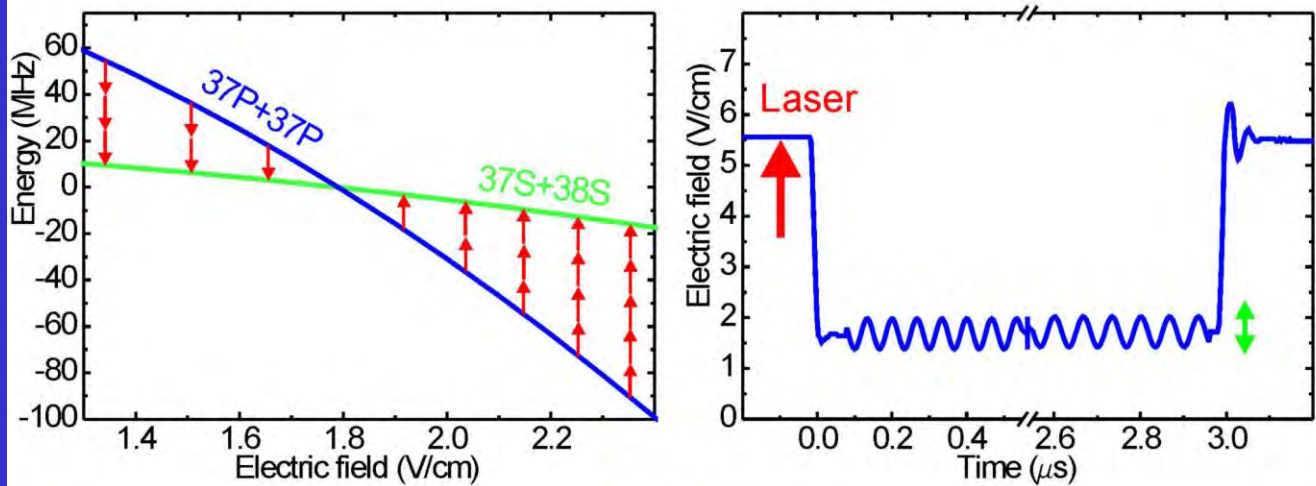
I.I.Ryabtsev, D.B.Tretyakov, I.I.Beterov, V.M.Entin, PRL 104 (2010) 073003

Förster resonances



D.B. Tretyakov et al., Phys. Rev. A **90**, 041403(R) (2014)
 E.A. Yakshina et al., Phys. Rev. A **94**, 043417 (2016)

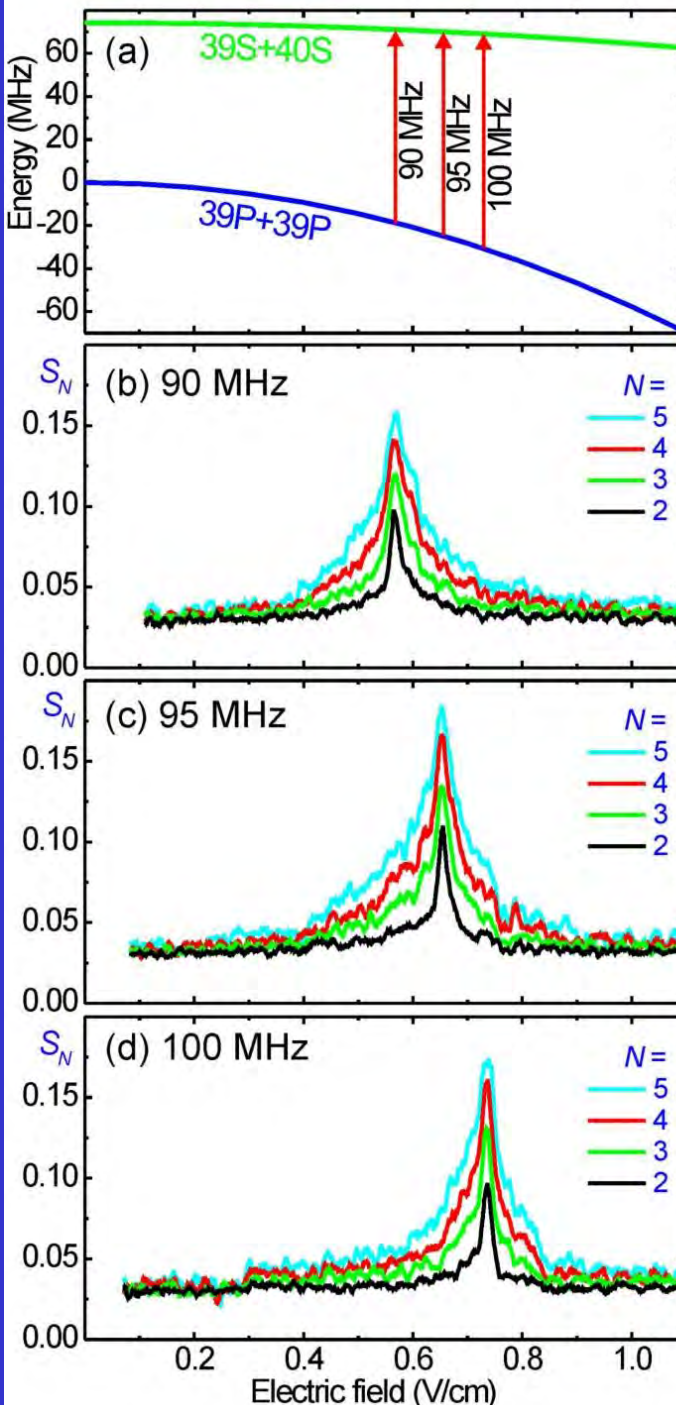
RF-assisted Förster resonances for $37P$ state at 15 MHz



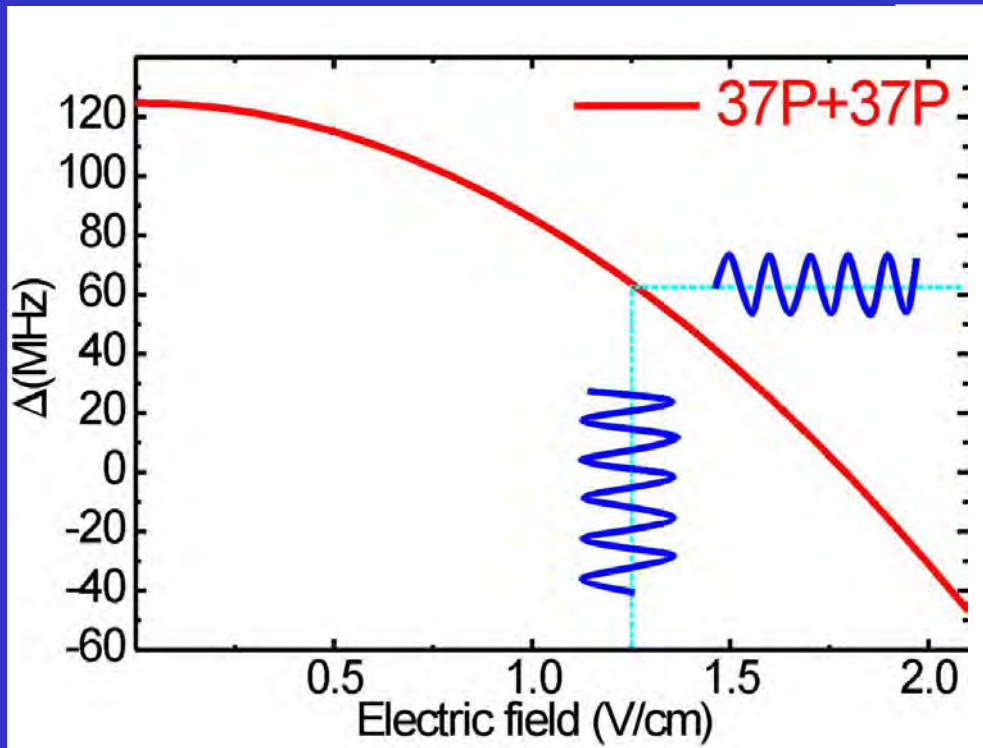
D.B. Tretyakov et al.,
Phys. Rev. A **90**,
041403(R) (2014)

RF-assisted Förster resonances for $39P$ state

D.B. Tretyakov et al.,
Phys. Rev. A **90**,
041403(R) (2014)



Floquet sidebands at rf-modulation of Rydberg states



Electric field

$$F = F_{dc} + F_{rf} \cos(\omega t)$$

Energy of nL Rydberg state

$$E_{nL} = -\alpha_{nL} F^2 / 2$$

$$E_{nL} = -\frac{1}{2} \alpha_{nL} [F_{dc}^2 + \frac{1}{2} F_{rf}^2 + 2F_{dc}F_{rf} \cos(\omega t) + \frac{1}{2} F_{rf}^2 \cos(2\omega t)]$$

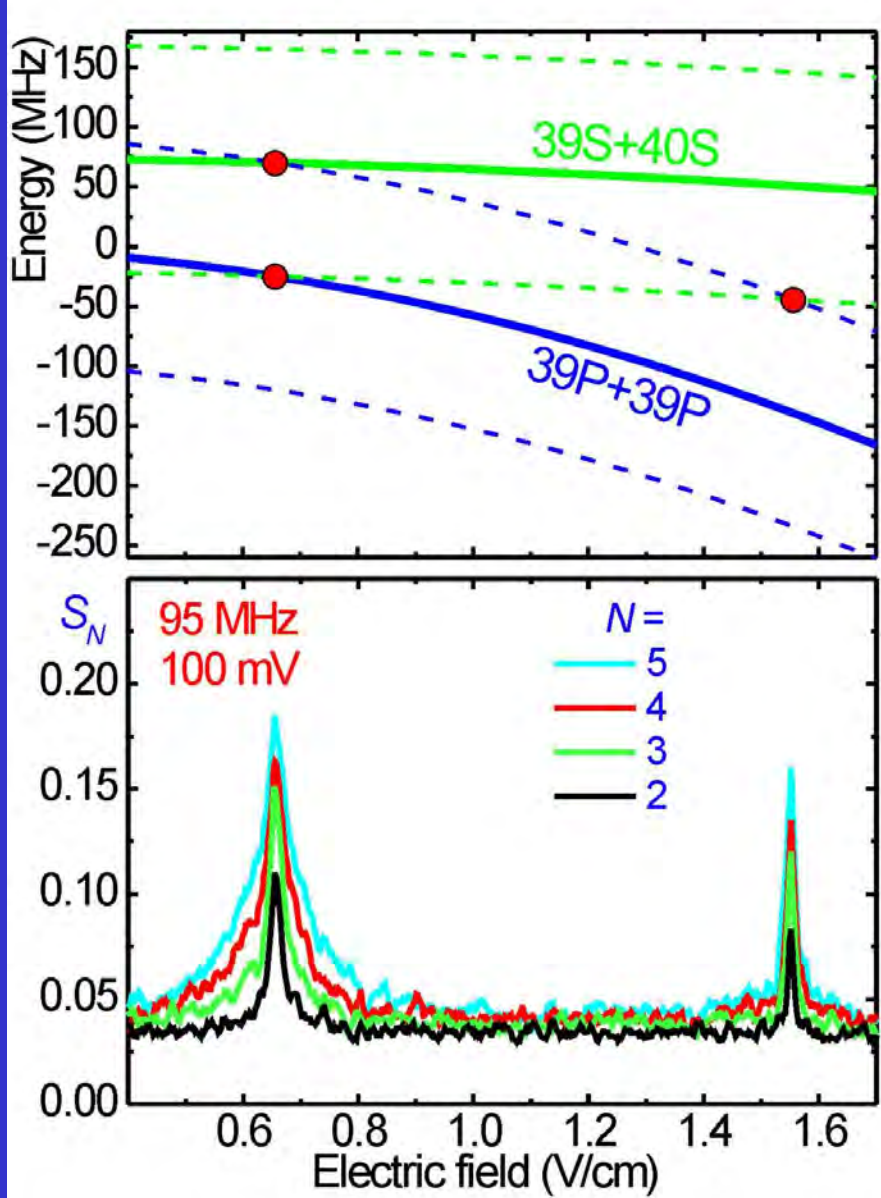
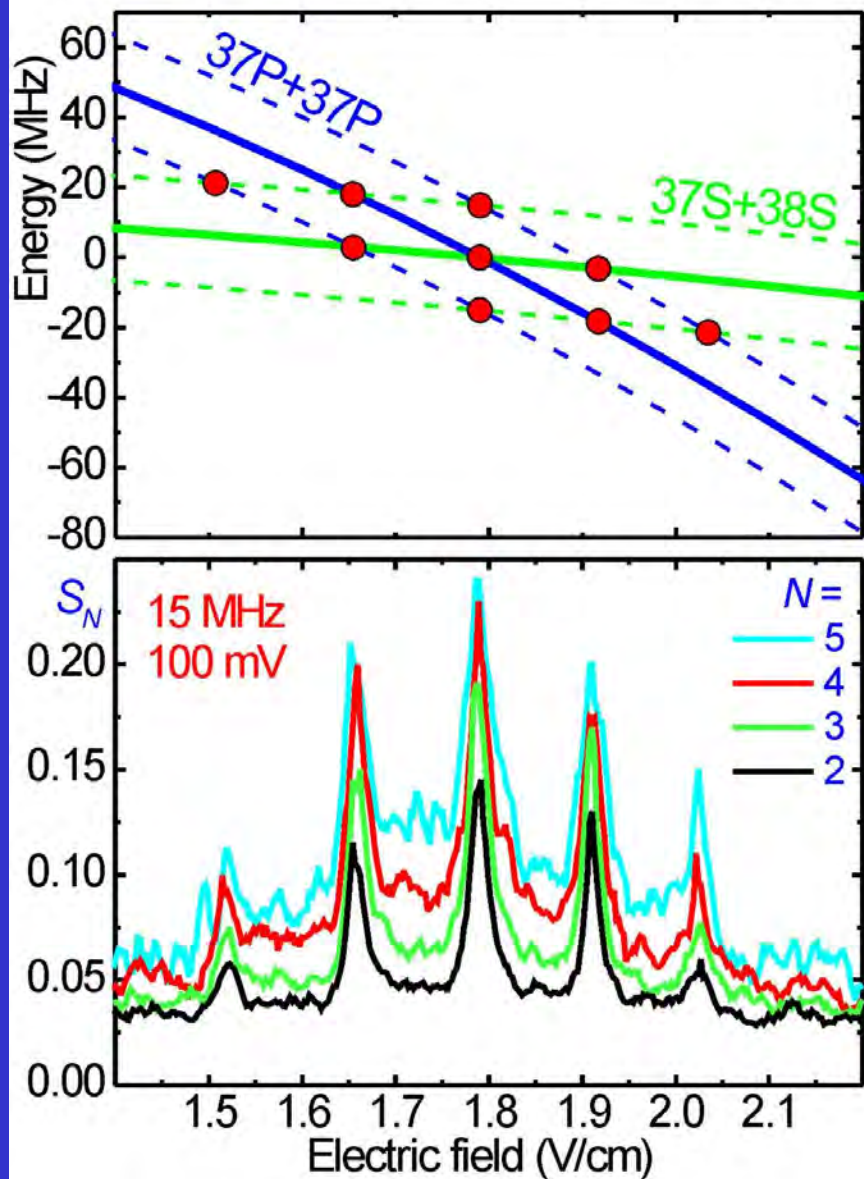
*Wave function
of Rydberg state*

$$\Psi_{nL}(r, t) = \psi_{nL}(r) e^{i\alpha(F_{dc}^2 + F_{rf}^2/2)t/2} \sum_{m=-\infty}^{\infty} a_{nL,m} e^{im\omega t}$$

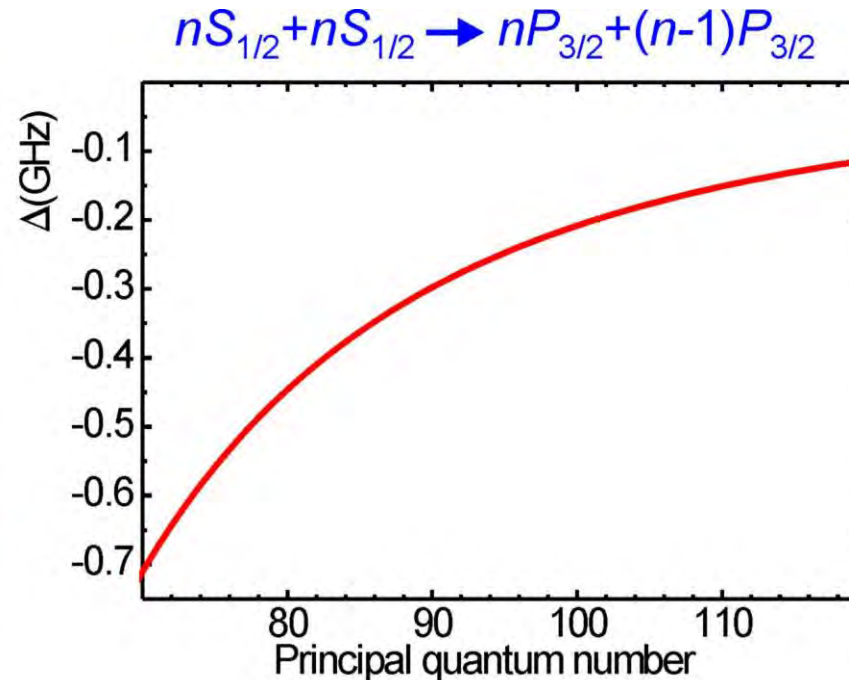
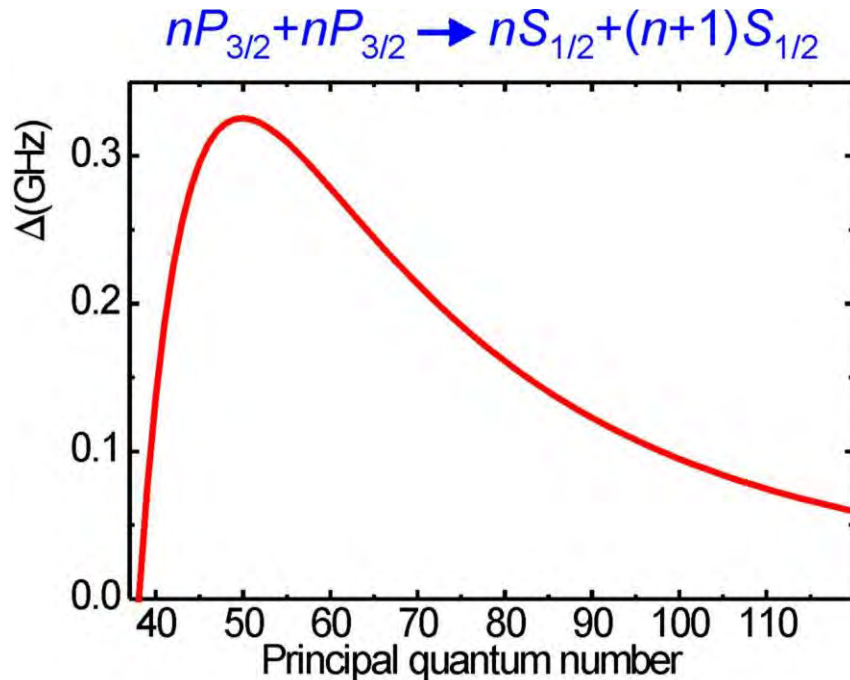
*Amplitudes of
Floquet states*

$$a_{nL,m} = \sum_{k=-\infty}^{\infty} J_{m-2k} \left(\frac{\alpha_{nL} F_{dc} F_{rf}}{\omega} \right) J_k \left(\frac{\alpha_{nL} F_{rf}^2}{8 \omega} \right)$$

RF-assisted Förster resonances in the Floquet states picture



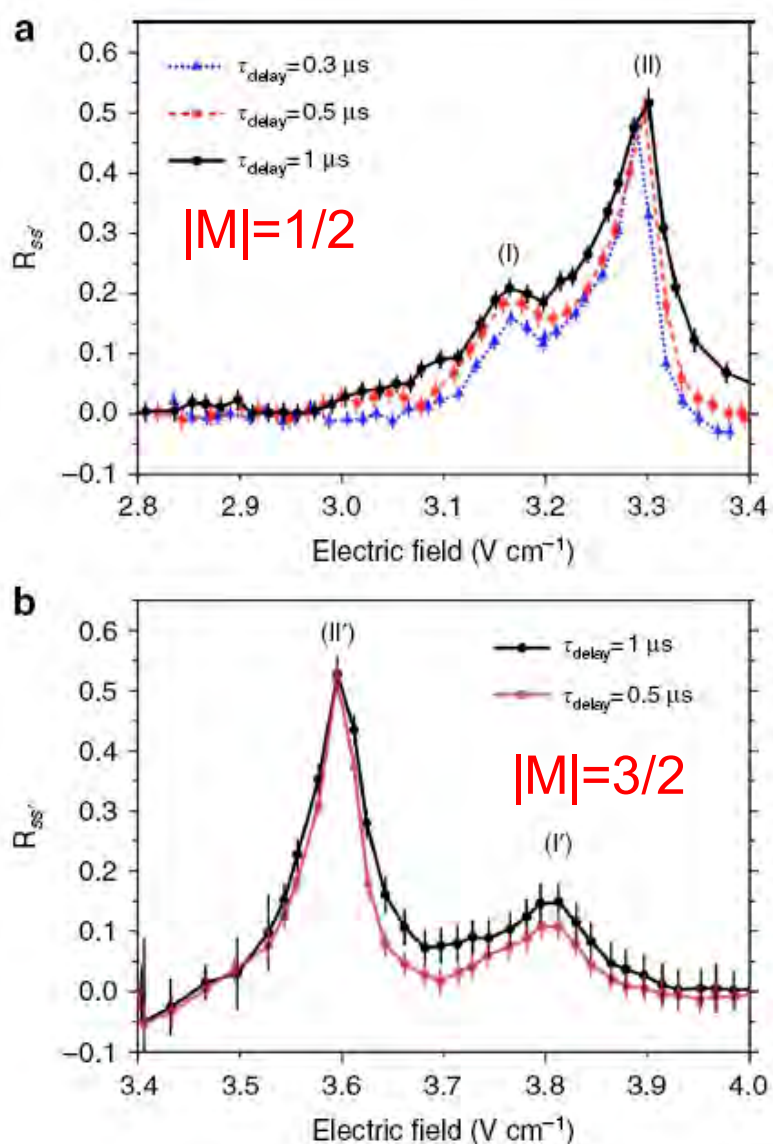
Energy defects of Förster resonances in Rb atoms



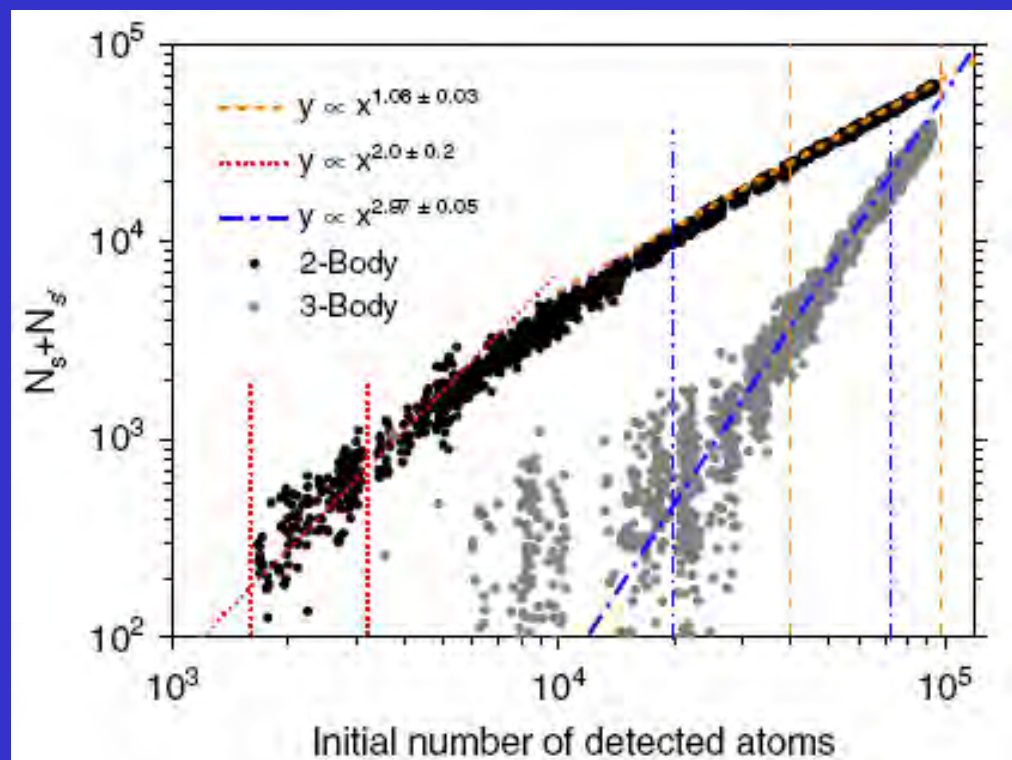
Interaction of any Rydberg atoms with large principal quantum number can be converted from van der Waals to resonant dipole-dipole using radio-frequency assisted Förster resonances with $\omega < 1$ GHz !

Borromean three-body FRET in frozen Rydberg gases

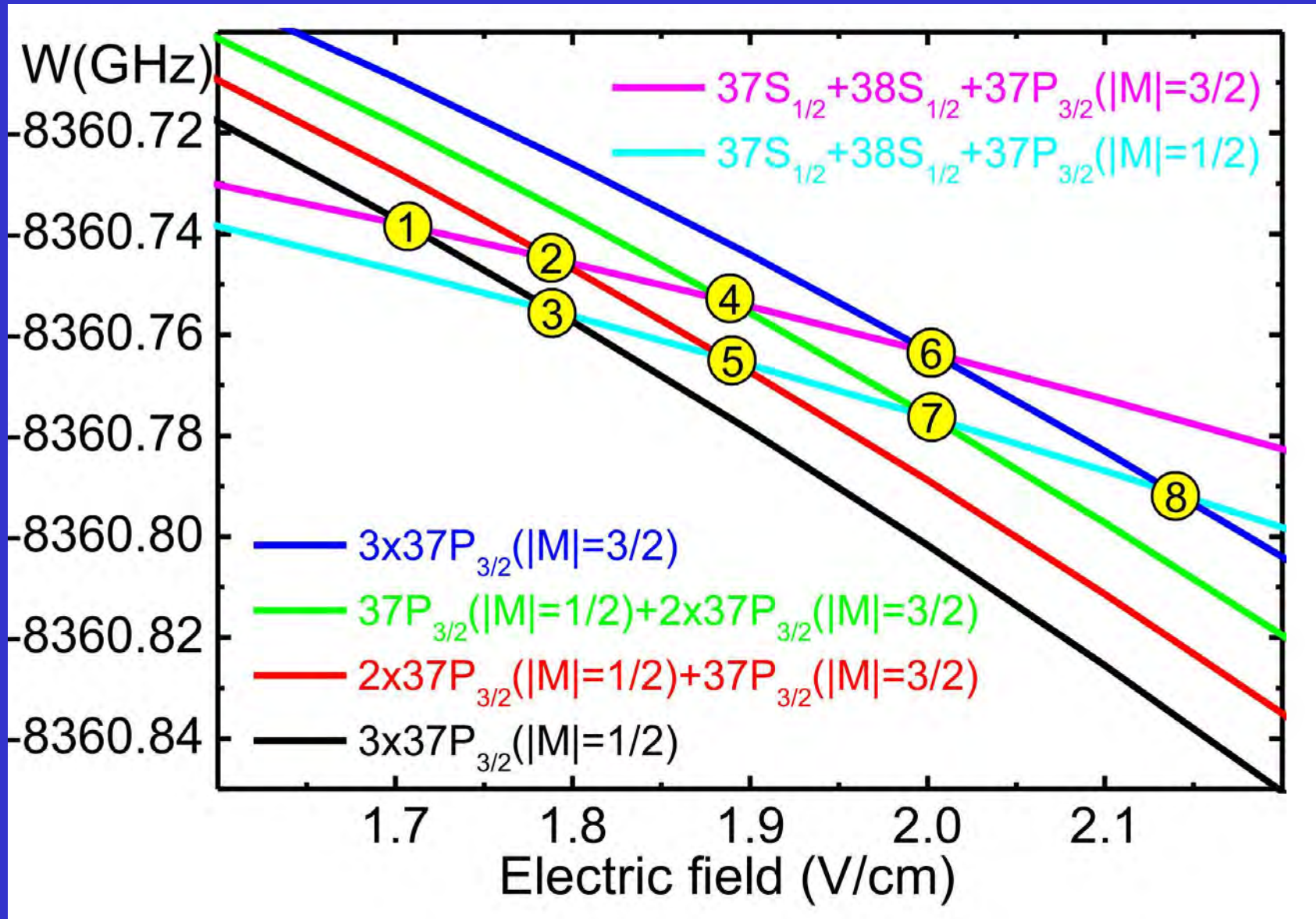
R. Faoro^{1,2}, B. Pelle¹, A. Zuliani¹, P. Cheinet¹, E. Arimondo^{2,3} & P. Pillet¹



$\sim 10^5 \text{ Cs}(35\text{P}_{3/2})$ atoms in the volume of $\sim 200 \mu\text{m}$ in size



Three-body Förster resonances for Rb($37P_{3/2}$) atoms



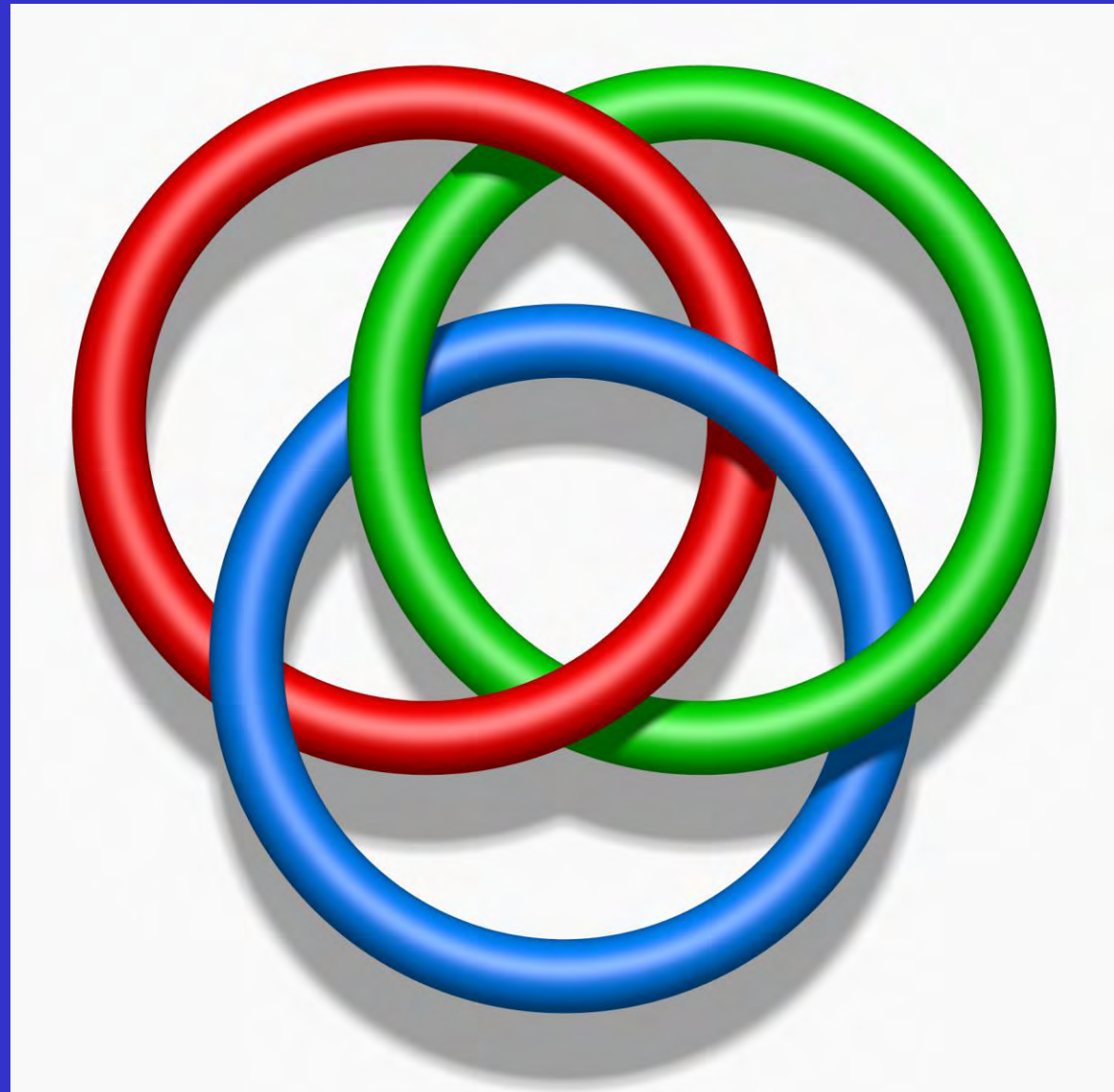
D.B. Tretyakov, I.I. Beterov, E.A. Yakshina, V.M. Entin, I.I. Ryabtsev,
P.Cheinet, and P.Pillet, Phys. Rev. Lett. 119, 173402 (2017)

Borromean three-body interactions of Rydberg atoms

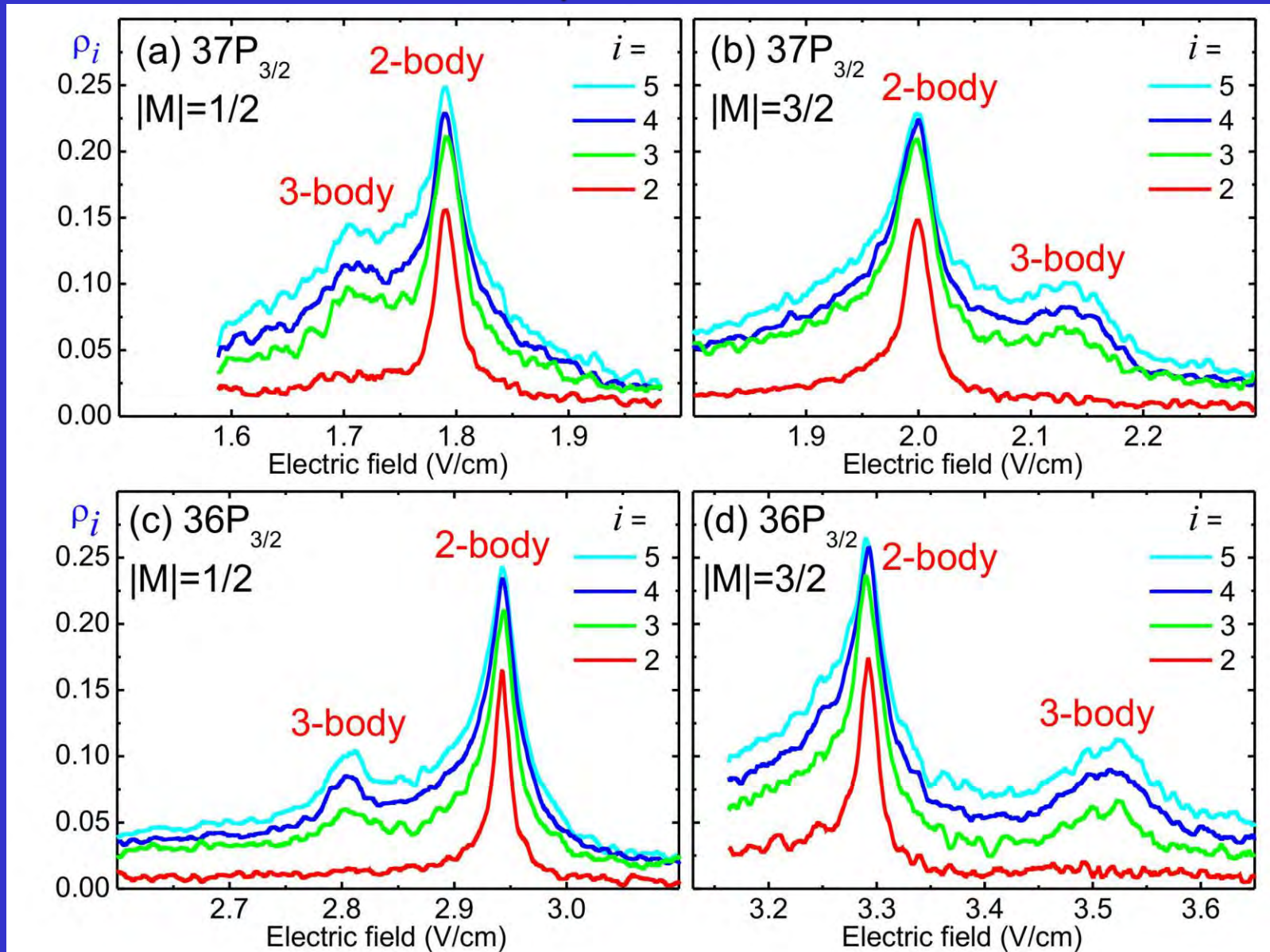
Why Borromean?

Borromean rings consist of three circles which are linked, but removing any ring results in two unlinked rings.

Borromean FRET is featured by the strong three-body interactions with a negligible contribution of two-body interactions.

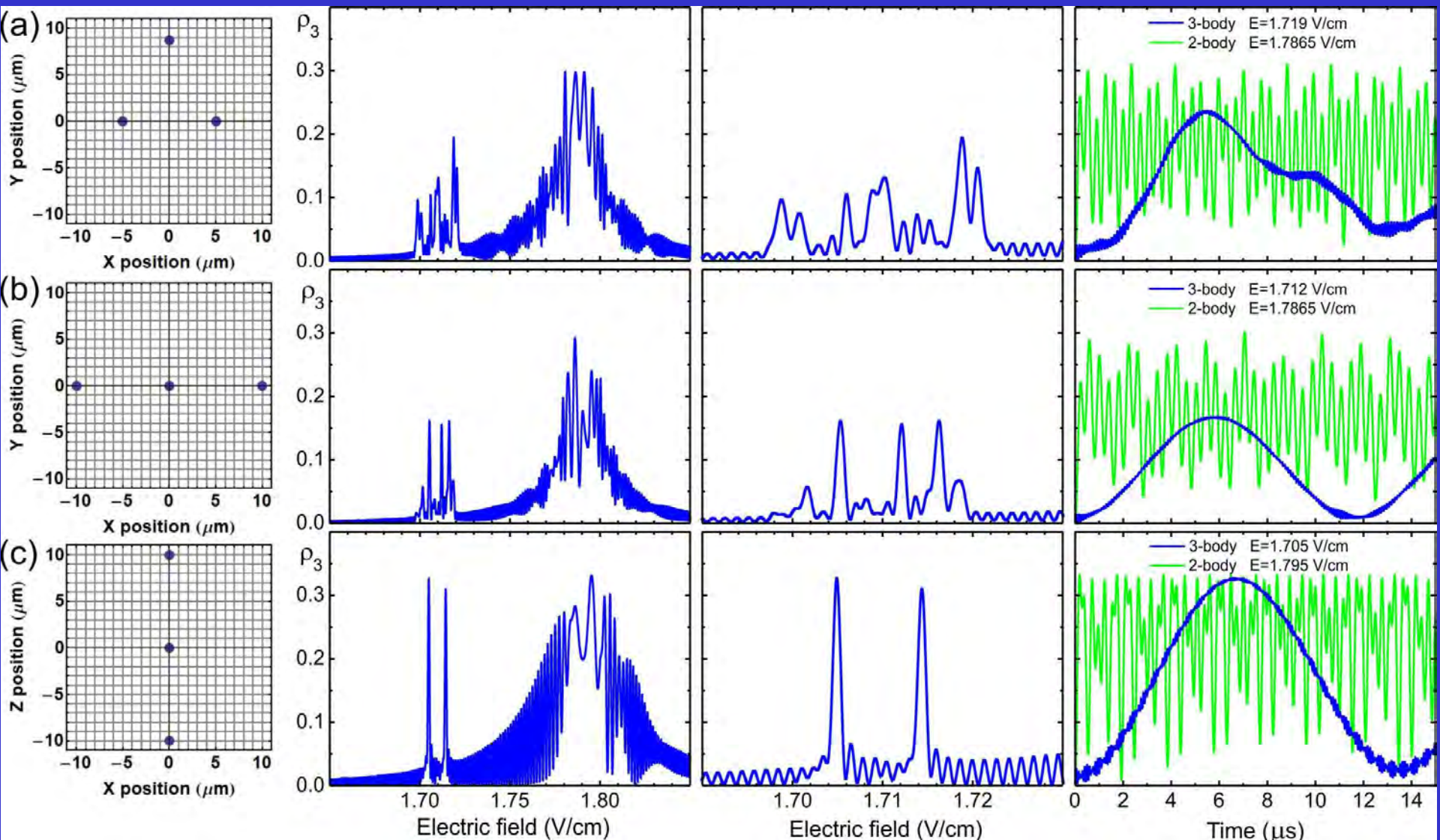


Observation of three-body Förster resonances in Rb atoms



D.B. Tretyakov, I.I. Beterov, E.A. Yakshina, V.M. Entin, I.I. Ryabtsev,
P.Cheinet, and P.Pillet, Phys. Rev. Lett. 119, 173402 (2017)

Coherence of three-body Förster resonances (full theory)



I.I.Ryabtsev, I.I.Beterov, D.B.Tretyakov, E.A.Yakshina, V.M.Entin,
P.Cheinet, and P.Pillet, Phys. Rev. A 98, 052703 (2018)

Three-qubit quantum gates

Toffoli gate

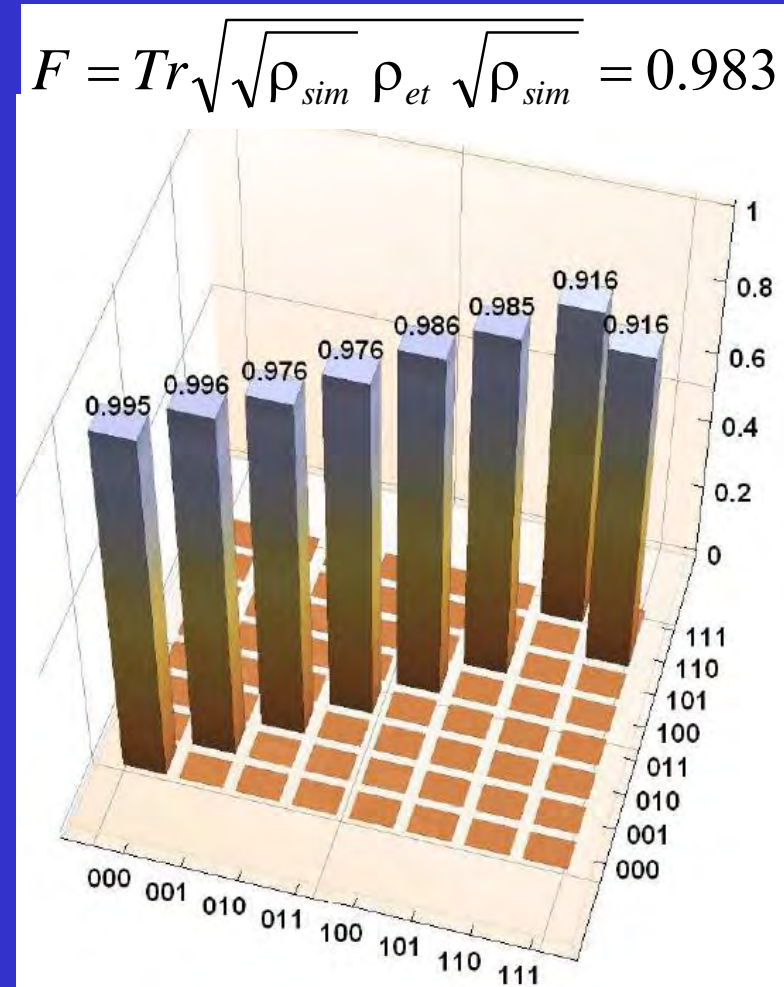
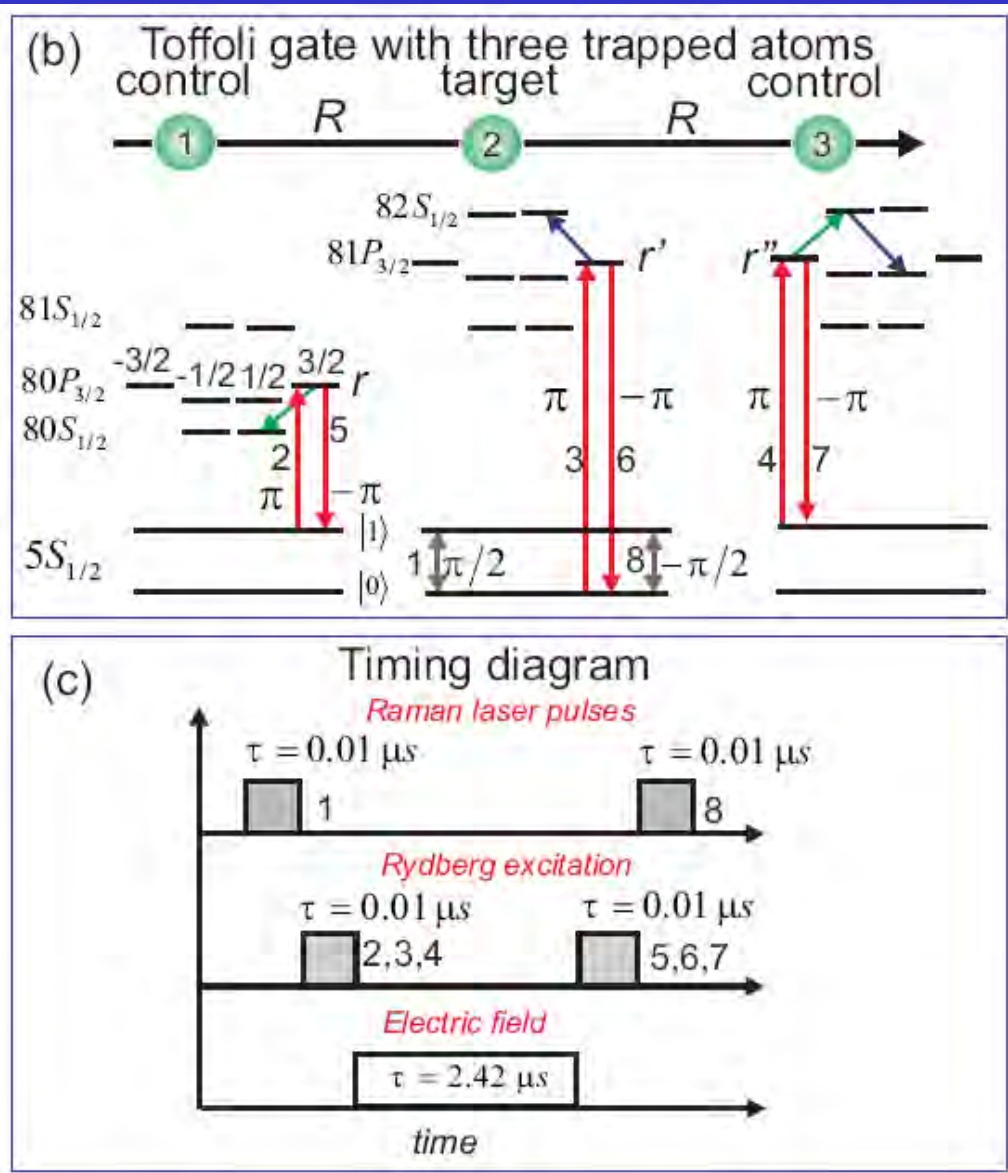
INPUT			OUTPUT		
0	0	0	0	0	0
0	0	1	0	0	1
0	1	0	0	1	0
0	1	1	0	1	1
1	0	0	1	0	0
1	0	1	1	0	1
1	1	0	1	1	1
1	1	1	1	1	0

Fredkin gate

INPUT			OUTPUT		
0	0	0	0	0	0
0	0	1	0	0	1
0	1	0	0	1	0
0	1	1	1	0	1
1	0	0	1	0	0
1	0	1	1	1	0
1	1	0	0	1	0
1	1	1	1	1	1

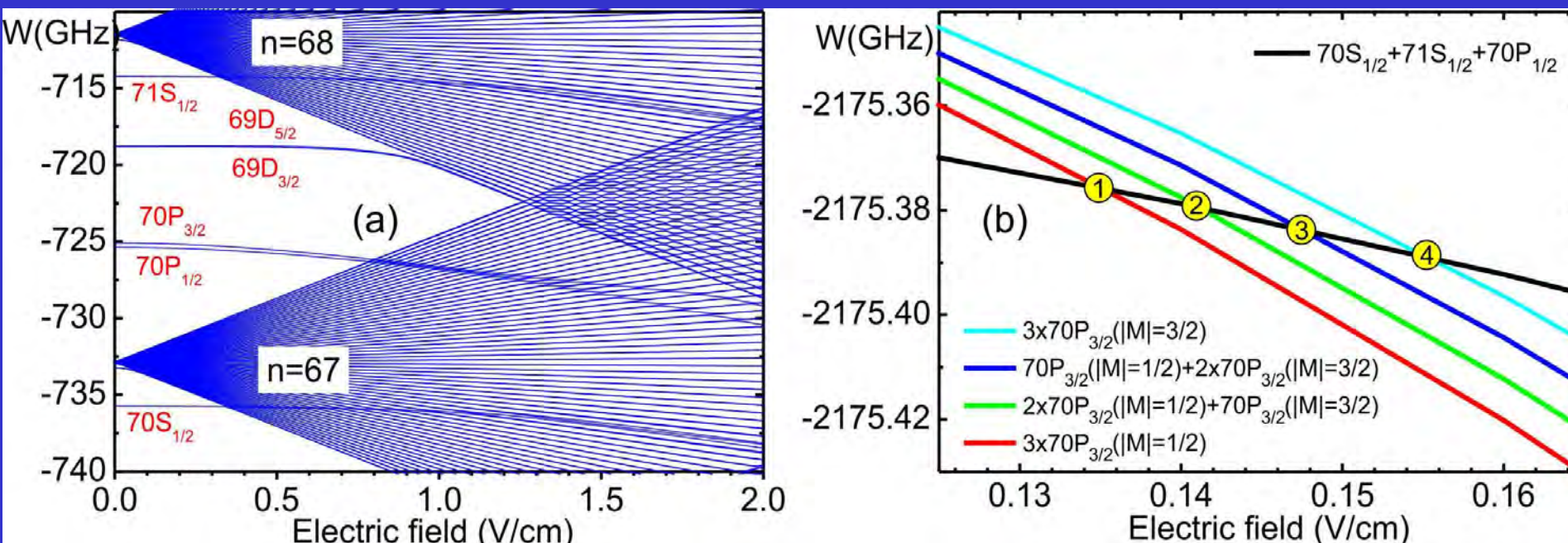
Useful for error correction and further speedup of quantum computation

Scheme of a 3-qubit Toffoli gate



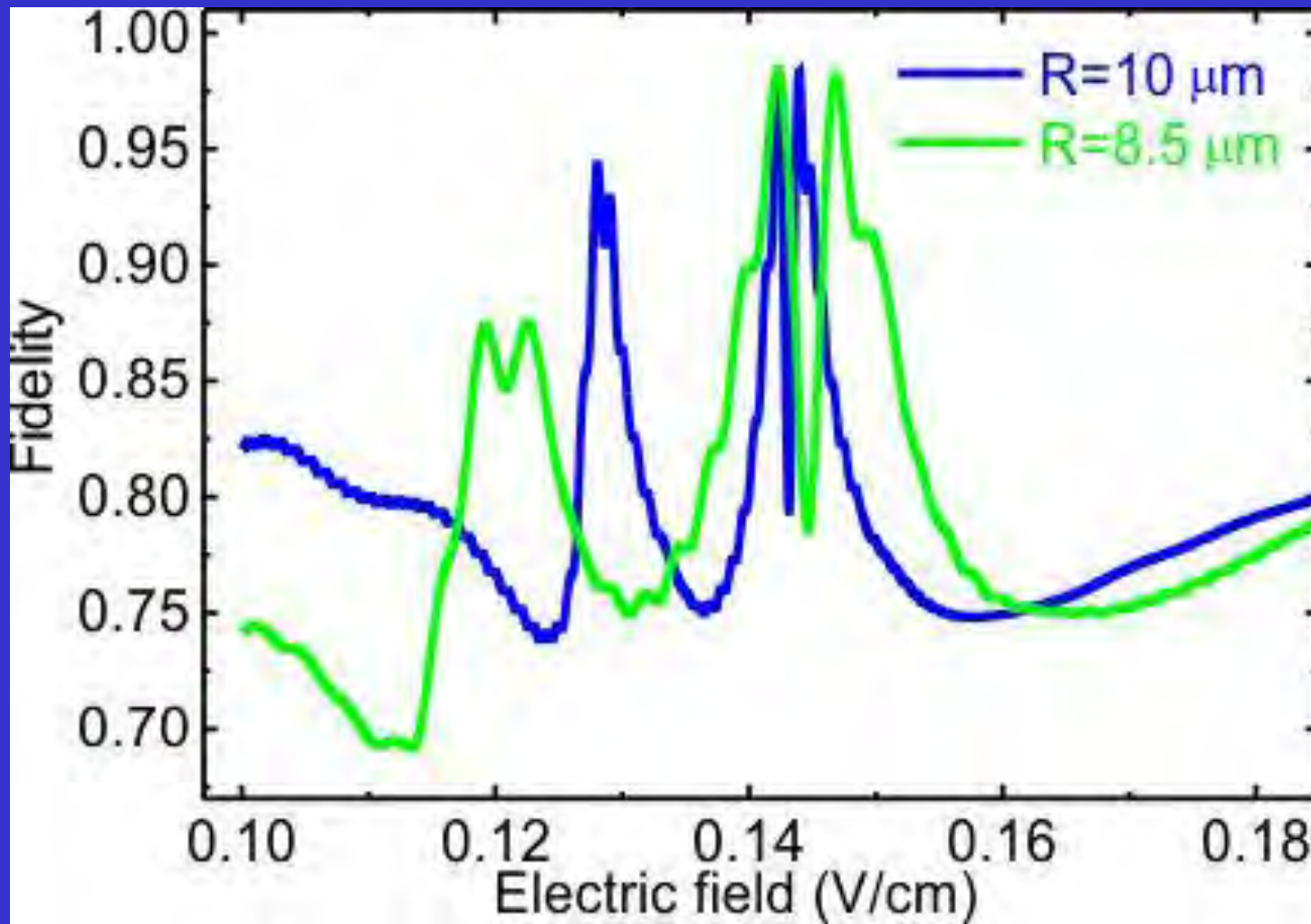
I.I.Beterov, I.N.Ashkarin, E.A.Yakshina,
D.B.Tretyakov, V.M.Entin, I.I.Ryabtsev,
P.Cheinet, P.Pillet, M.Saffman, Phys. Rev.
A **98**, 042704 (2018)

Three-body Förster resonance of a new type $3 \times nP_{3/2} \rightarrow nS_{1/2} + (n+1)S_{1/2} + nP_{1/2}$ for Rb atoms



(a) Calculated Stark map of Rydberg states of Rb atoms near the $70P$ state.
(b) Calculated Stark structure of a new-type Förster resonance for three Rb Rydberg atoms. Crossings of collective states (indicated by numbers) correspond only to three-body Förster resonances, when all three atoms change their states, while two-body resonances are absent.

Numerical results for the fidelity of new Toffoli gate



Dependence of the fidelity of the Toffoli gate on the dc electric field for interatomic distances of 10 and $8.5 \mu\text{m}$. The maximum achievable fidelity is 98.5%.

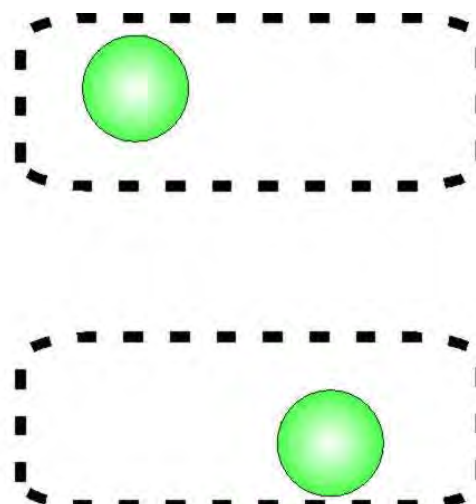
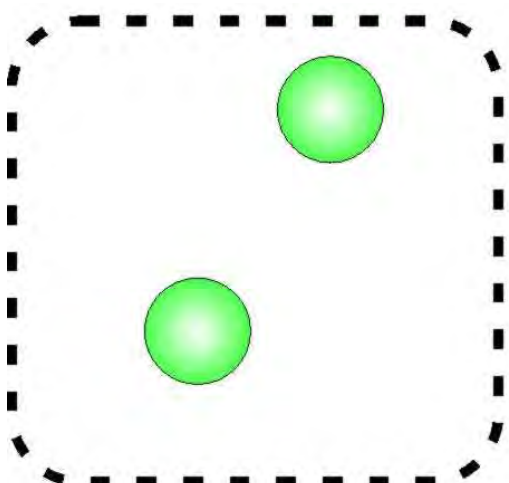
Conditional Quantum Phase Gate $|ab\rangle \rightarrow \exp(i \pi \delta_{a1} \delta_{b1}) |ab\rangle$

*Evolution of population
at Förster resonance
in two frozen atoms:*

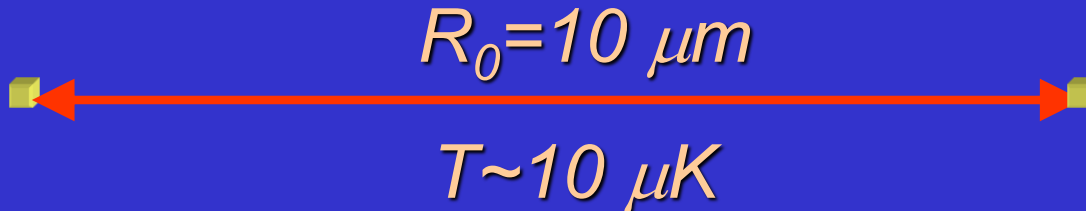
$$\rho_2(t) = \frac{1}{2} \sin^2\left(\sqrt{2} \Omega_{ab} t\right)$$

$$\Omega_{ab} \cong \frac{d_1 d_2}{\hbar R^3}$$

Spatial configurations for two trapped Rydberg atoms

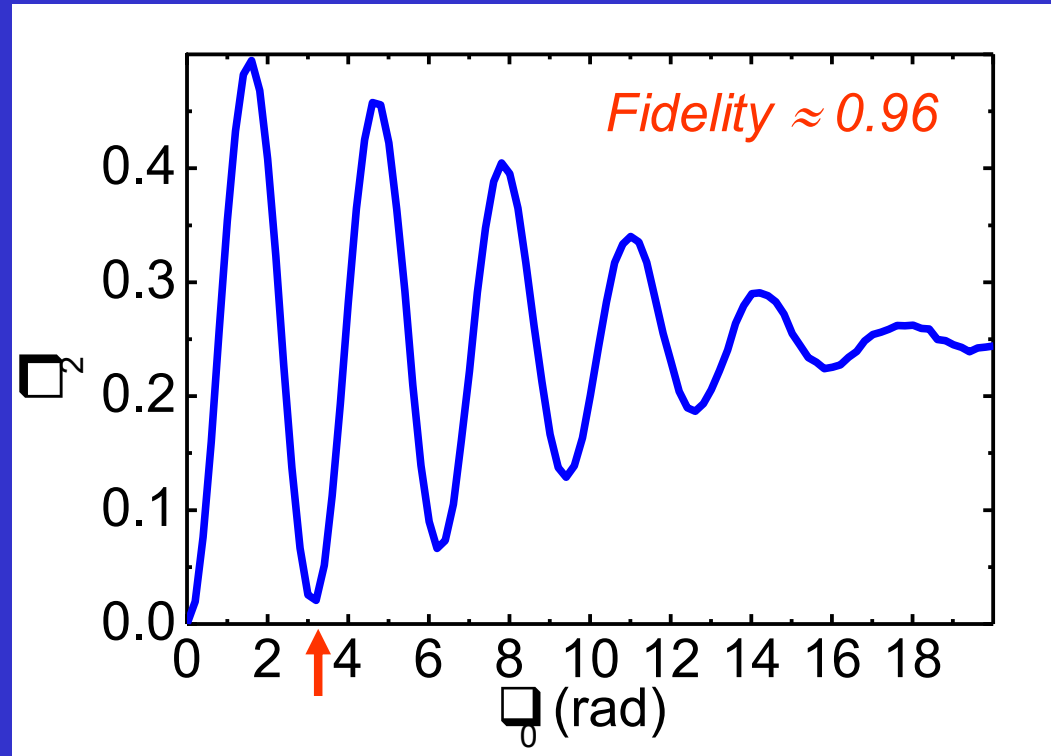


Numerical modeling for Conditional Quantum Phase Gate

$$|ab\rangle \rightarrow \exp(i \pi \delta_{a1} \delta_{b1}) |ab\rangle$$


$$\rho_2(t) = \frac{1}{2} \sin^2(\theta_0)$$

$$\theta_0 = \frac{2\sqrt{2}d_1 d_2 t_0}{4\pi\varepsilon_0 \hbar R_0^3}$$

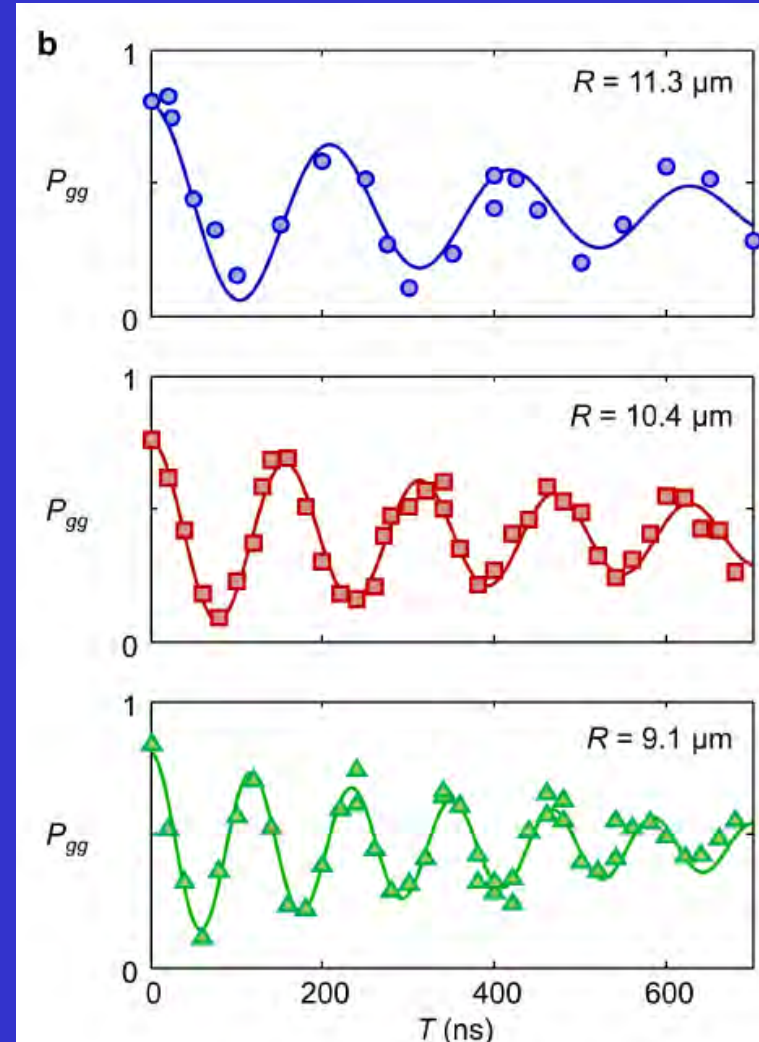
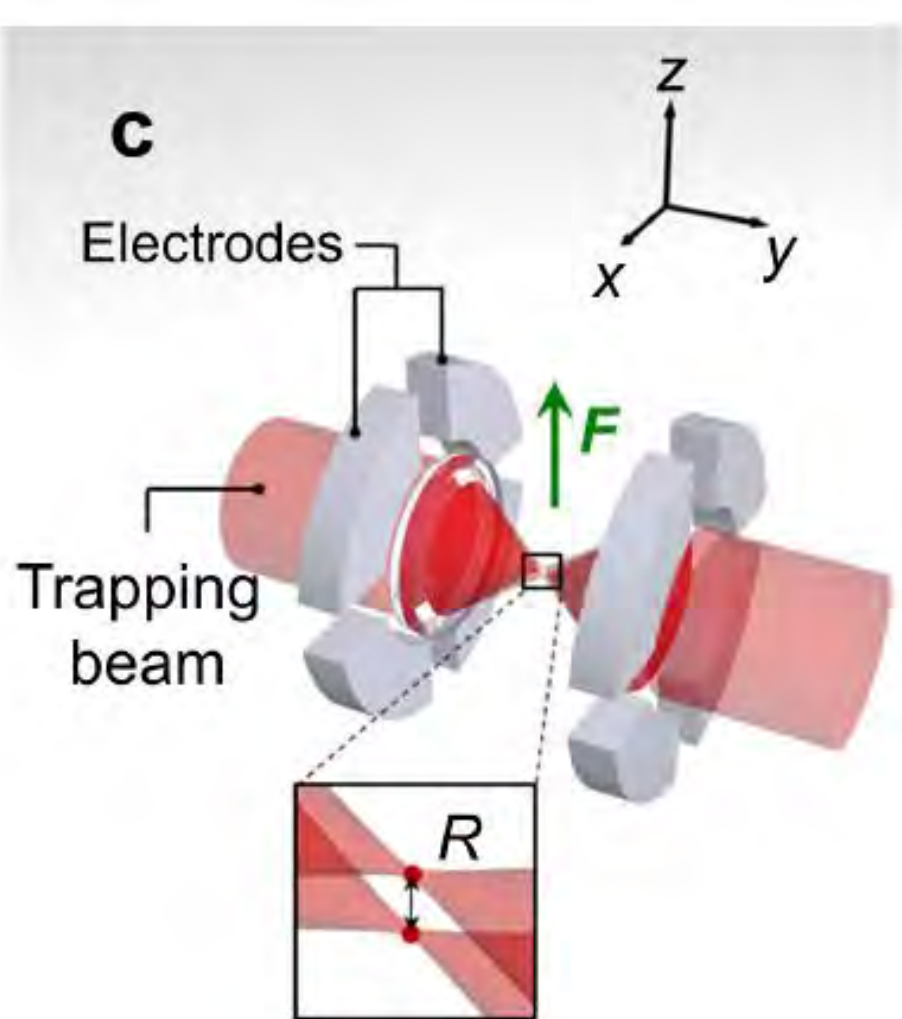


I.I.Ryabtsev et al., Phys. Rev. A 82, 053409 (2010)

Coherent dipole-dipole coupling between two single atoms at a Förster resonance

S. Ravets, H. Labuhn, D. Barredo, L. Béguin, T. Lahaye, and A. Browaeys

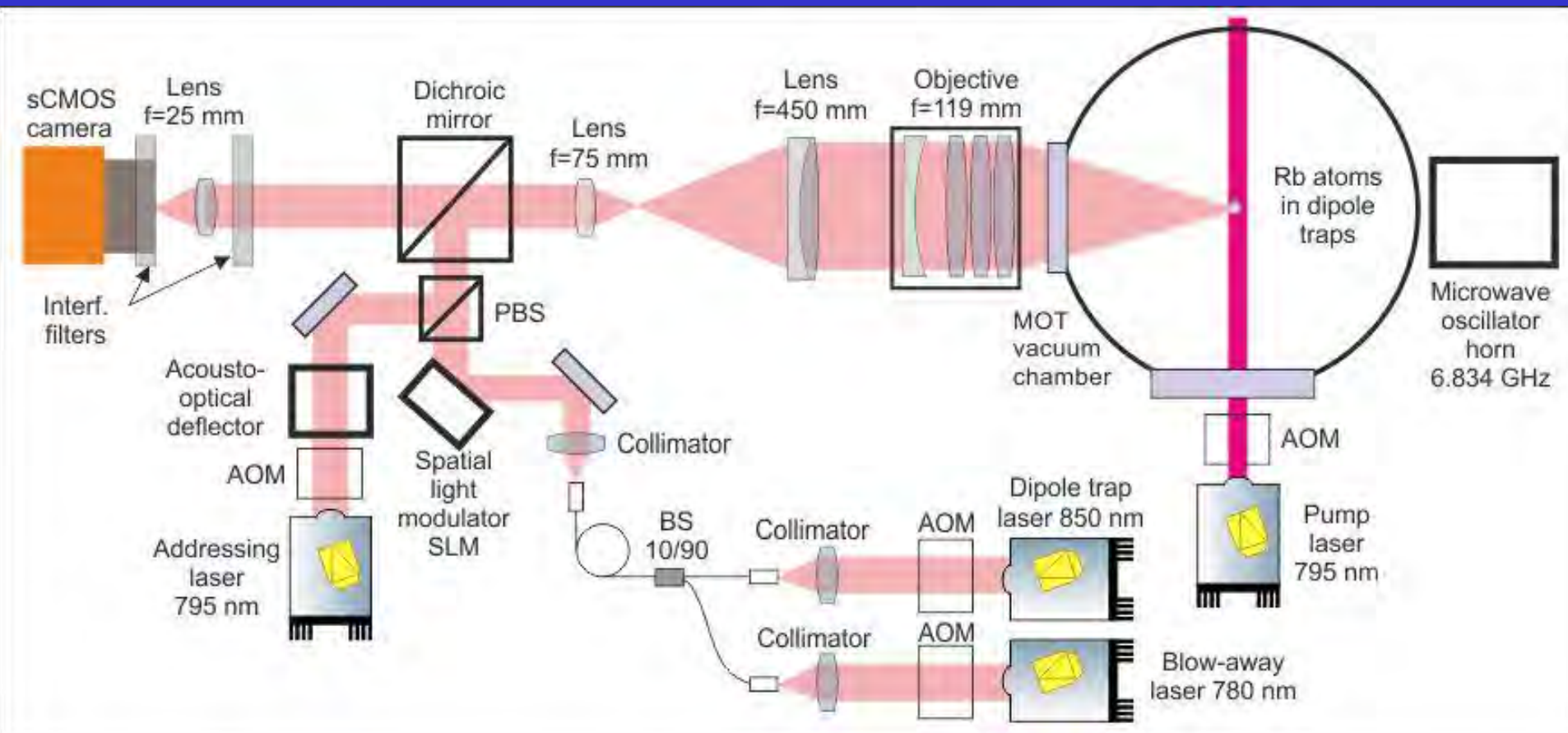
*Laboratoire Charles Fabry, UMR 8501, Institut d'Optique, CNRS, Univ Paris Sud 11,
2 avenue Augustin Fresnel, 91127 Palaiseau Cedex, France*



Experimental setup for implementing individually-addressed quantum gates with ^{87}Rb atoms in an array of optical dipole traps

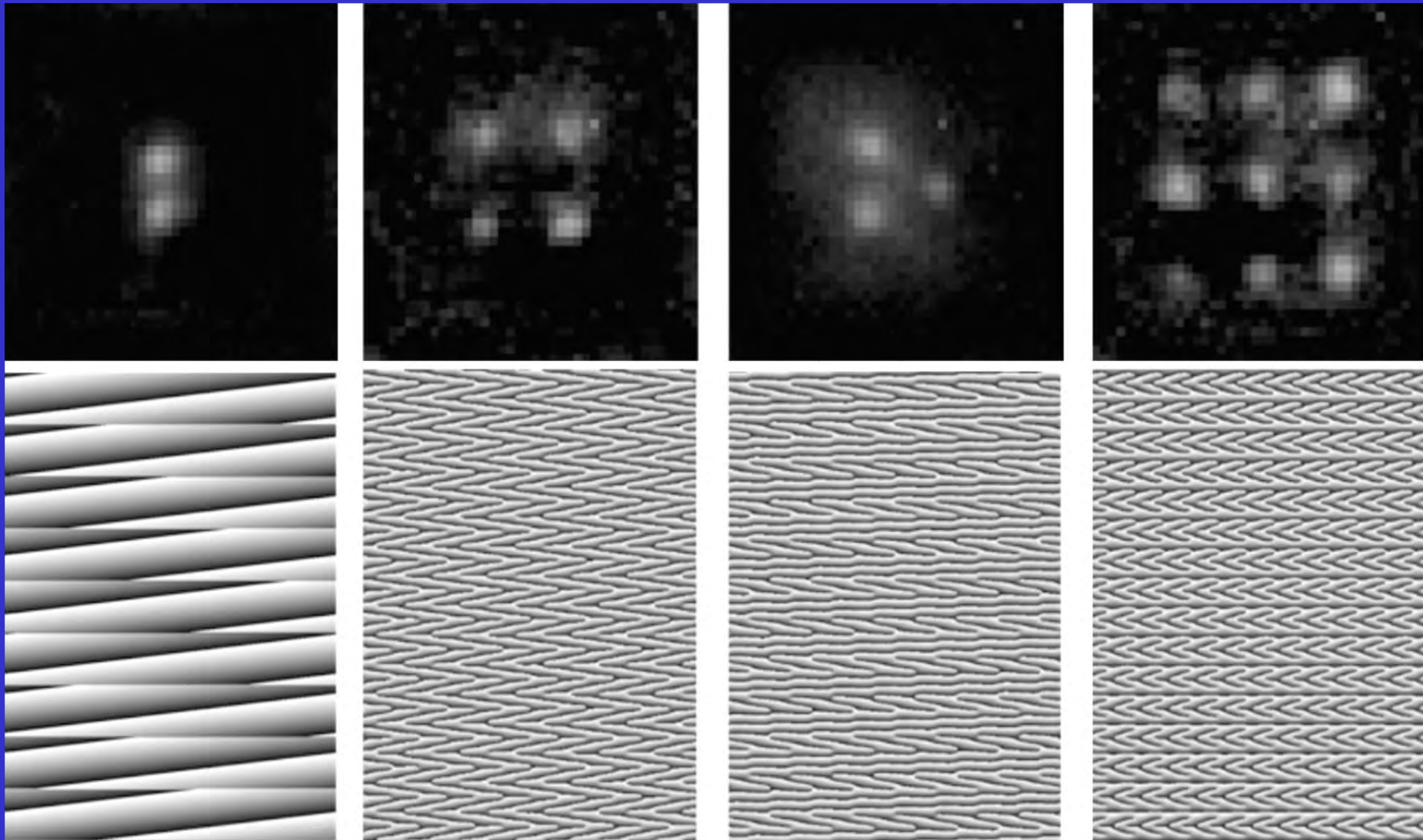


Experimental setup for implementing individually-addressed one-qubit gates with ^{87}Rb atoms in an array of optical dipole traps

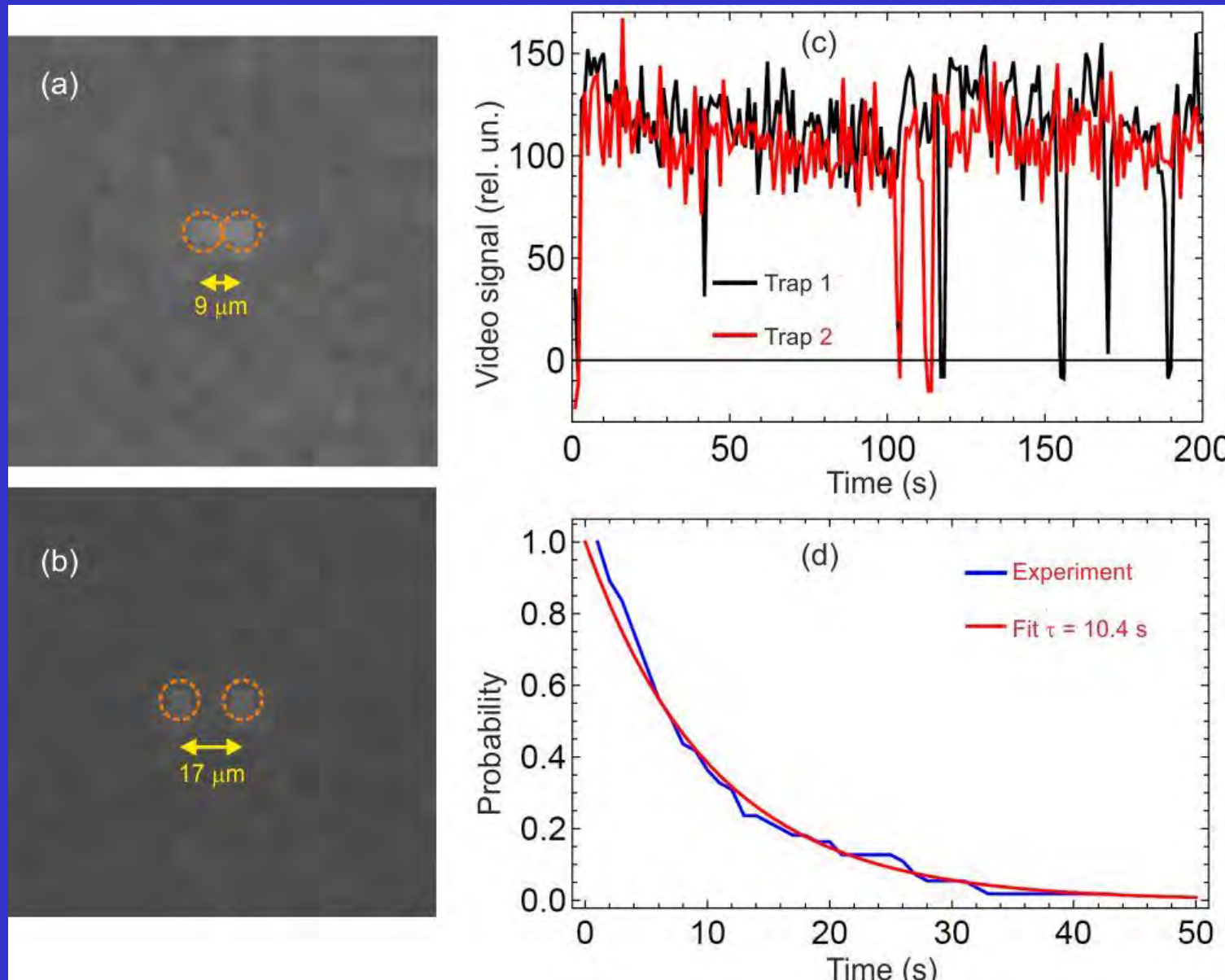


A spatial light modulator SLM forms a trap array, and addressing laser 795 nm with acousto-optical deflector (AOD) is used for individual addressing. SLM is a mirror split to many 20 micron-sized elements controlled independently. It forms a mask for the laser wave front. After focusing, an array of optical dipole traps of arbitrary dimensions can be formed.

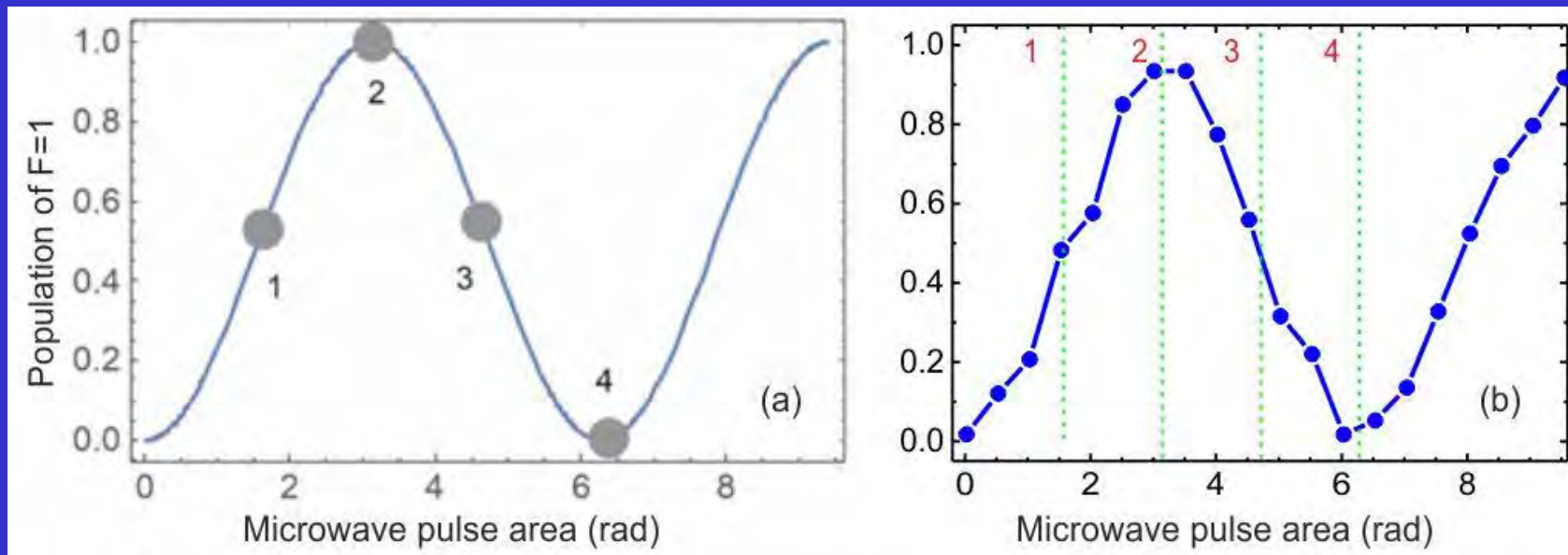
Trapping of Rb atoms in arrays of various dimensions with separation of $15 \mu\text{m}$, and corresponding phase masks of SLM



Trapping of two ^{87}Rb atoms into two optical dipole traps separated by 9-17 μm and measurement of simultaneous trapping time



Rabi oscillations on a "clock" microwave transition in a single ^{87}Rb atom and the truth table for one-qubit gates



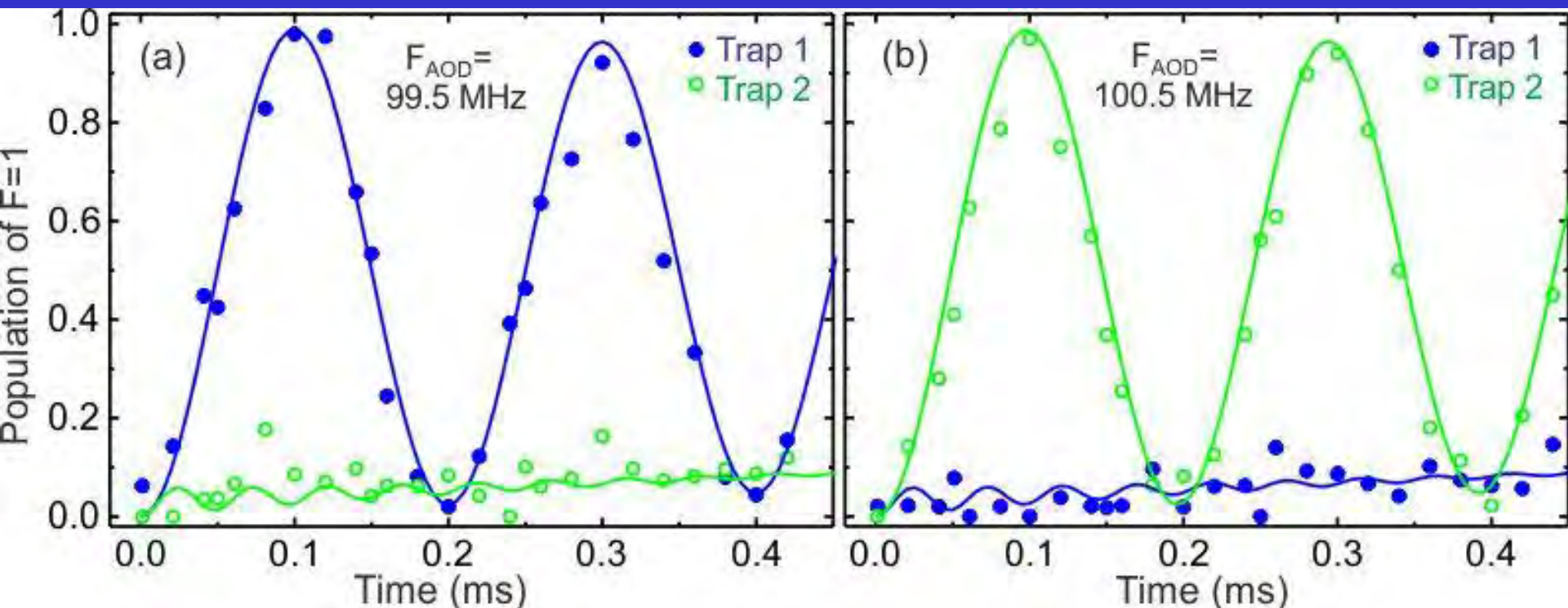
Various points correspond to various one-qubit gates:

- | | |
|-----------------------------------|------------------------------|
| 1 - Hadamard gate form state "0"; | 2 - NOT gate from state "0"; |
| 3 - Hadamard gate form state "1"; | 4 - NOT gate from state "1". |

Initial qubit state	Result of performing the gate H	Fidelity of performing the gate H	Result of performing the gate NOT	Fidelity of performing the gate NOT
0	0.489 ± 0.02	$97.8 \pm 4\%$	0.935 ± 0.02	$93.5 \pm 2\%$
1	0.465 ± 0.02	$93 \pm 4\%$	0.035 ± 0.02	$96.5 \pm 2\%$

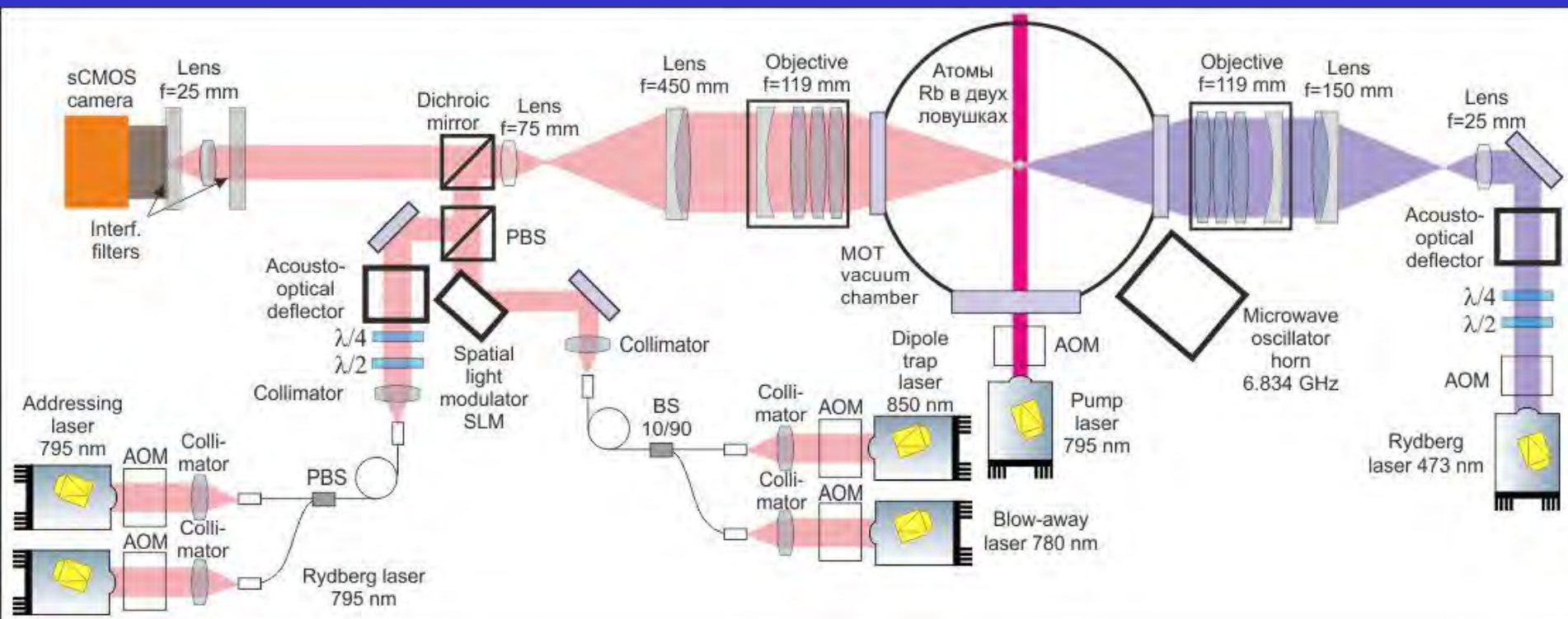
The average fidelity of one-qubit gates is $95.2 \pm 3\%$.

Rabi oscillations on a "clock" microwave transition in two ^{87}Rb atoms with individual addressing



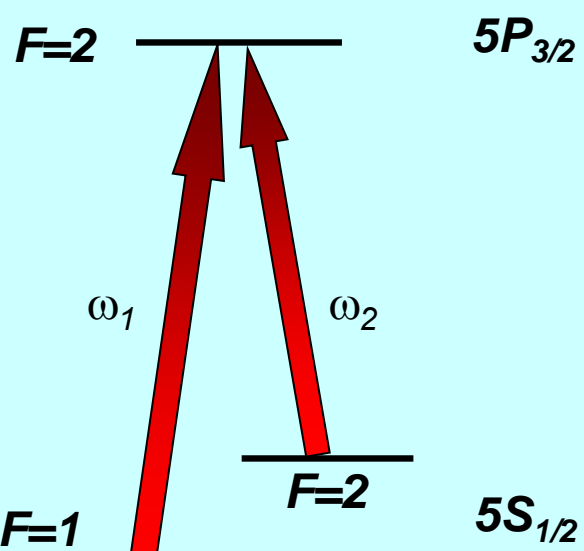
The Rabi frequency is 5 kHz, contrast is 97%, and coherence time is 4 ms. The average fidelity of one-qubit gates is $91.8 \pm 3\%$, crosstalk is $4.7 \pm 1\%$. For SPAM error taken into account, the fidelity of one-qubit rotations is $97 \pm 3\%$. To reduce SPAM error, we need to increase the fidelity of optical pumping and reduce the parasitic repumping at blowing-away detection. But it is already possible to start experiments on two-qubit gates.

Experimental setup for implementing two- and three-qubit quantum gates with ^{87}Rb atoms in an array of optical dipole trap

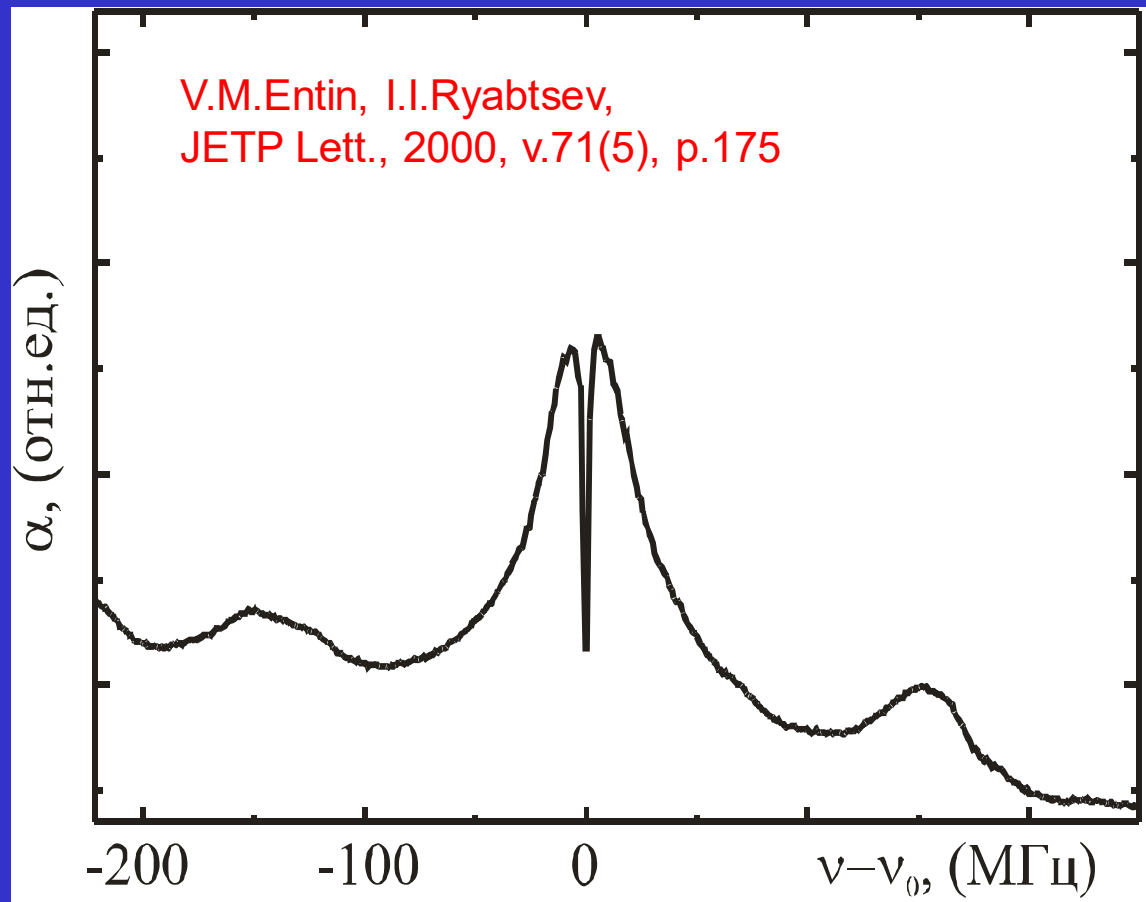


Added are the lasers of the first (795 nm) and second (473 nm) excitation steps of Rydberg states and an optical system to focus the second-step laser radiation. The experiments are in progress.

Electromagnetically induced transparency (EIT)



*Two long-lived
ground-state levels*



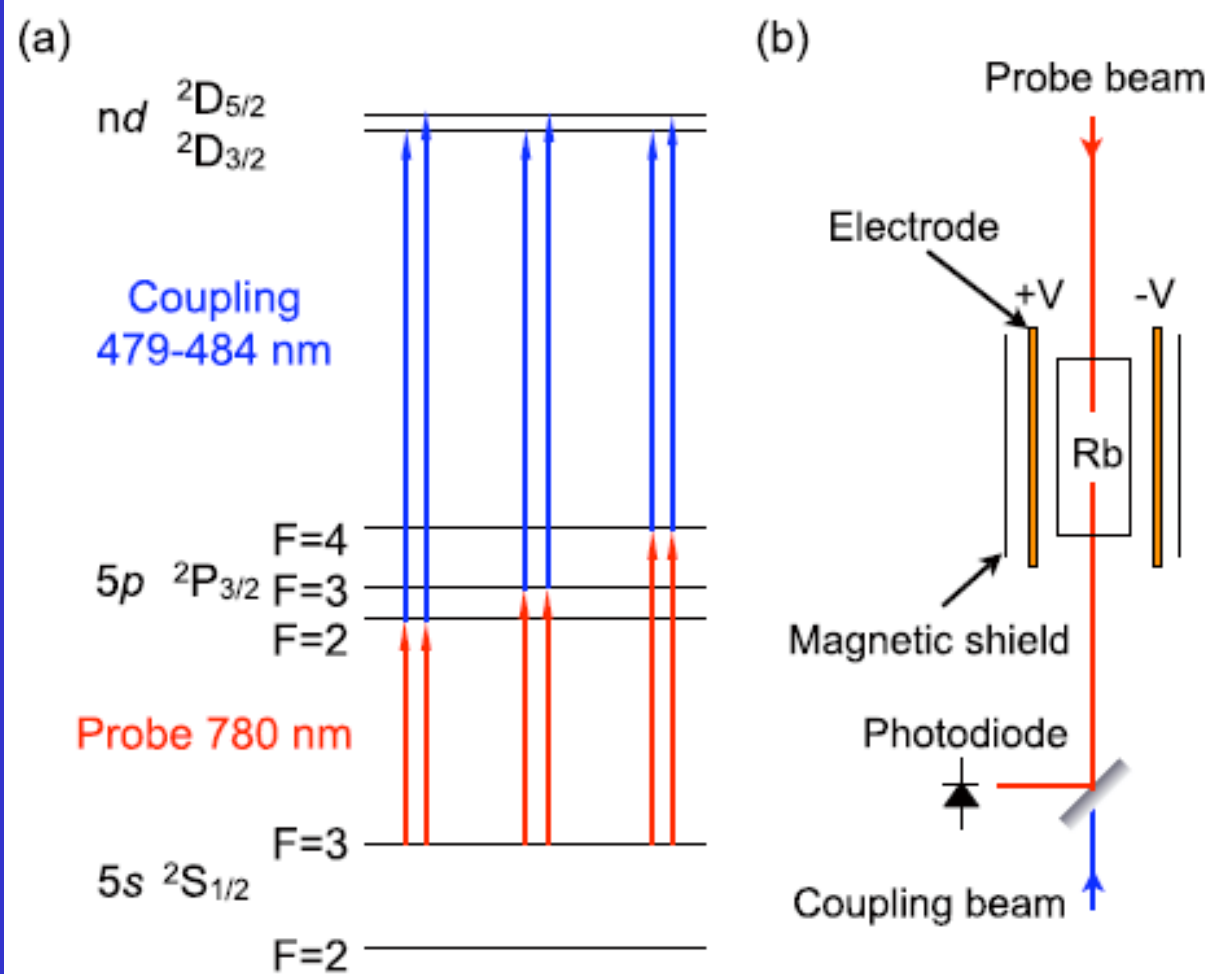
The width of the narrow EIT dip is determined by the lifetimes of ground-state levels or by transit time

Coherent Optical Detection of Highly Excited Rydberg States Using Electromagnetically Induced Transparency

A. K. Mohapatra, T. R. Jackson, and C. S. Adams

Department of Physics, Durham University, Rochester Building, South Road, Durham DH1 3LE, United Kingdom

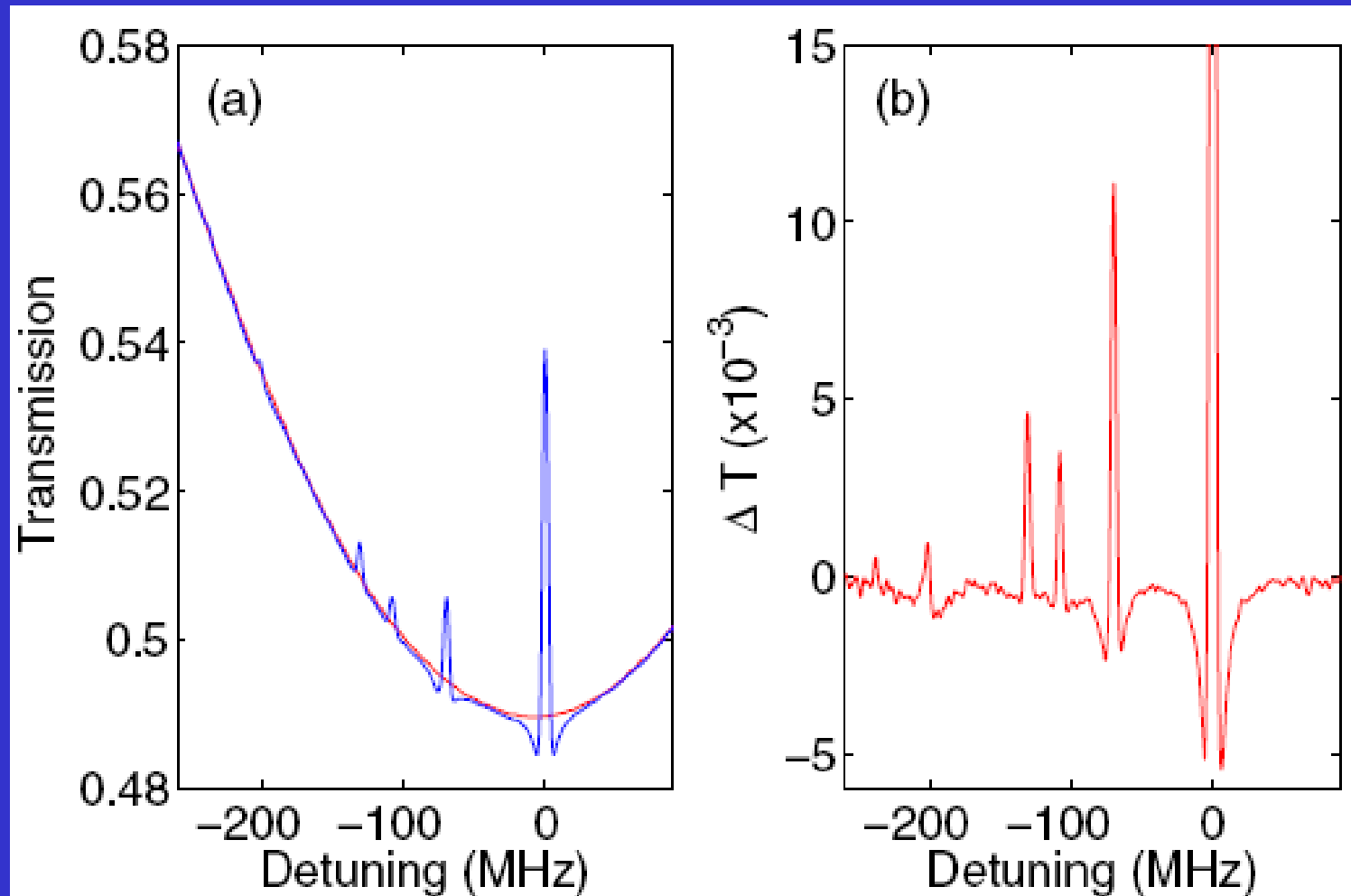
One of the long-lived ground-state level is replaced by a long-lived Rydberg state



Coherent Optical Detection of Highly Excited Rydberg States Using Electromagnetically Induced Transparency

A. K. Mohapatra, T. R. Jackson, and C. S. Adams

Department of Physics, Durham University, Rochester Building, South Road, Durham DH1 3LE, United Kingdom



A giant electro-optic effect using polarizable dark states

Nature Physics 4,
890 (2008)

ASHOK K. MOHAPATRA^{1*}, MARK G. BASON¹, BJÖRN BUTSCHER², KEVIN J. WEATHERILL¹
AND CHARLES S. ADAMS^{1*}

Table 1 The value of the Kerr coefficient, B_0 , for various media.

Medium	$B_0 (\times 10^{-18} \text{ m V}^{-2})$
Gas (CO ₂ , 1 atm) ³⁵	10 ⁰
Water ³⁶	10 ²
Glass ³⁶	10 ⁴
Nitrobenzene ³⁶	10 ⁶
Rydberg dark states (this experiment)	> 10 ¹²

Measurement of the electric dipole moments for transitions to rubidium Rydberg states via Autler–Townes splitting

New Journal of Physics
13 (2011) 093012

M J Piotrowicz¹, C MacCormick^{1,3}, A Kowalczyk¹,
S Bergamini^{1,3}, I I Beterov² and E A Yakshina²

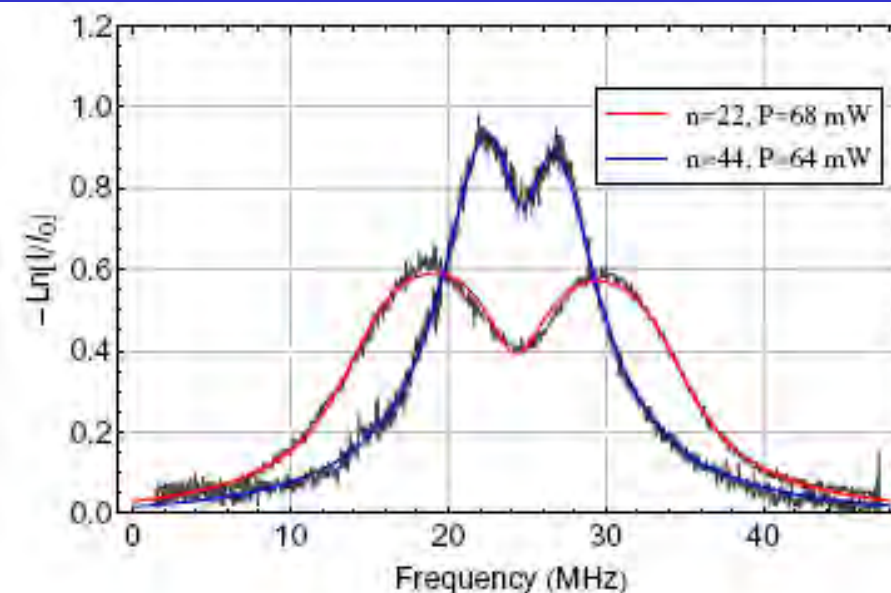
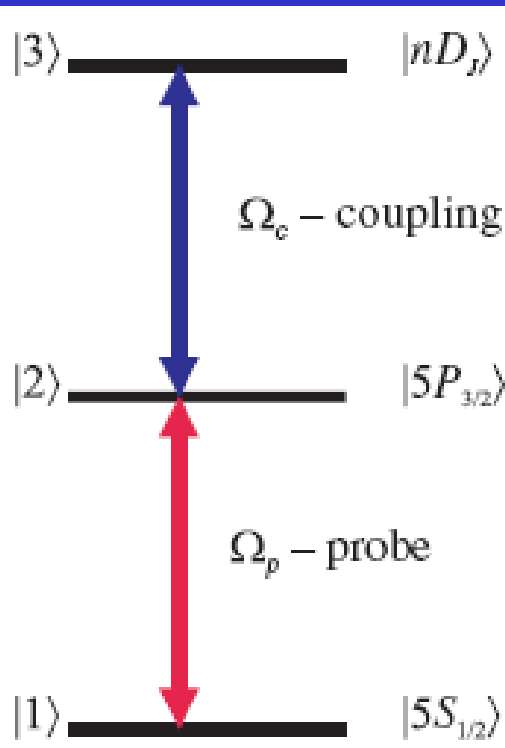
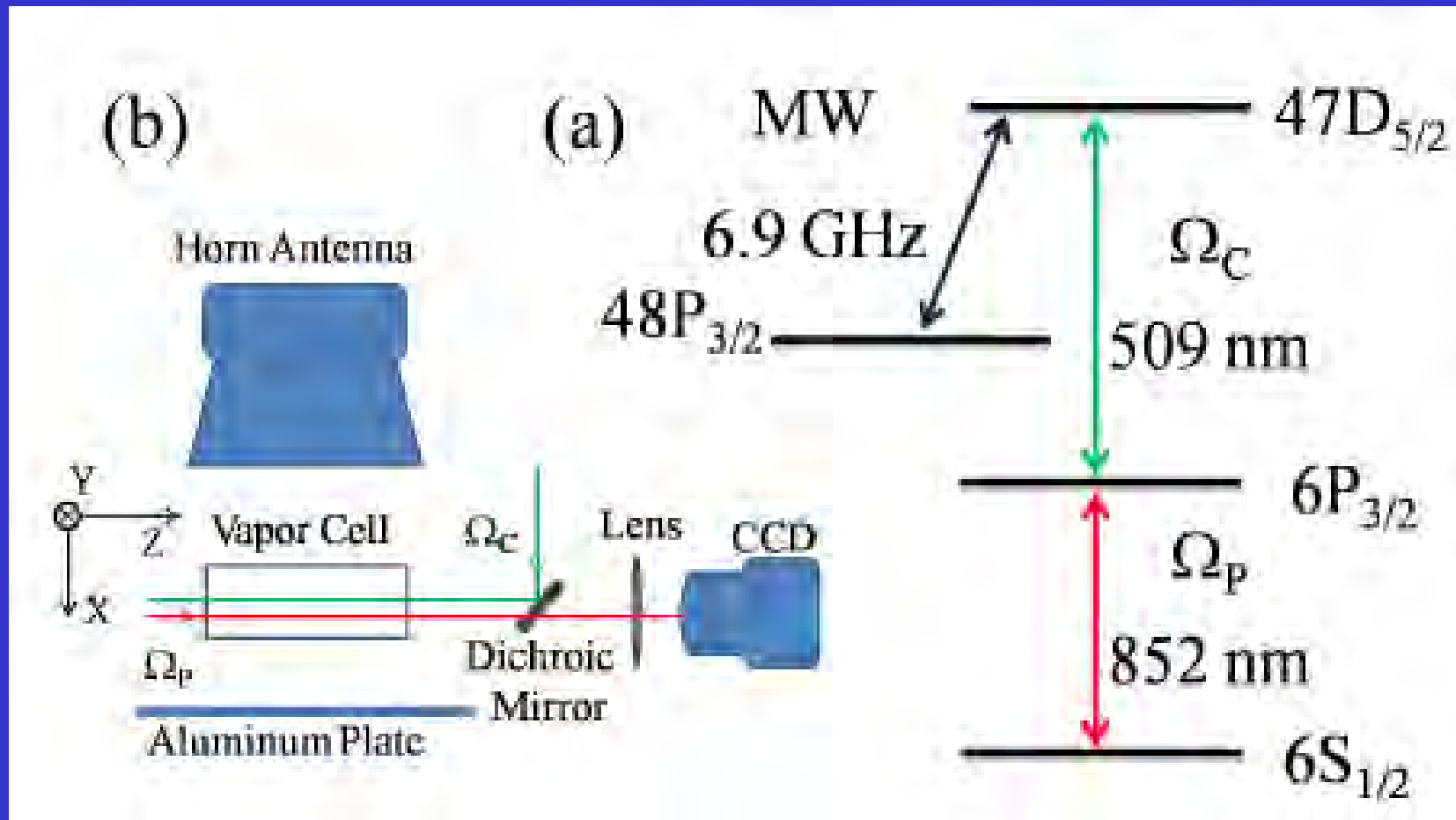


Figure 3. Typical AT spectra recorded for the upper state $44D_{5/2}$ and $22D_{5/2}$. Solid lines show the modeling of the lineshape.

Sub-wavelength microwave electric field imaging using Rydberg atoms inside atomic vapor cells

H.Q. Fan,¹ S. Kumar,¹ R. Daschner,² H. Kübler,^{1,2} and J. P. Shaffer^{1,*}

Optics Letters Vol. 39, Issue 10, pp. 3030-3033 (2014)

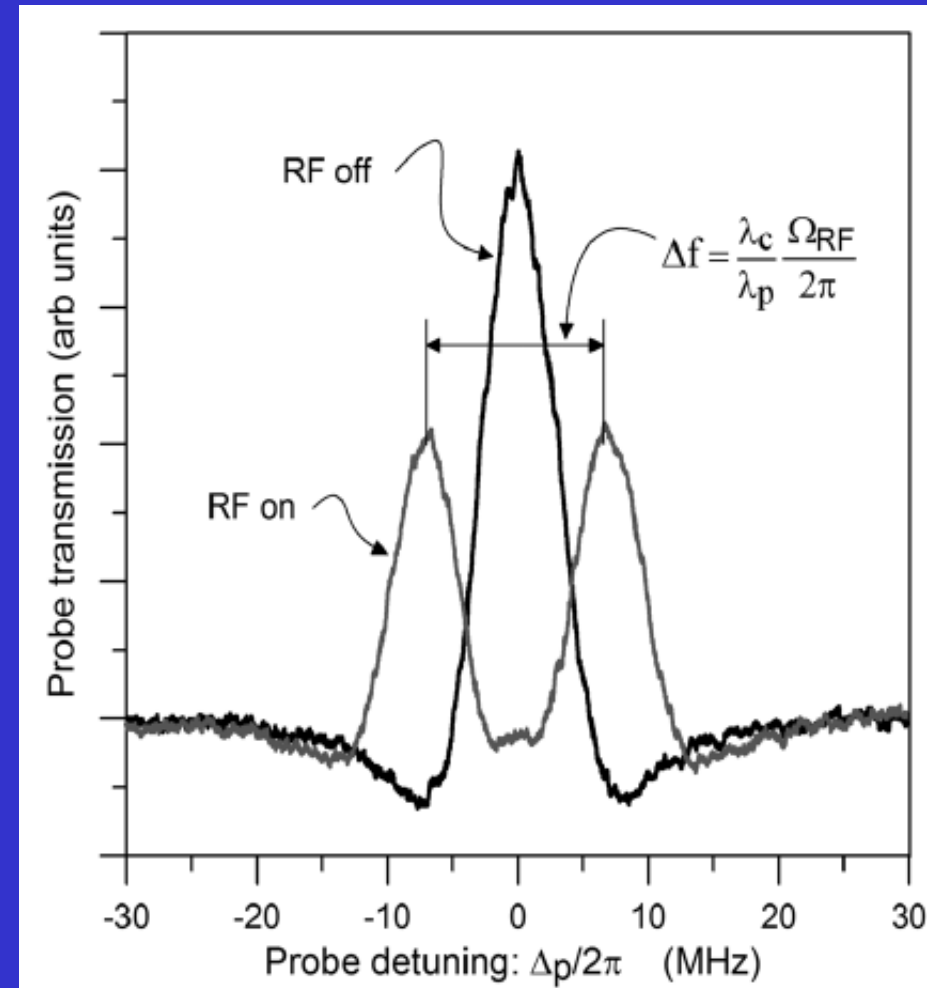
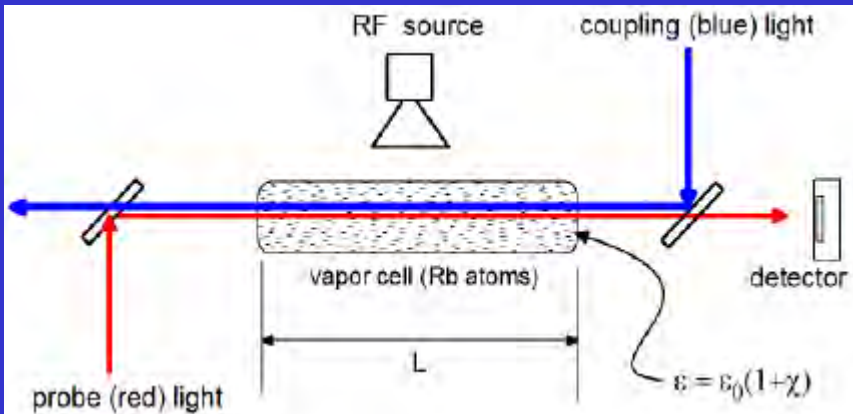


Sub-Wavelength Imaging and Field Mapping

via EIT and Autler-Townes Splitting In Rydberg Atoms*

Christopher L. Holloway,^{1,†} Joshua A. Gordon,¹ Andrew Schwarzkopf,² David A. Anderson,² Stephanie A. Miller,² Nithiwadee Thaicharoen,² and Georg Raithel²

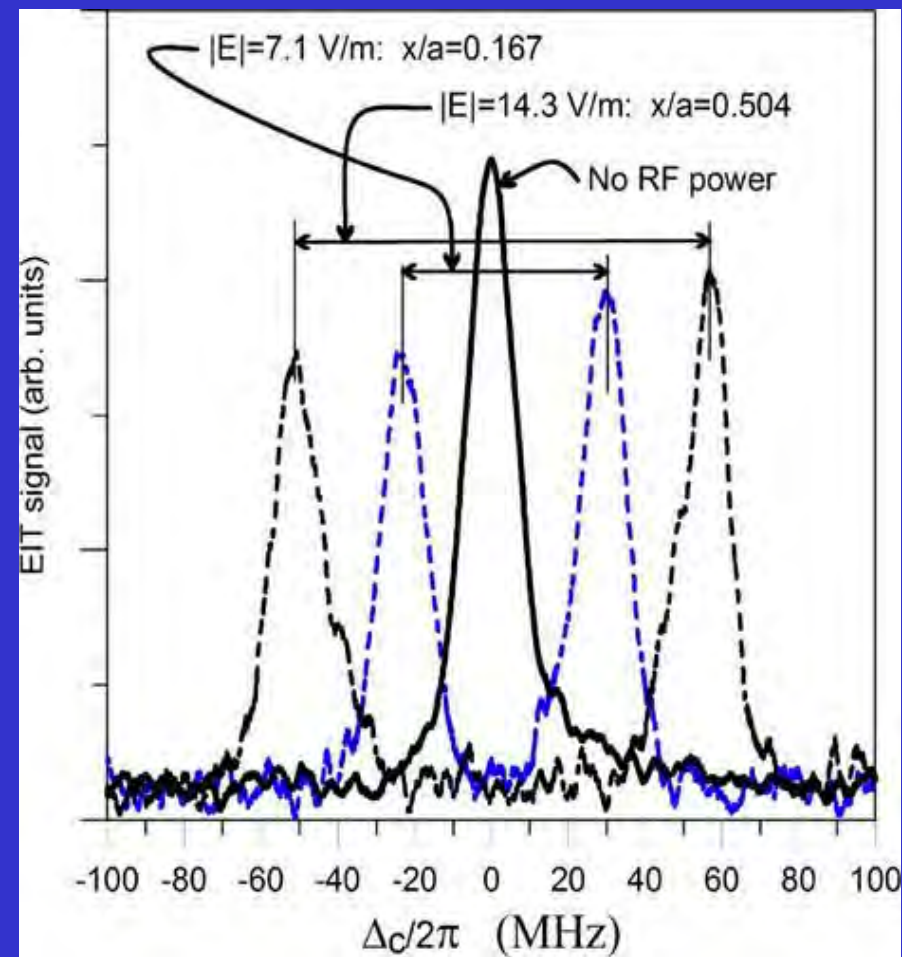
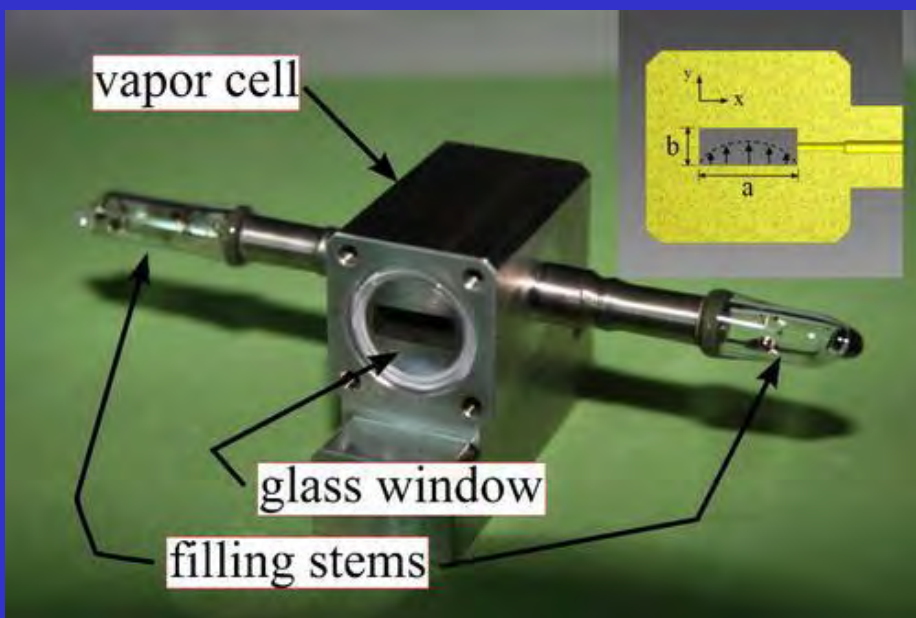
Appl. Phys. Lett.
104, 244102 (2014)



A New Quantum-Based Power Standard: Using Rydberg Atoms for a SI-Traceable Radio-Frequency Power Measurement Technique in Rectangular Waveguides^{a)}

Christopher L. Holloway,^{1,b)} Matthew T. Simons,¹ Marcus D. Kautz,¹ Abdulaziz H. Haddab,¹ Joshua A. Gordon,¹ and Thomas P. Crowley²

Appl. Phys. Lett. 113,
094101 (2018)

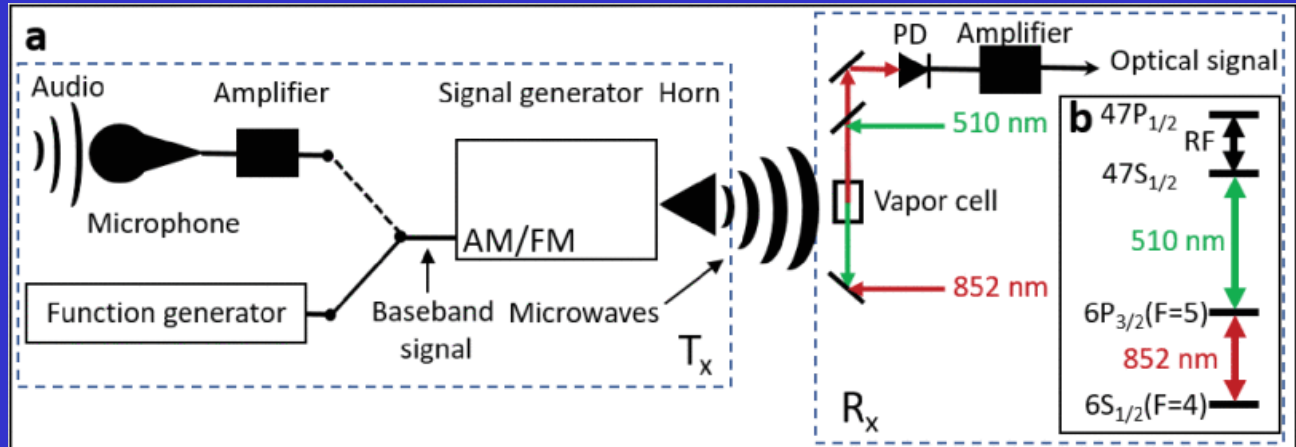


An atomic receiver for AM and FM radio communication

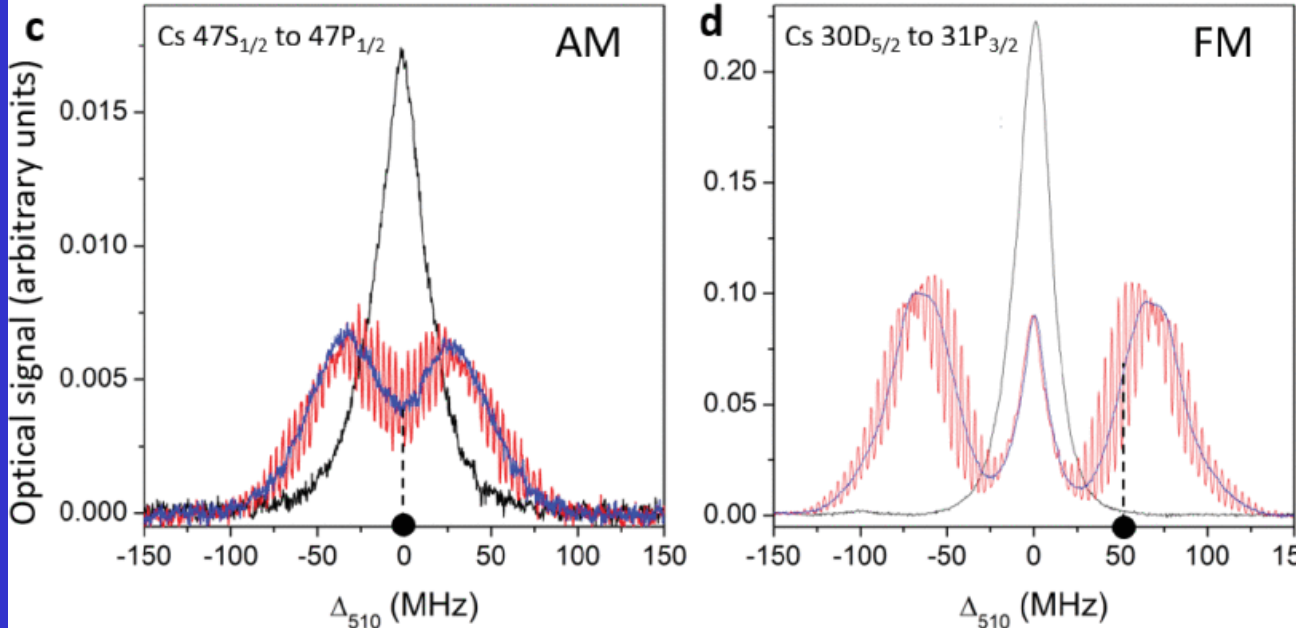
D. A. Anderson^{1,*}, R. E. Sapiro¹, and G. Raithel^{1,2}

1. Rydberg Technologies, Ann Arbor, MI 48104 USA and

2. Department of Physics, University of Michigan, Ann Arbor, MI 48109 USA



IEEE
Transactions on
Antennas and
Propagation, v.69,
p.2455 (2021)



A self-calibrating SI-traceable broadband Rydberg atom-based radio-frequency electric field probe and measurement instrument.

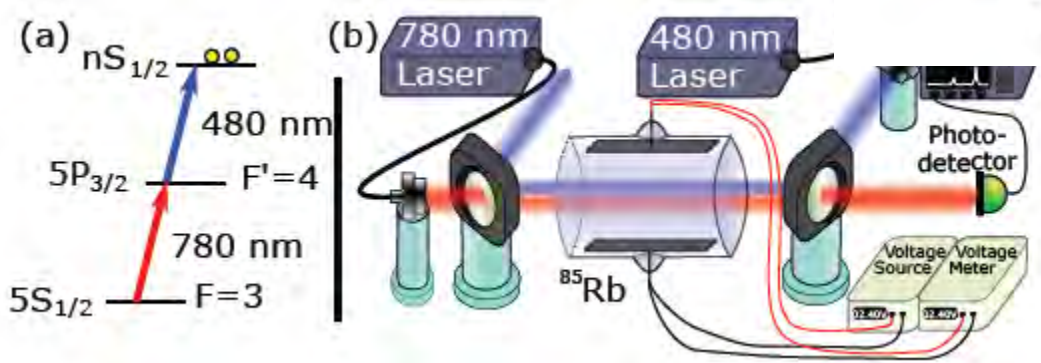
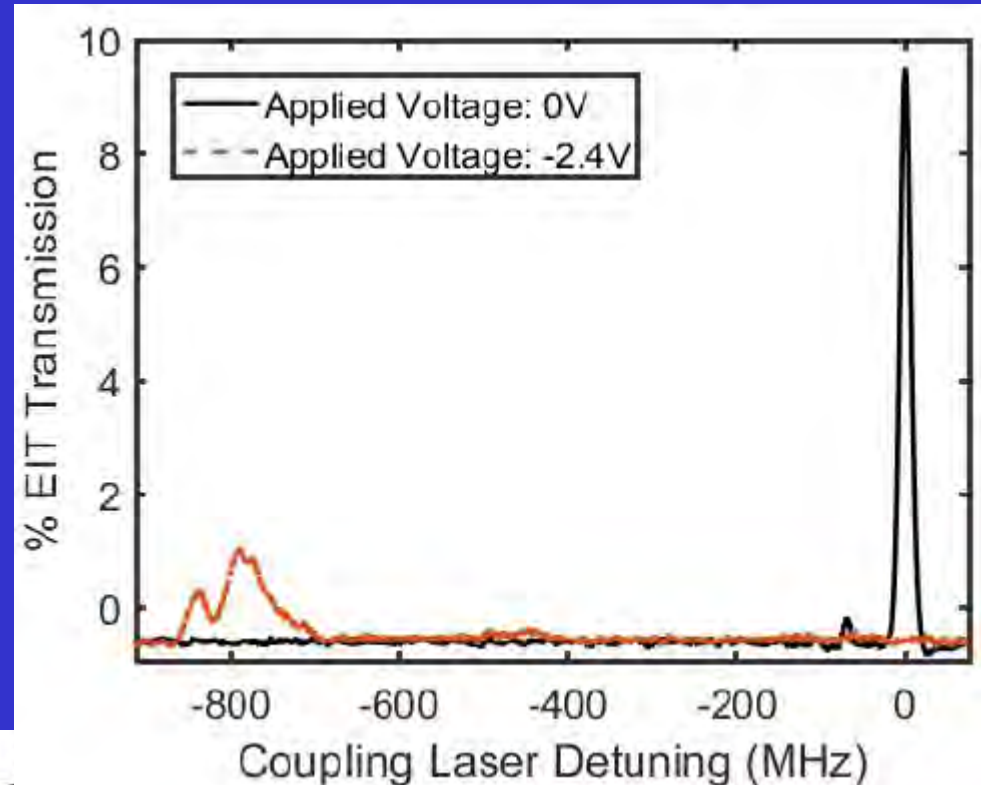
David Alexander Anderson, Rachel Elizabeth Sapiro, and Georg Raithel



IEEE
Transactions on
Antennas and
Propagation v.69,
p.5931 (2021)

Electromagnetically induced transparency based Rydberg-atom sensor for quantum-based voltage measurements^{a)}

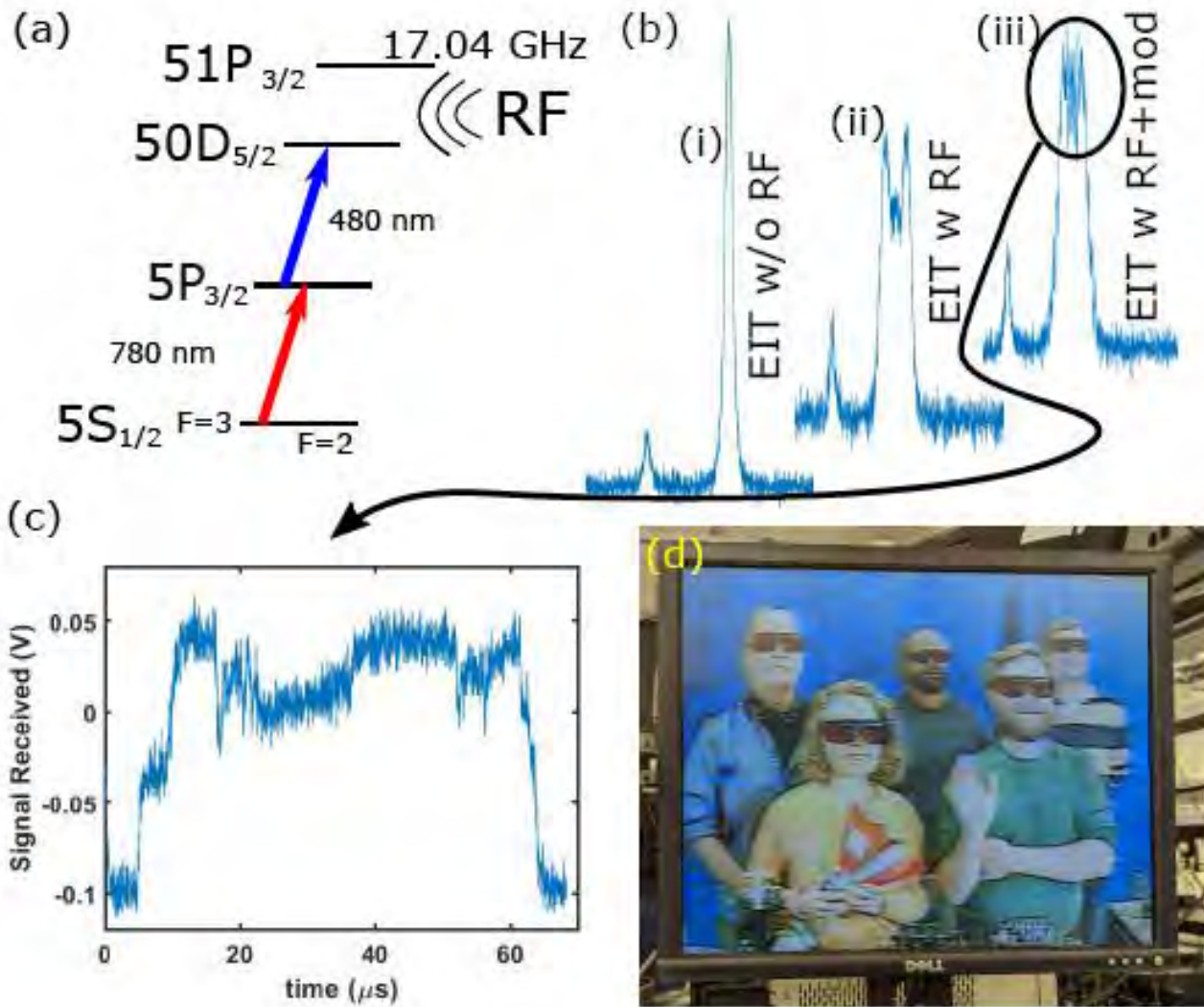
Christopher L. Holloway,¹ Nikunjkumar Prajapati,^{1, 2} John Kitching,¹ Jeffery A. Sherman,¹ Carson Teale,¹ Alain Rüfenacht,¹ Alexandra B. Artusio-Glimpse,¹ Matthew T. Simons,¹ Amy K. Robinson,³ and Eric B. Norrgard⁴



arXiv:2110.02335

TV and Video Game Streaming with a Quantum Receiver: A Study on a Rydberg atom-based receiver's bandwidth and reception clarity^{a)}

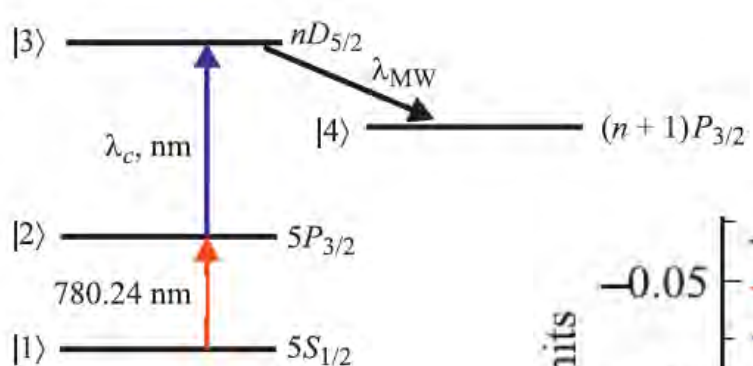
Nikunjkumar Prajapati, Andrew P. Rotunno, Samuel Berweger, Matthew T. Simons, Alexandra B. Artusio-Glimpse, and Christopher L. Holloway



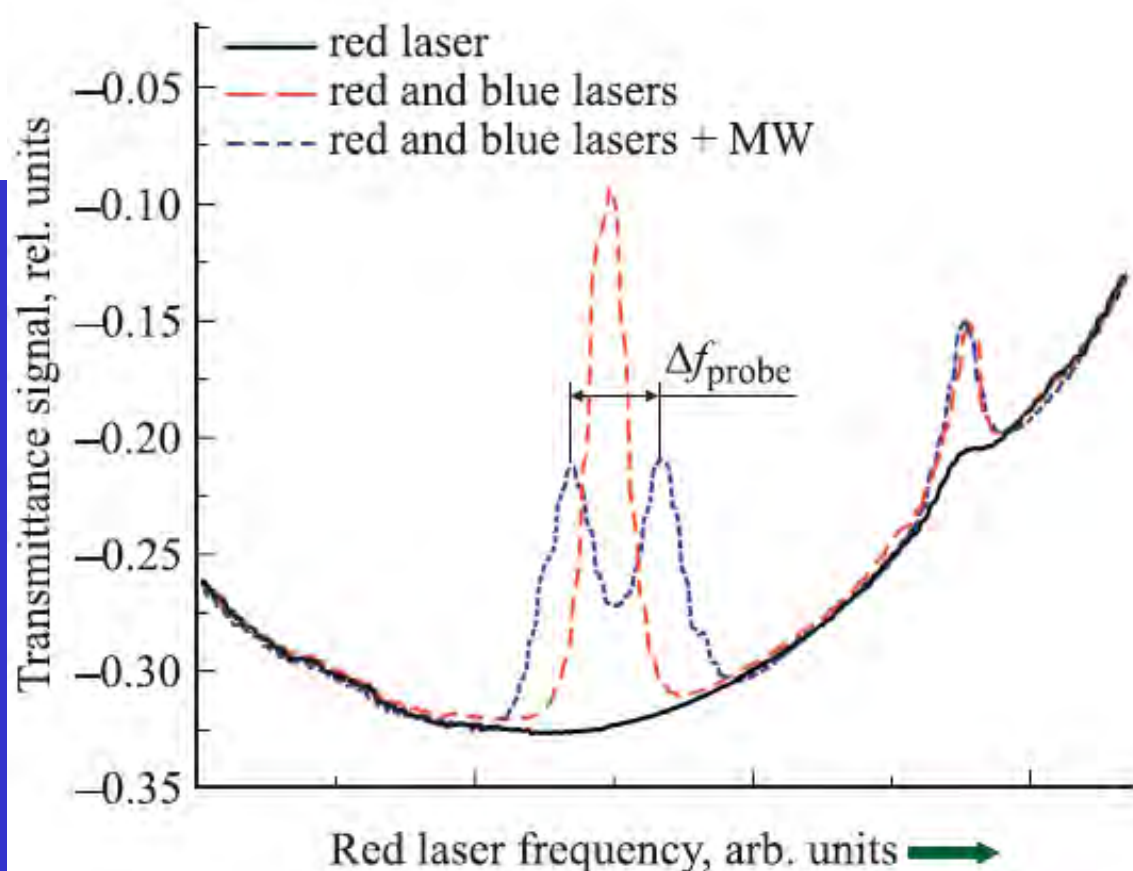
arXiv: 2205.02716

Измерение напряженности электрического поля СВЧ излучения на частоте радиационного перехода между ридберговскими состояниями атомов ^{85}Rb

© Е.Ф. Стельмашенко¹, О.А. Клезович¹, В.Н. Барышев¹, В.А. Тищенко¹, И.Ю. Блинов¹,
В.Г. Пальчиков^{1,2}, В.Д. Овсянников^{1,3}

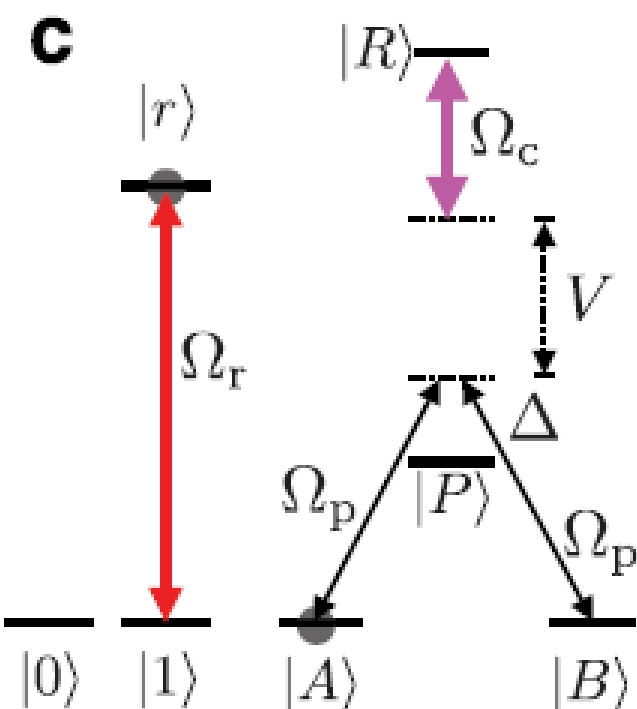
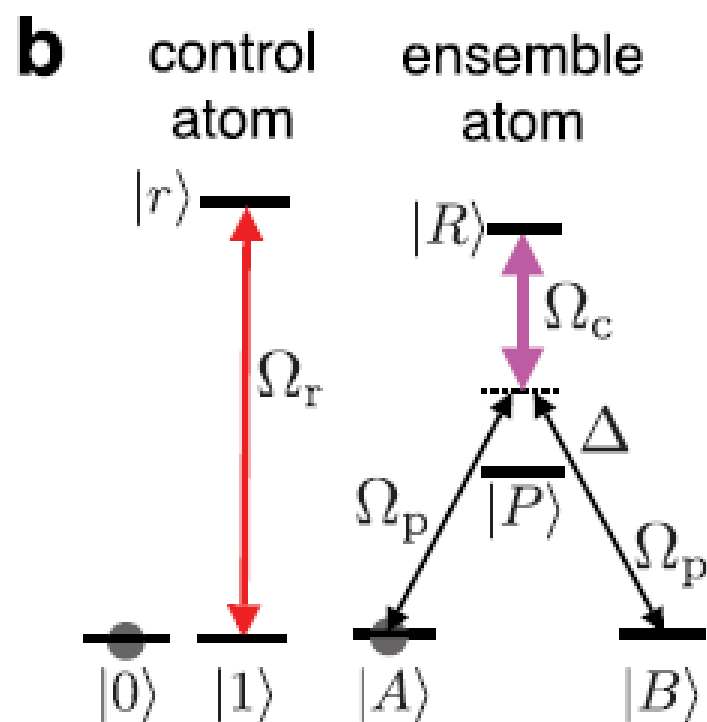
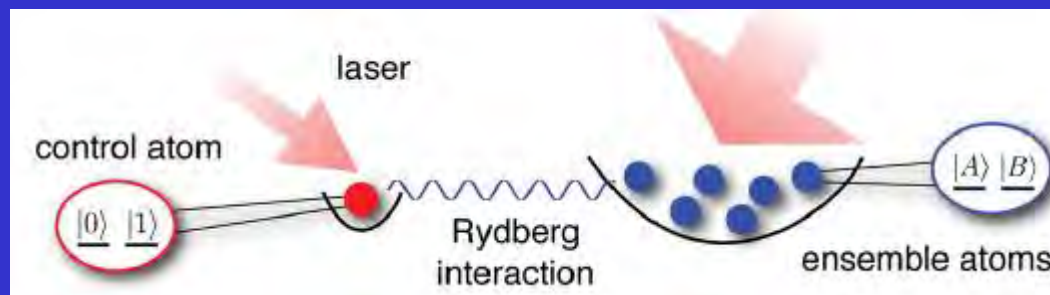


Оптика и спектроскопия,
2020, том 128, вып. 8, 1063



Mesoscopic Rydberg Gate Based on Electromagnetically Induced Transparency

M. Müller,¹ I. Lesanovsky,¹ H. Weimer,² H. P. Büchler,² and P. Zoller¹

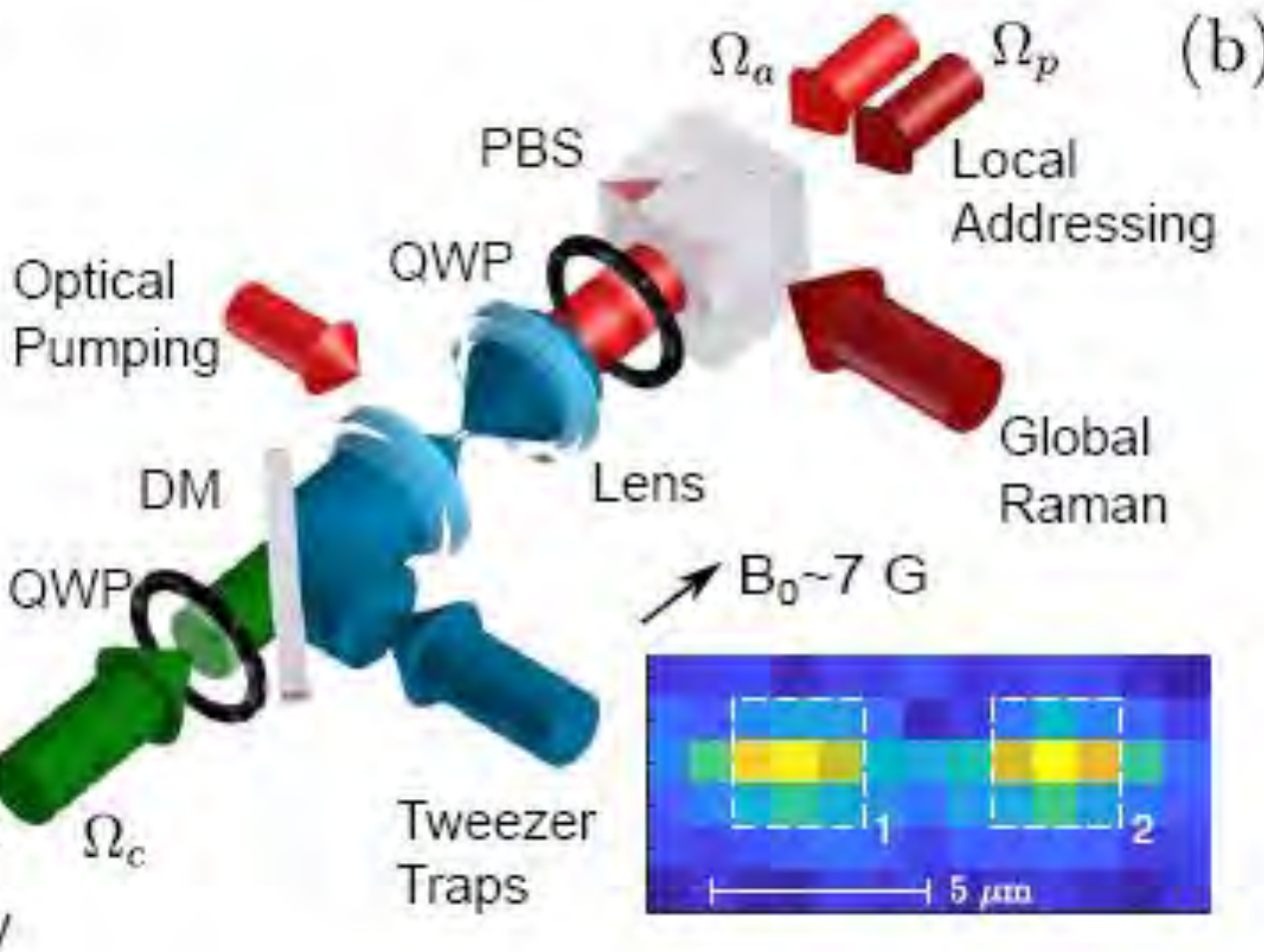


Demonstration of a Quantum Gate using Electromagnetically Induced Transparency

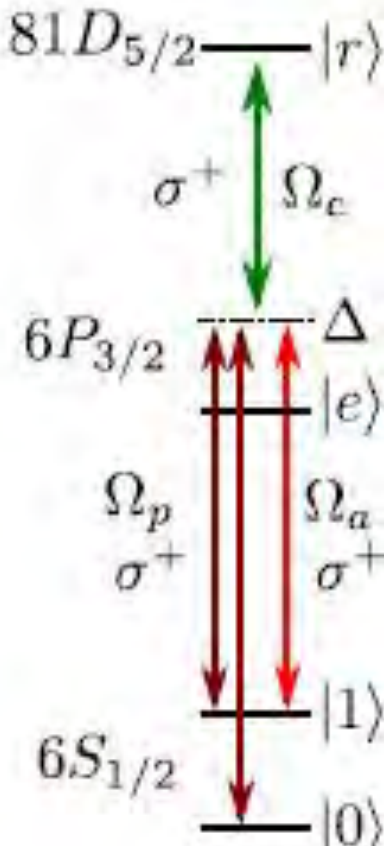
K. McDonnell, L.F. Keary, and J.D. Pritchard*

EQOP, Department of Physics, University of Strathclyde, SUPA, Glasgow G4 0NG, UK

(a)



(b)



arXiv: 2204.03733

Demonstration of a Quantum Gate using Electromagnetically Induced Transparency

K. McDonnell, L.F. Keary, and J.D. Pritchard*

EQOP, Department of Physics, University of Strathclyde, SUPA, Glasgow G4 0NG, UK

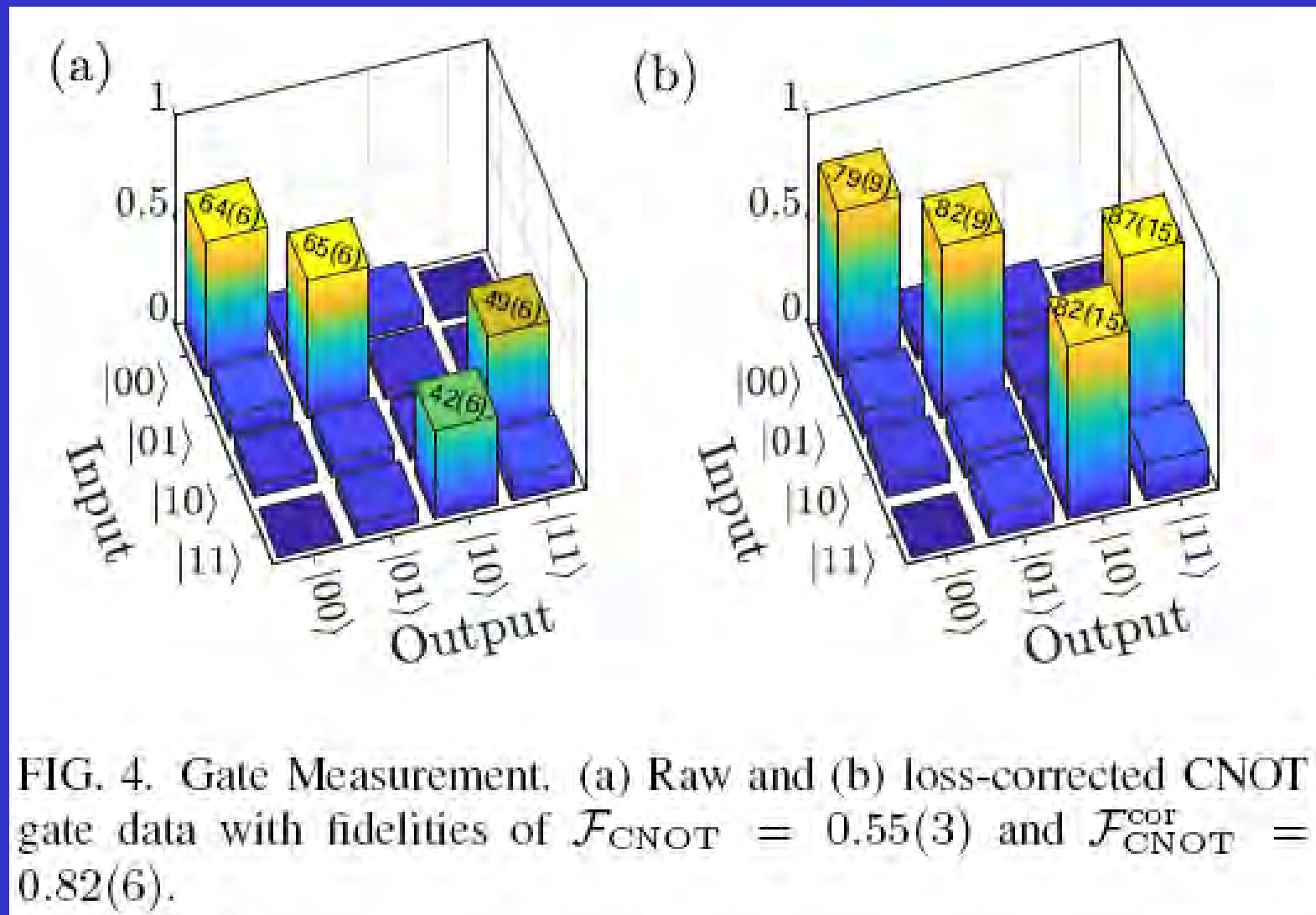
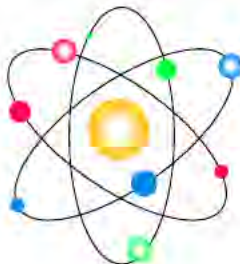


FIG. 4. Gate Measurement. (a) Raw and (b) loss-corrected CNOT gate data with fidelities of $\mathcal{F}_{\text{CNOT}} = 0.55(3)$ and $\mathcal{F}_{\text{CNOT}}^{\text{cor}} = 0.82(6)$.

SUMMARY

- Rydberg atoms have unique properties compared to low-excited atoms and are of great interest for high-resolution laser and microwave spectroscopy.
- Cold Rydberg atoms demonstrate strong long-range interactions which can be used to implement two- and three-qubit gates in quantum information processing with neutral atoms in optical lattices.
- Stark-tuned and rf-assisted Förster resonances provide fine and flexible control of many-body interactions between Rydberg atom.
- Rydberg atoms in optical gas cells demonstrate narrow EIT resonances which can be used as high-precision sensors of dc and ac electric fields.
- Our current aim is to build a medium-scale quantum computer and simulator with qubits based on single Rb atoms. We have demonstrated optical dipole traps, single atom loading and detection, initialization and one-qubit gates with individual addressing.
- Our experiments on two- and three-qubit gates with coherent interactions of Rydberg atoms in optical traps are in progress.

Федеральное государственное бюджетное учреждение
науки Институт физики полупроводников им. А.В.Ржанова
Сибирского отделения Российской академии наук



ИНСТИТУТСКИЙ СЕМИНАР

Административный корпус
Конф. зал

29 апреля 2013 г.
Понедельник, 9:30

Alain Aspect
*Augustin Fresnel Professor,
Institut d'Optique, Palaiseau, France*

*Coherent Back Scattering
and Anderson Localization
of Ultra Cold Atoms*



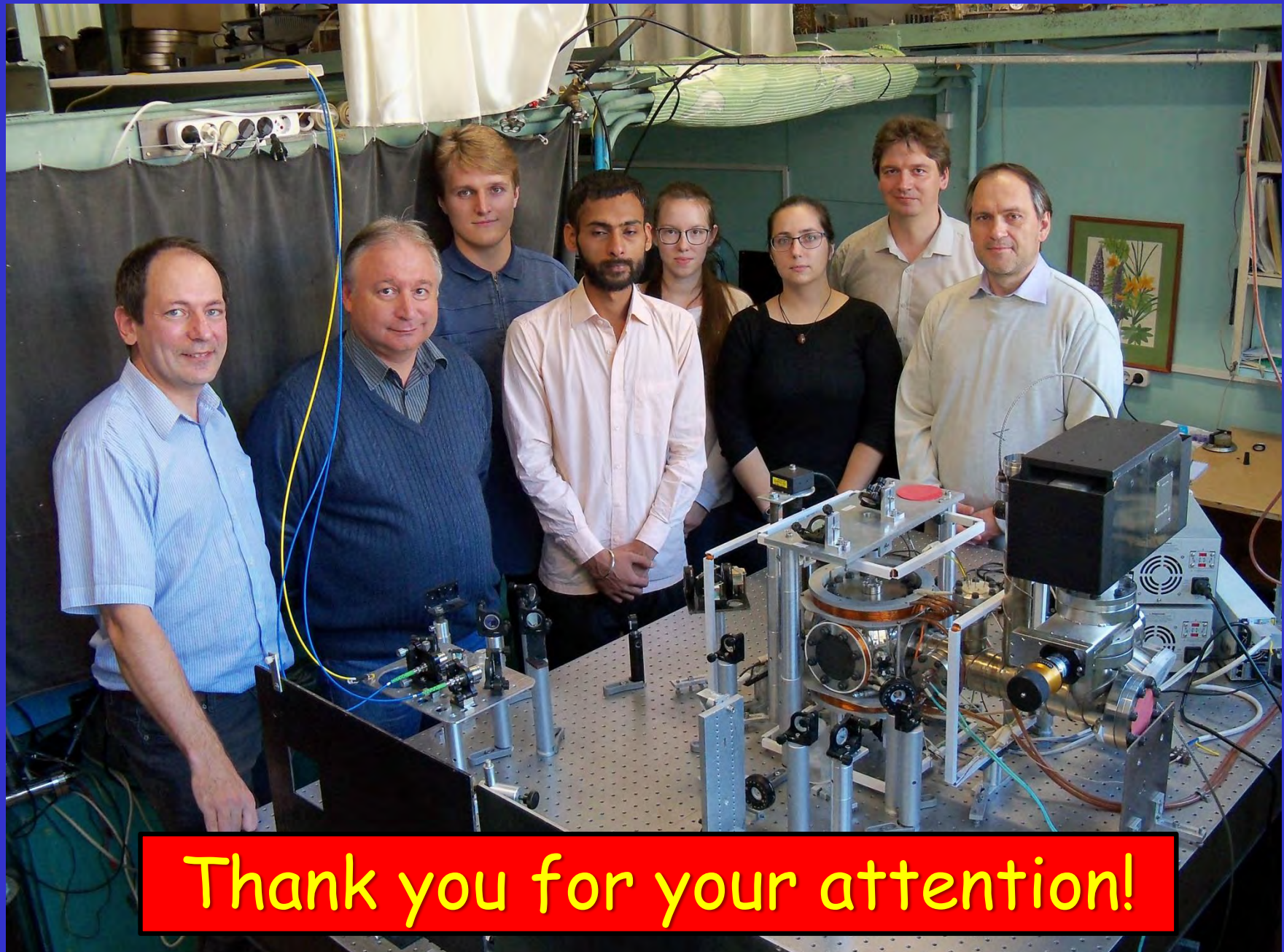
16-я Всероссийская научная конференция с международным участием
"Физика ультрахолодных атомов – 2022"

Организаторы: ИЛФ СО РАН, ИФП СО РАН, ИАиЭ СО РАН, НГУ

19-21 декабря 2022 года, Новосибирск, Академгородок, проспект Лаврентьева 15 Б,
конференц-зал Института лазерной физики СО РАН

Сайт конференции: ultracoldatoms2022.laser.nsc.ru

The team and assembled setup with Rb trap array



Thank you for your attention!